Evolution of the shell structure in medium-mass nuclei:

Search for the $2d_{5/2}$ neutron orbital in ^{69}Ni

Mohamad Moukaddam
Université de Strasbourg - IPHC/CNRS

Shell Model as a Unified View of Nuclear structure
08 - 10 Oct., Strasbourg, France

Introduction

- Structure evolution of neutron-rich nuclei at N=40.

- Light-mass region :
  - HO shell closures : 2, 8, 20
- heavy-mass region :
  - Spin-orbit shell closures : 50, 82..

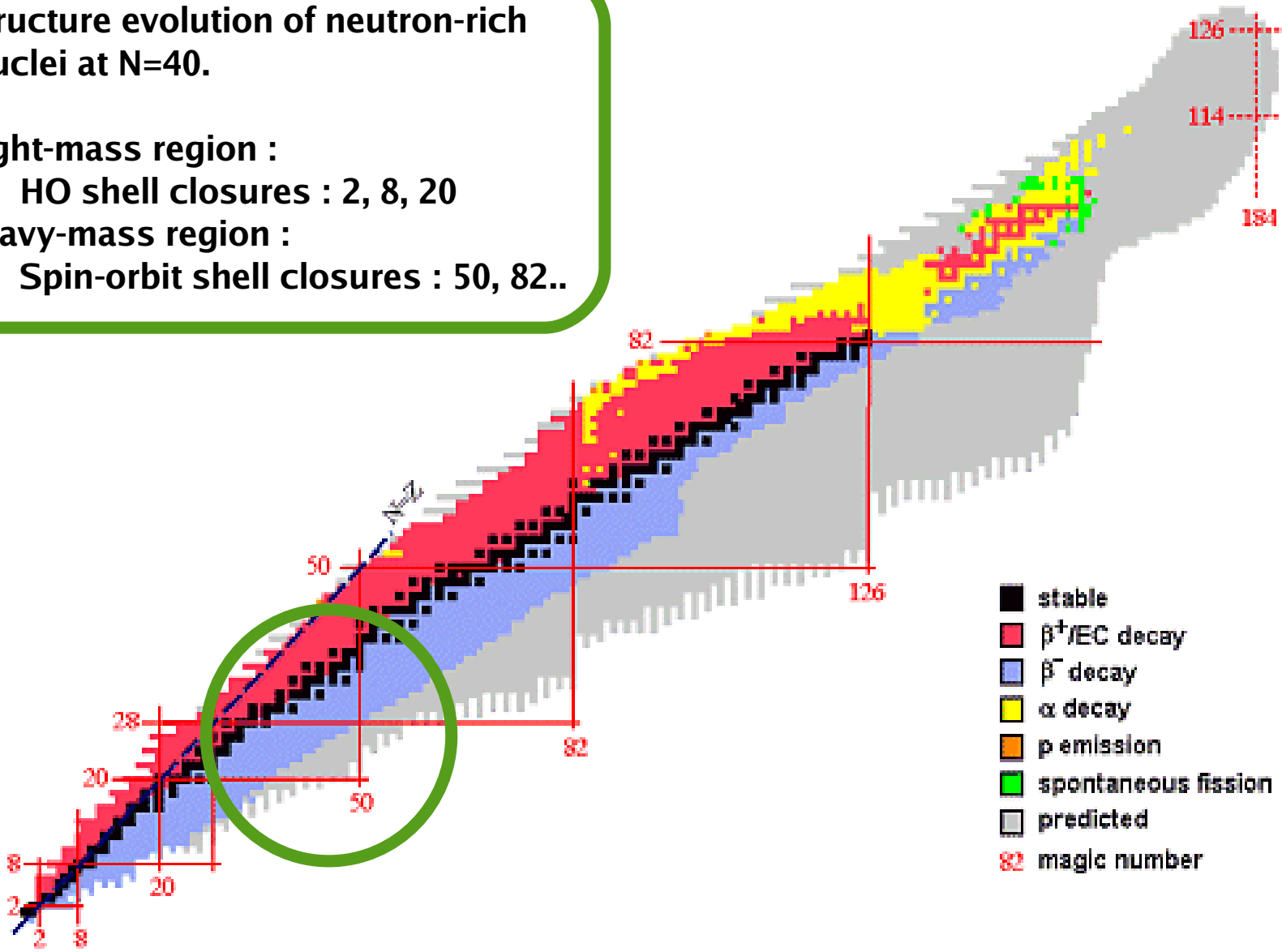

^{68}Ni and Deformation in Fe et Cr

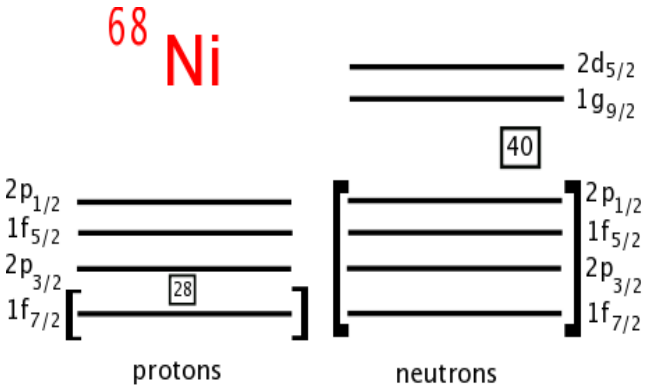

- Semi-magic nucleus (Z=28)
- E(2^+) ~ 2 MeV
  Broda et al, PRL, 74, 868, 1995
- B(E2) ~ 3.2 W.u.
  Sorlin, PRL, 88, 092501, 2002

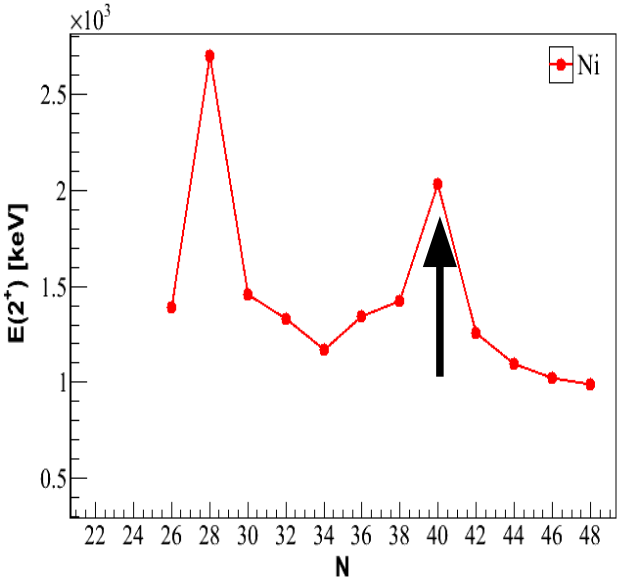

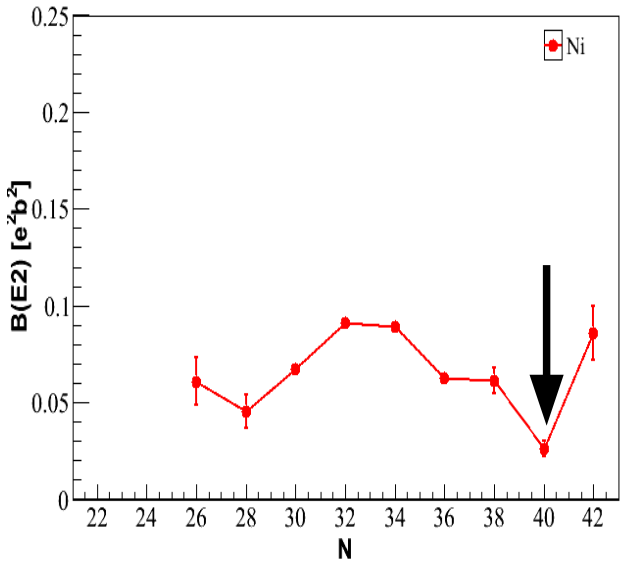

^{68}Ni and Deformation in Fe et Cr

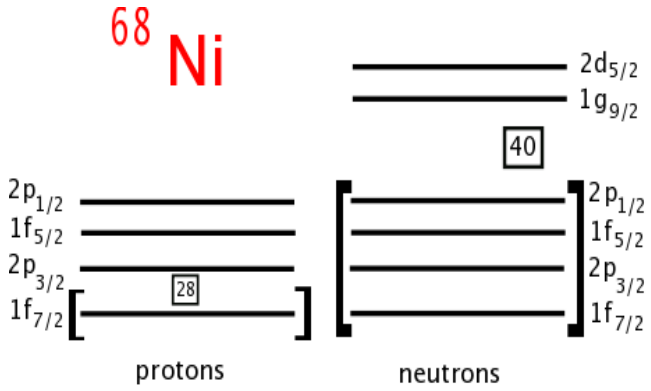

- Noyau Semi-magique (Z=28)
- $E(2^+)$ ~ 2 MeV
  Broda et al, PRL, 74, 868, 1995
- B(E2) ~ 3.2 W.u.
  Sorlin, PRL, 88, 092501, 2002

No trace for magicity according to S_{2n}
Rahaman, EPJ, 32, 87, 2007

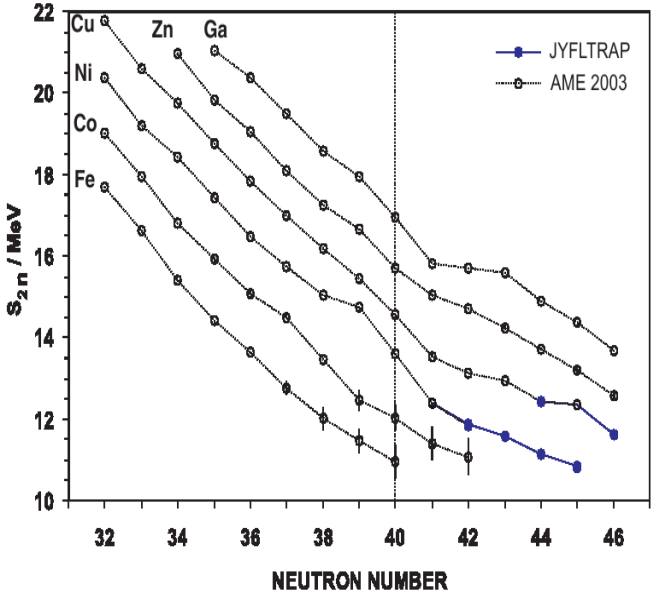

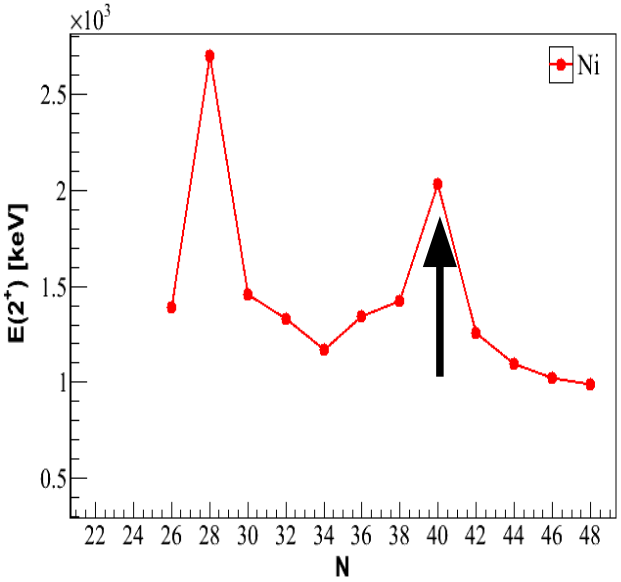

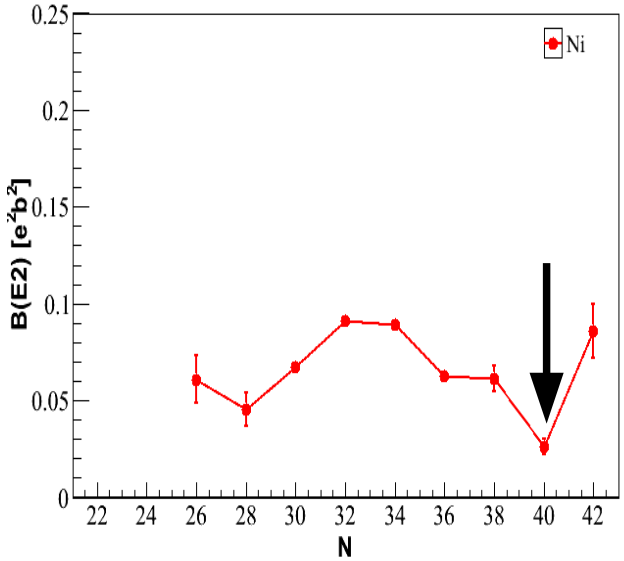

^{68}Ni and Deformation in Fe et Cr

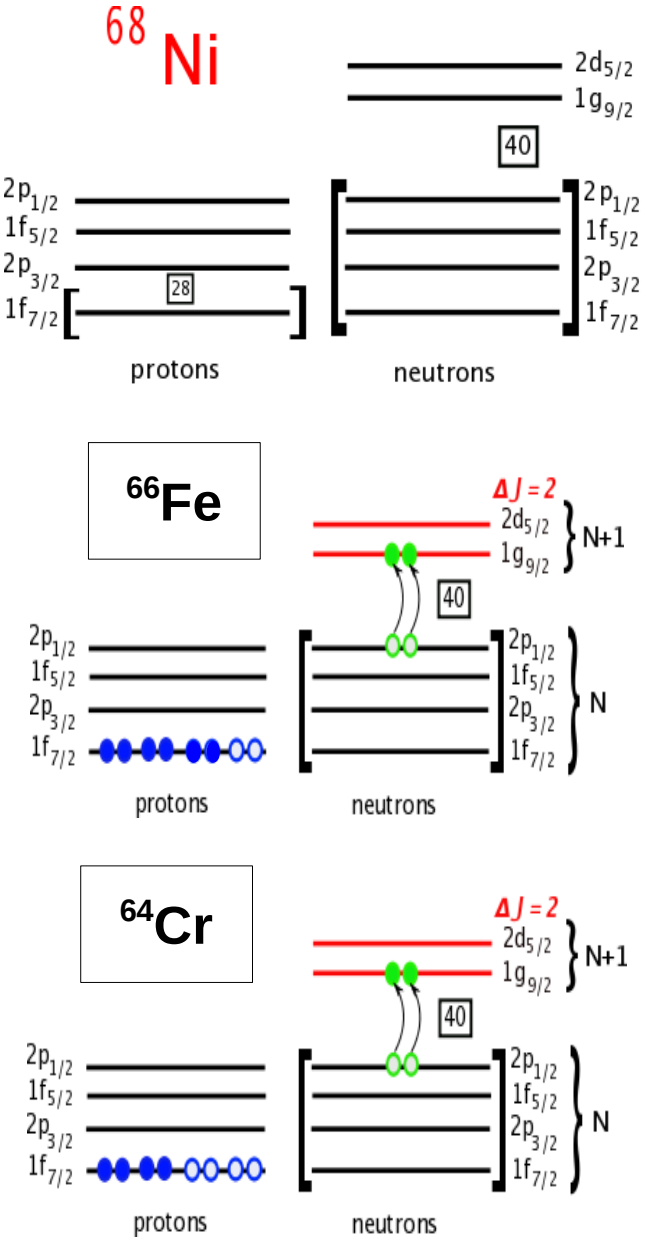

- Semi-magic nucleus (Z=28)
- $E(2^+) \sim 2$ MeV
  Broda et al, PRL, 74, 868, 1995
- B(E2) ~ 3.2 W.u.
  Sorlin, PRL, 88, 092501, 2002

No trace for magicity according to S_{2n}
Rahaman, EPJ, 32, 87, 2007

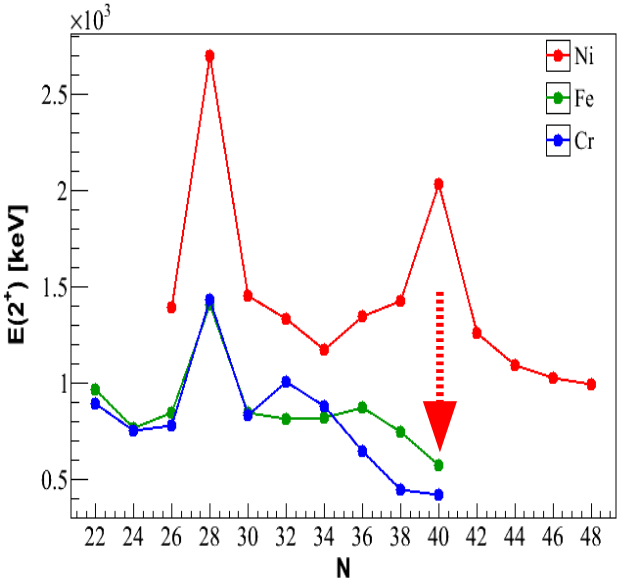

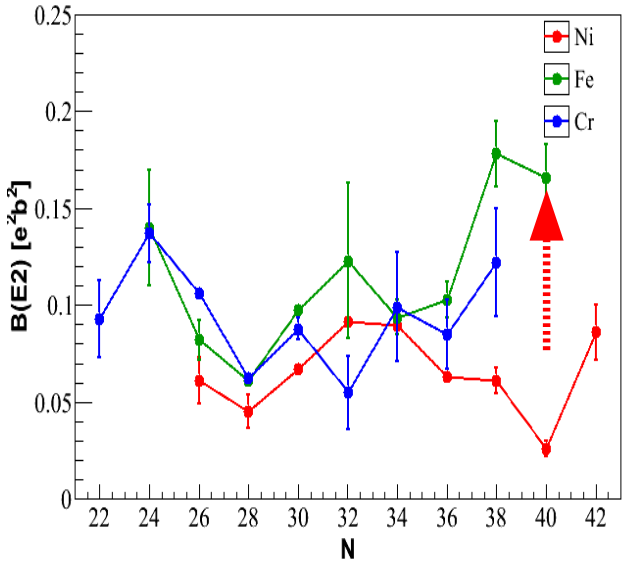

- N = 40 HO shell-closure is quickly washed out with removal of proton pairs.

Caurier et al. EPJ, A, 15, 2002, 145

Island of inversion and quadrupole deformations

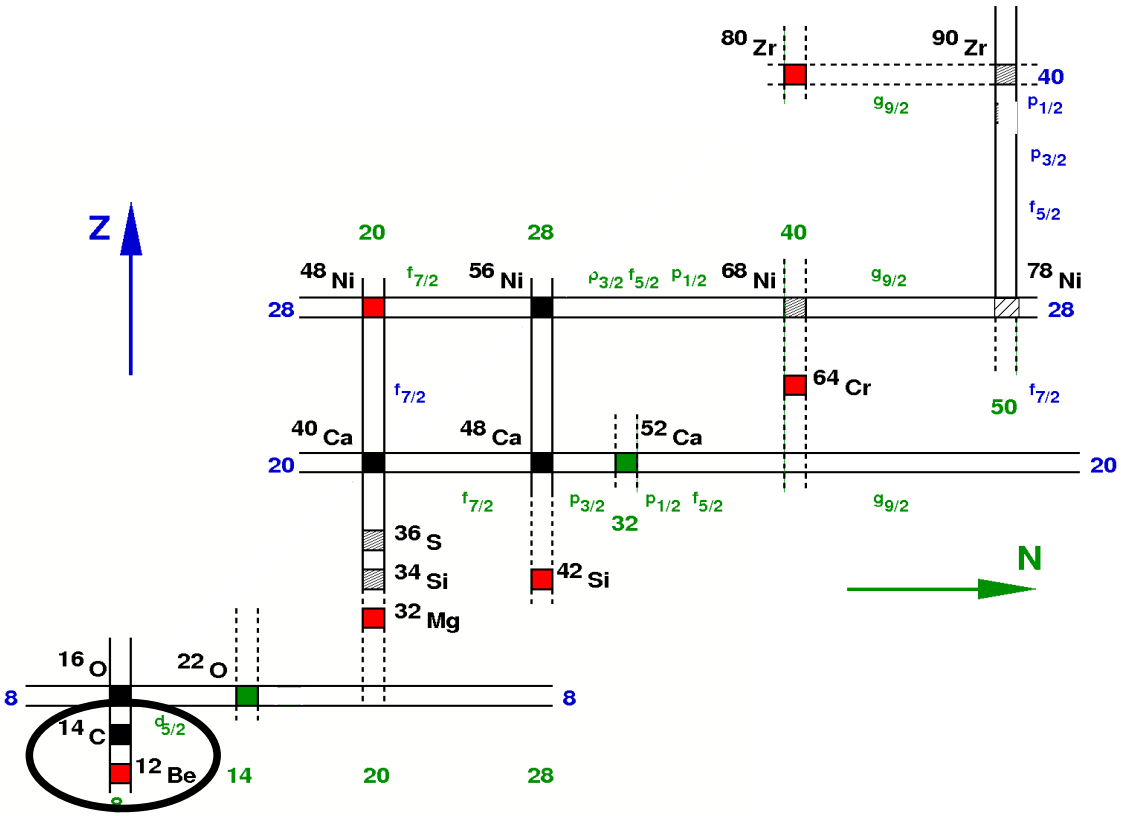

- Presence of quadrupole deformation at HO shell closures (N = 8, 20, 40)
- Island of inversion at N = 40

Caurier et al. EPJ, A, 15, 2002, 145

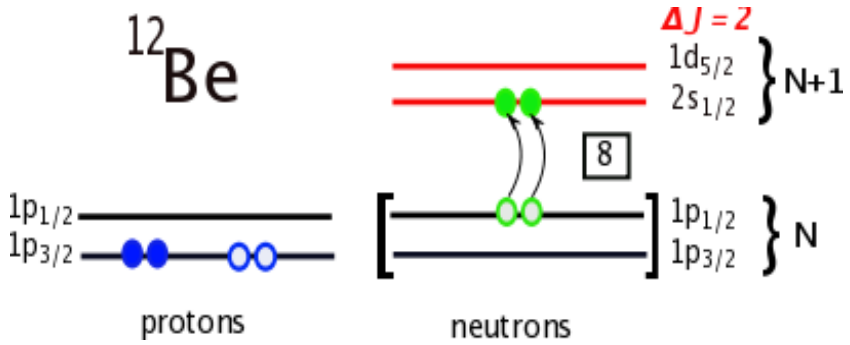

Island of inversion and quadrupole deformations

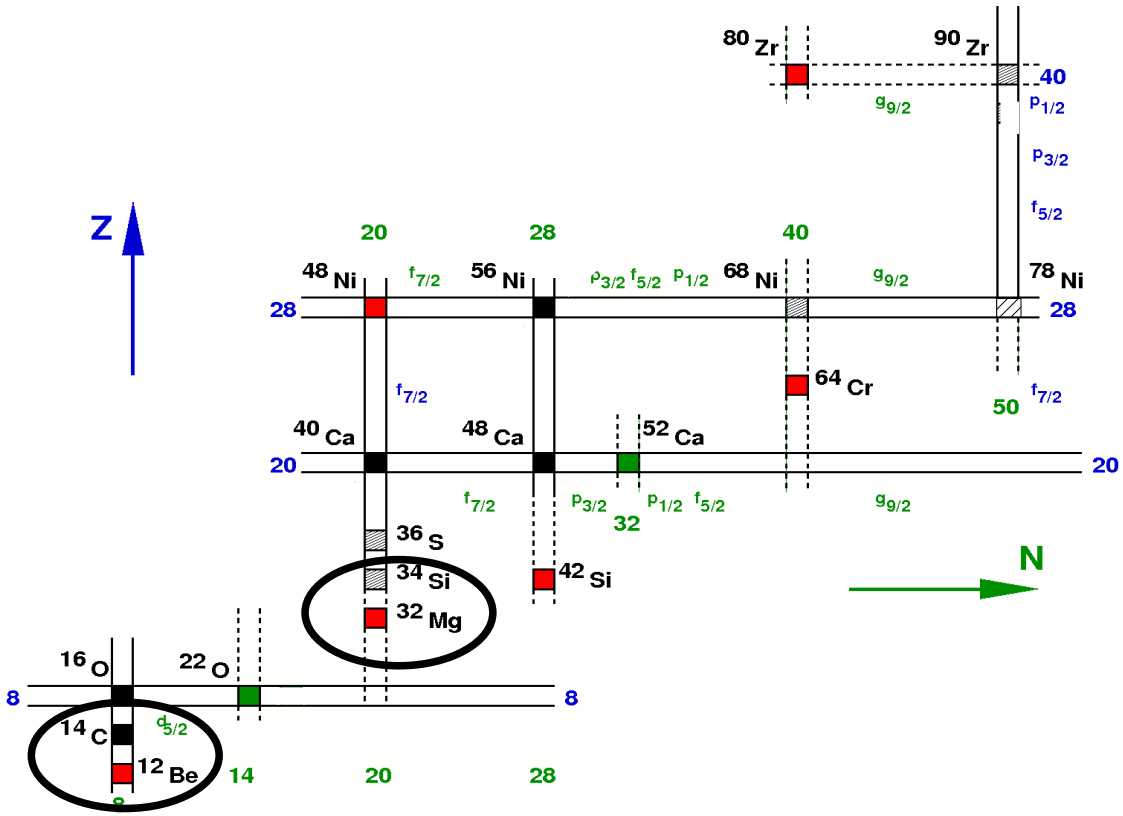

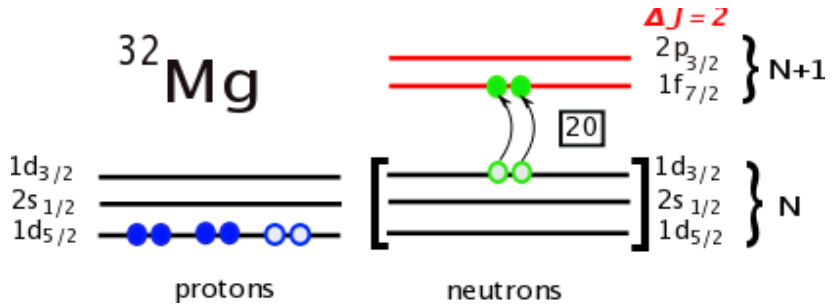

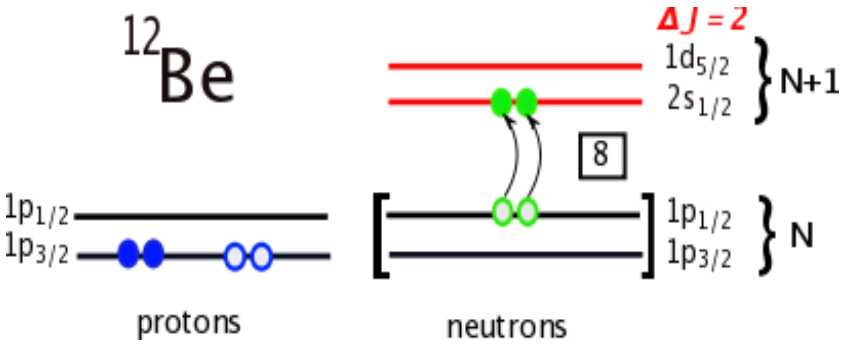

- Presence of quadrupole deformation at HO shell closures (N = 8, 20, 40)
- Island of inversion at N = 40

Caurier et al. EPJ, A, 15, 2002, 145

Island of inversion and quadrupole deformations

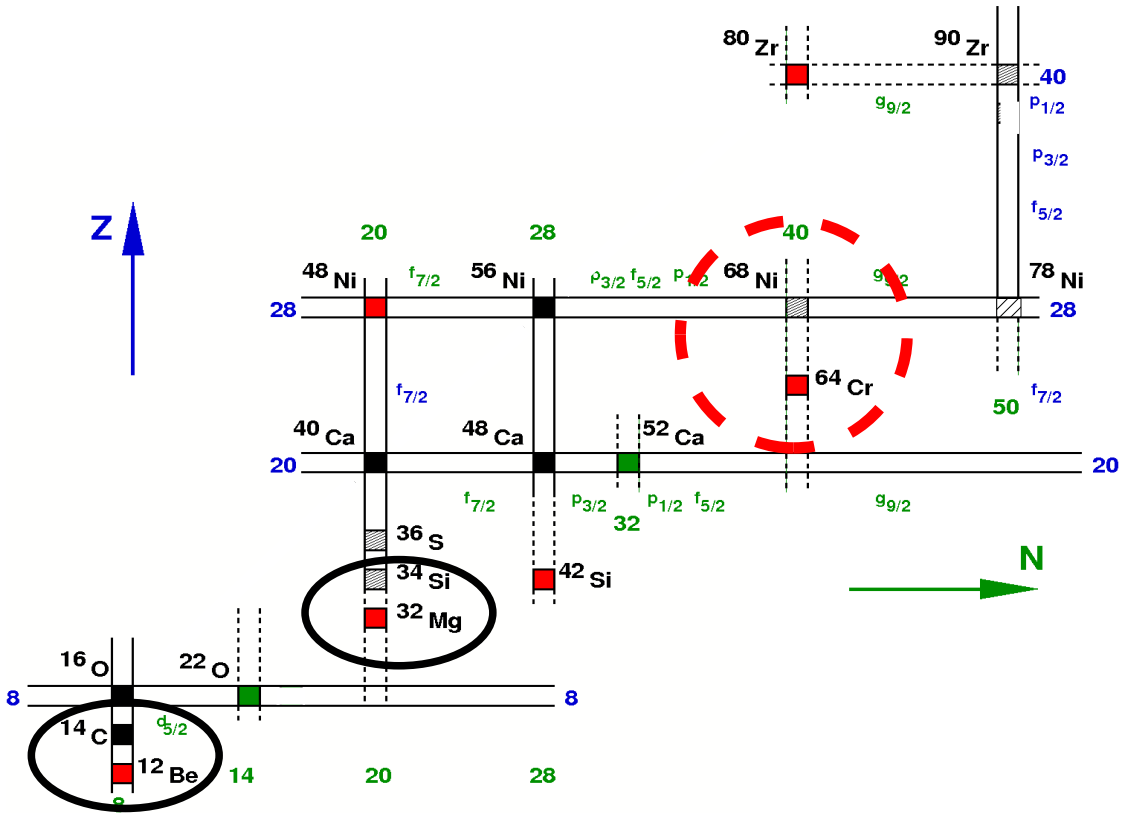

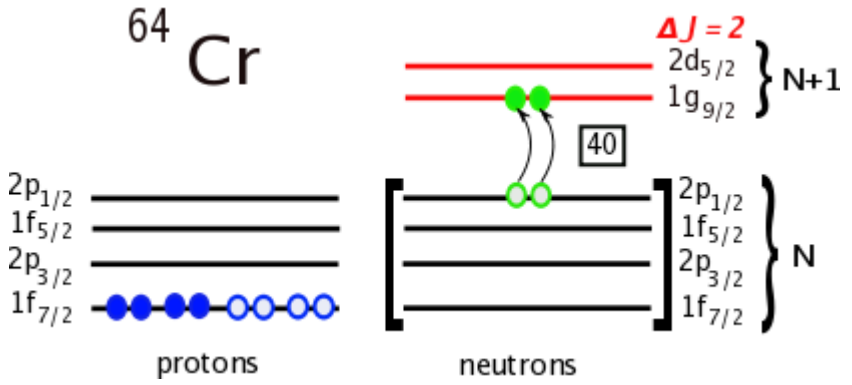

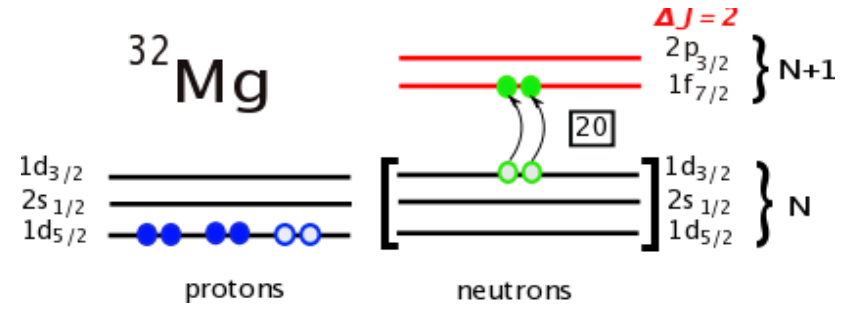

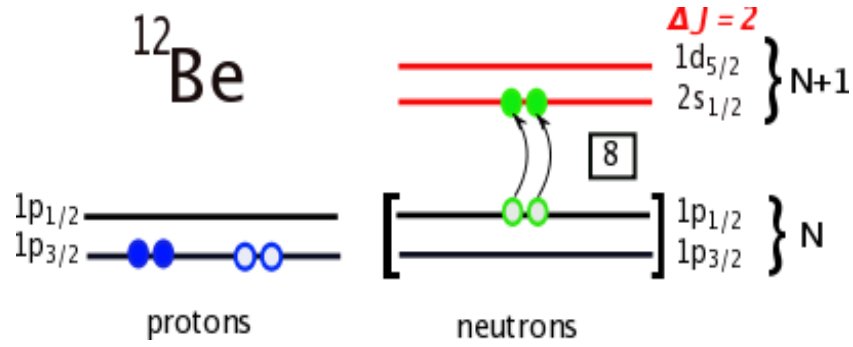

- Presence of quadrupole deformation at HO shell closures (N = 8, 20, 40)
- Island of inversion at N = 40

Caurier et al. EPJ, A, 15, 2002, 145

Island of inversion and quadrupole deformations

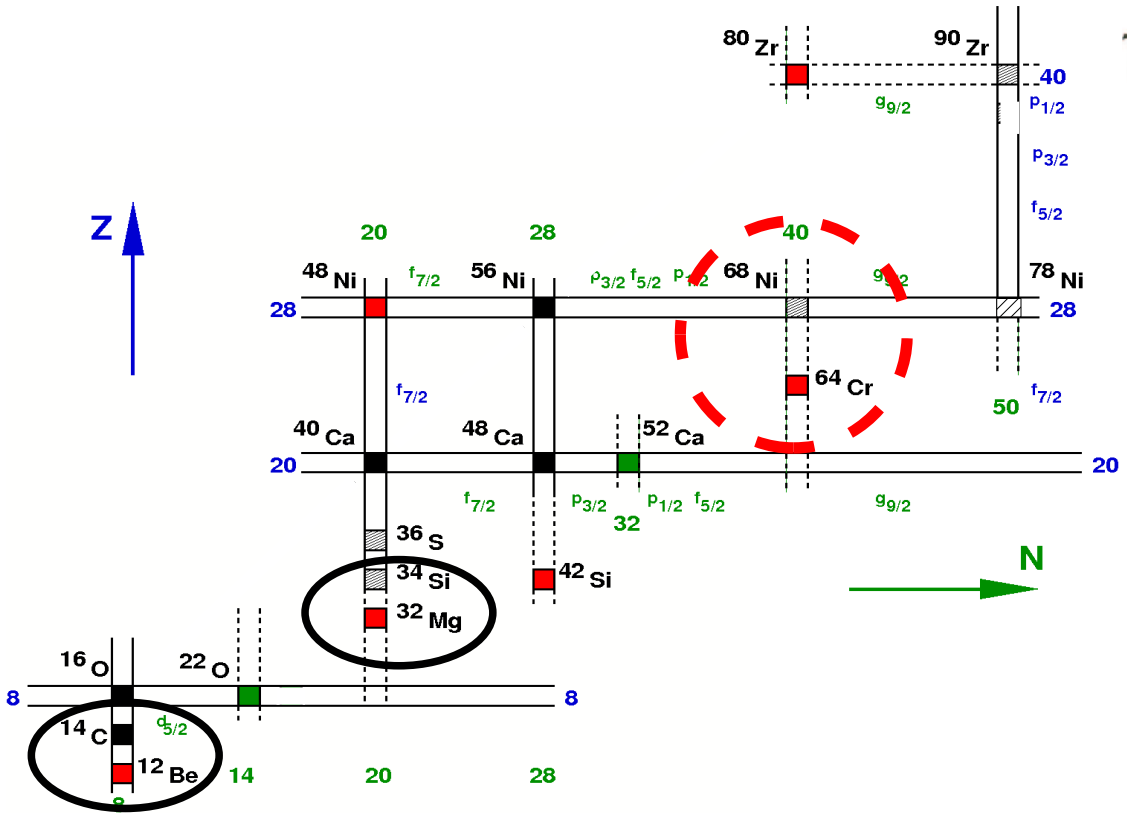

- Presence of quadrupole deformation at HO shell closures (N = 8, 20, 40)
- Island of inversion at N = 40

Caurier et al. EPJ, A, 15, 2002, 145

The Physics around the doubly-magic ^{78}Ni Nucleus

Leuven, Belgium
November 4-5, 1996

A. Poves

^{64}Cr

$g(0ph-2ph) = 5.70$
$g(0ph-4ph) = 8.30$

$Q = -9.0\ b^2$ CS < 1%
$BE2 = 19.8\ b^4$ $n(d_{5/2}) = 1.1$

$\frac{E(4^+)}{E(2^+)} = 2.7$ $\left[\frac{E(4^+)}{E(2^+)} = (3.2)(3.4)\right]$
in the intruder configurations.

A SITUATION THAT REMINDS WHAT IS KNOWN AT N=20 FFS.

^{69}Ni : search for the $2d_{5/2}$ neutron orbital

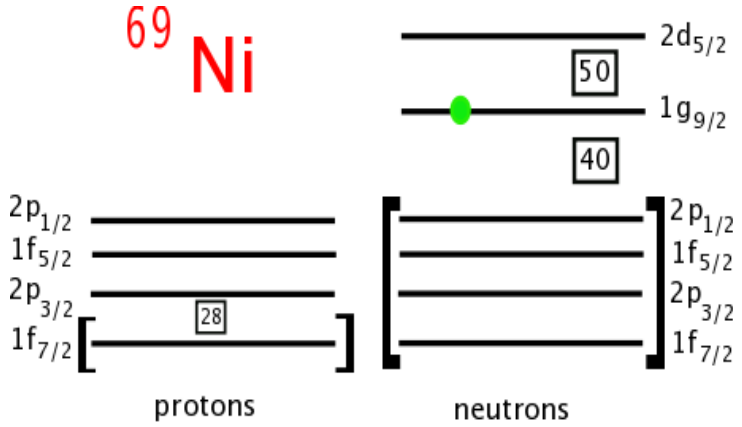

^{69}Ni : search for the $2d_{5/2}$ neutron orbital

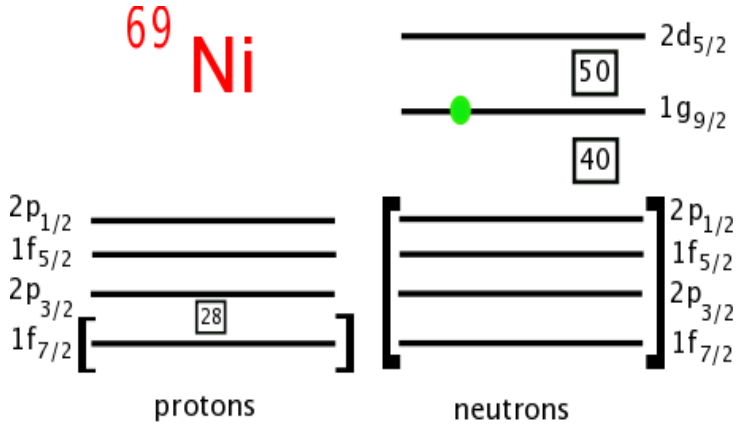

Previous experiments

- Isomer-state decay
  (Grzywacz et al., PRL, 81, 766, 1998)
- β-decay
  (*Mueller et al., PRL, 83, 3613, 1999*)

5/2+ neutron states are not observed

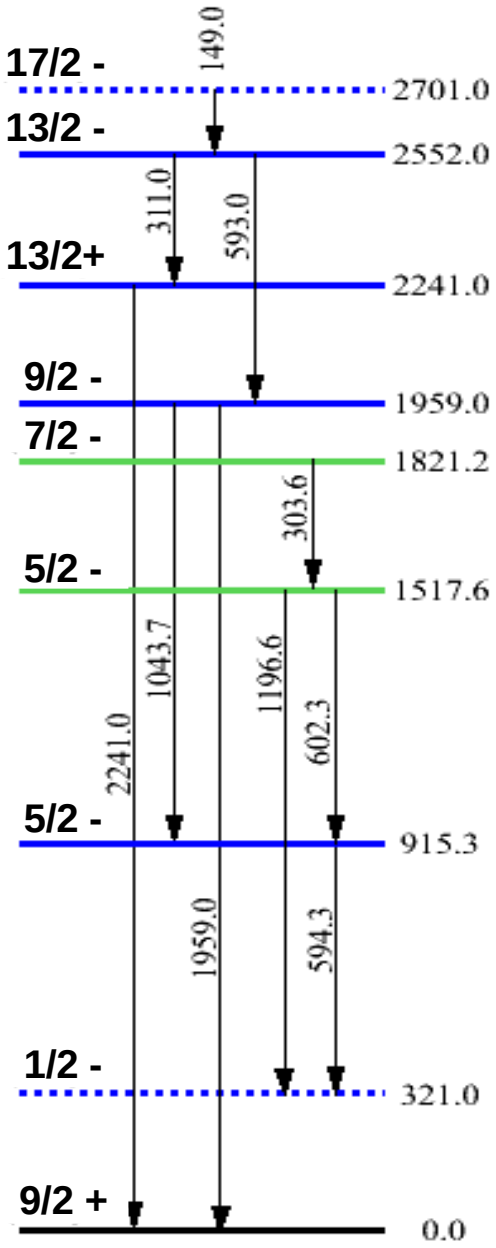

^{69}Ni : search for the $2d_{5/2}$ neutron orbital

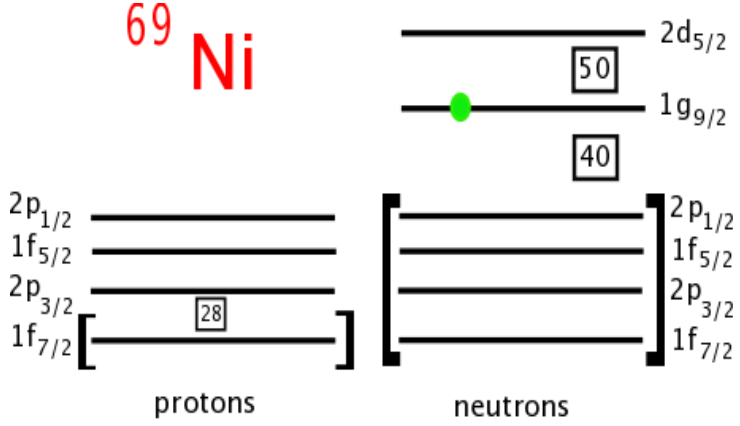

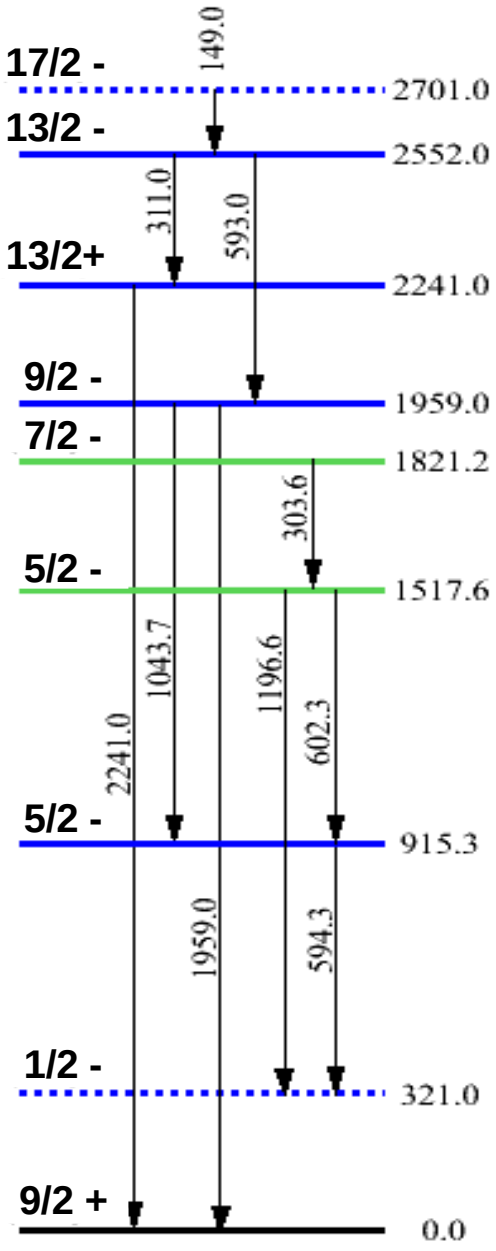

Previous experiments

- Isomer-state decay
  (Grzywacz et al., PRL, 81, 766, 1998)
- β-decay
  (*Mueller et al., PRL, 83, 3613, 1999*)

5/2+ neutron states are not observed

Main goal of this work

Search for the neutron $2d_{5/2}$ orbital in ^{69}Ni

$d(^{68}Ni,p)^{69}Ni$

Beam production

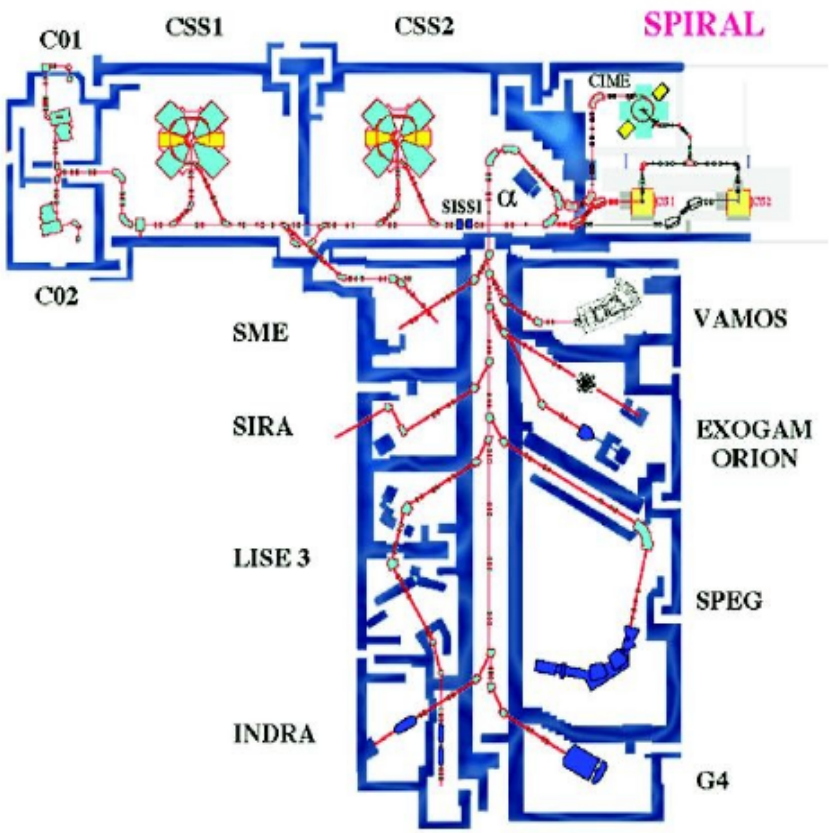

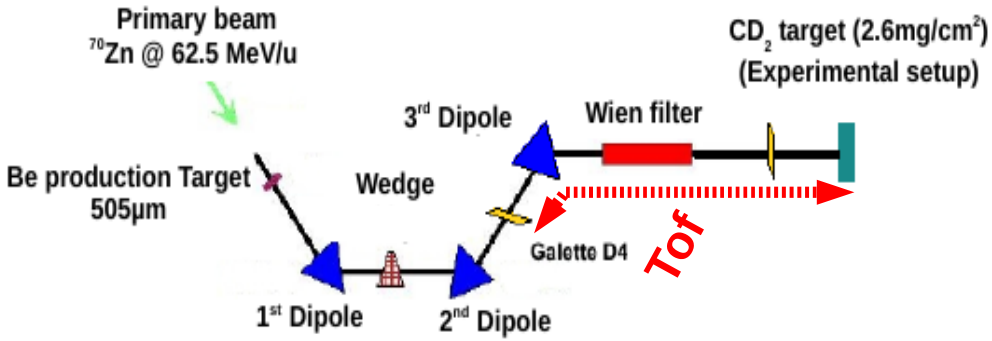

- Primary beam : ^{70}Zn (@62.5 AMeV)
- Primary beam intensity : 1.5 µAe
- Production target : ^{9}Be (505µm, 0°)
- Wedge : ^{9}Be (1099µm)
- Wien filter at 1kV
- Secondary beam intensity ~ 8.10^{4} pps @ 25.14 MeV/u
- **Purity ~ 86%**

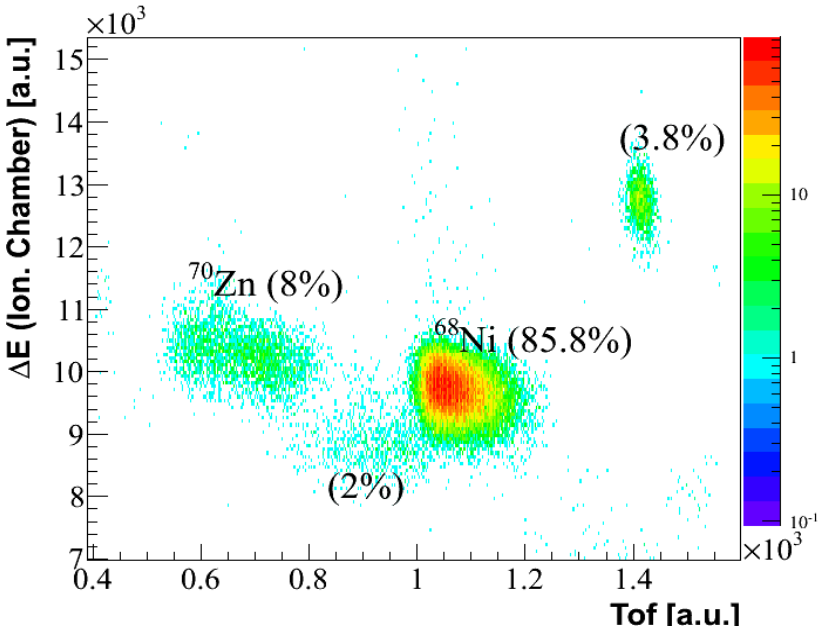

Experimental set-up

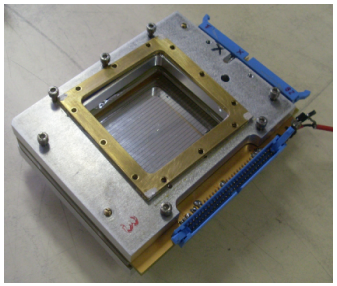

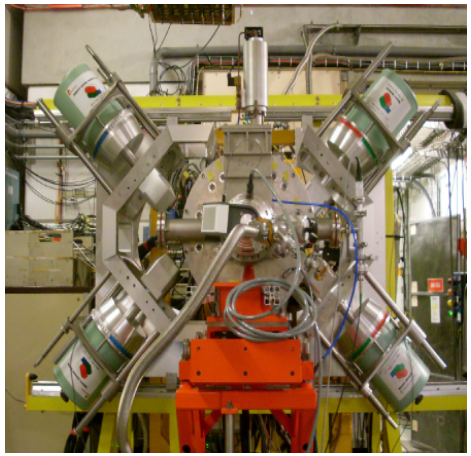

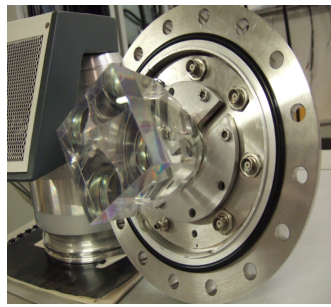

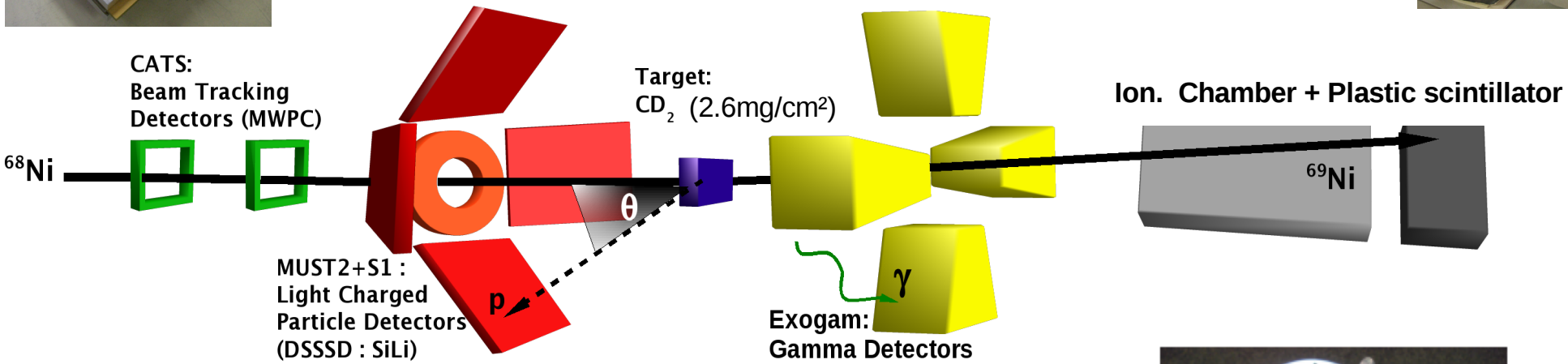

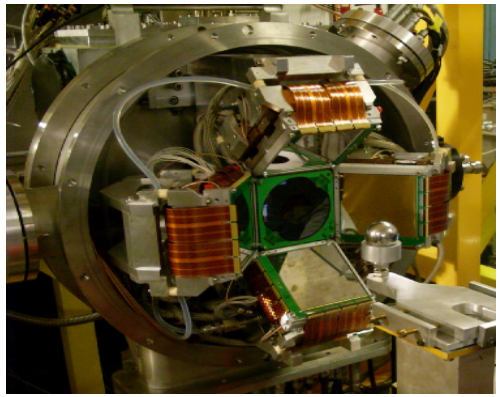

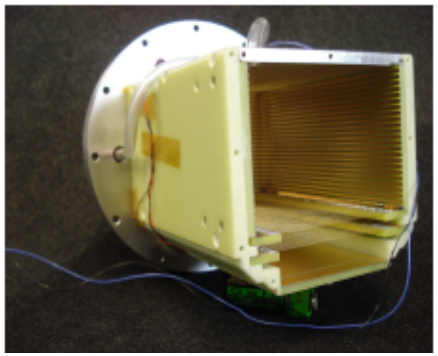

Experimental set-up

Beam reconstruction
In the target plane

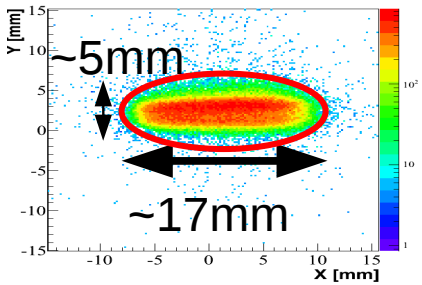

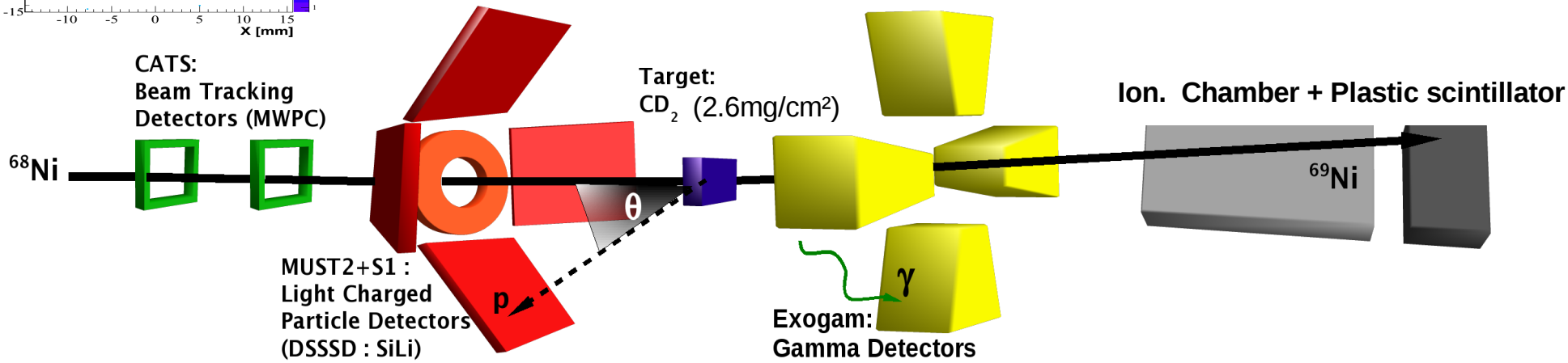

Experimental set-up

Beam reconstruction
In the target plane

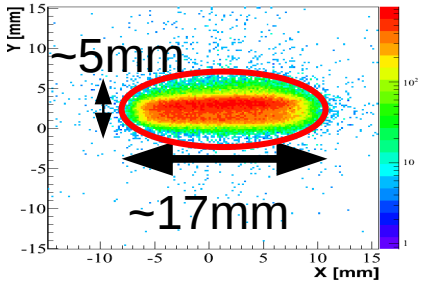

MUST2 : Si(Li)

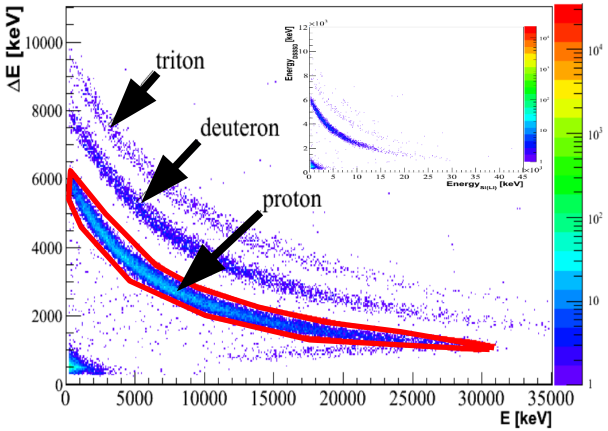

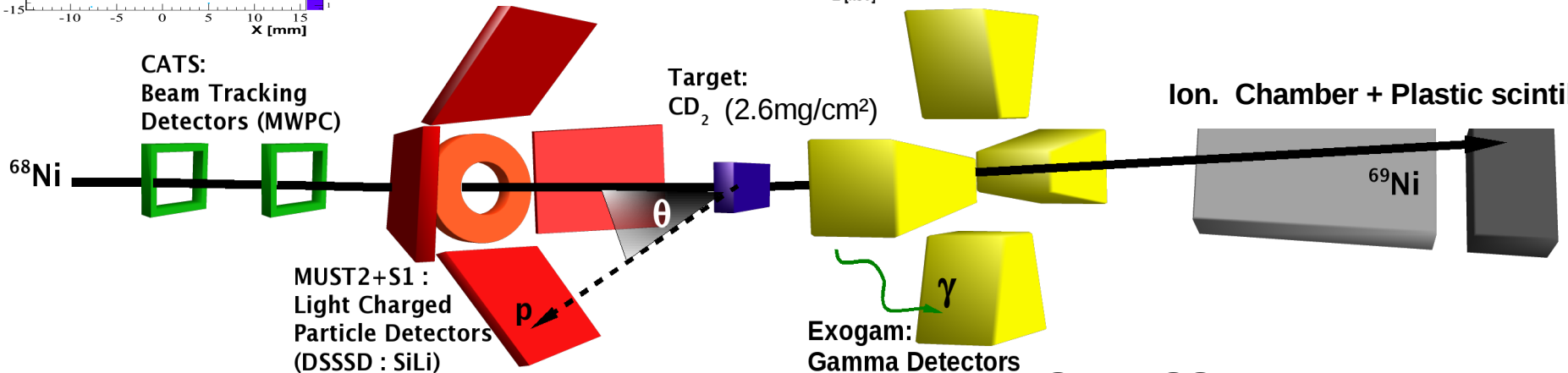

MUST2 : DSSD

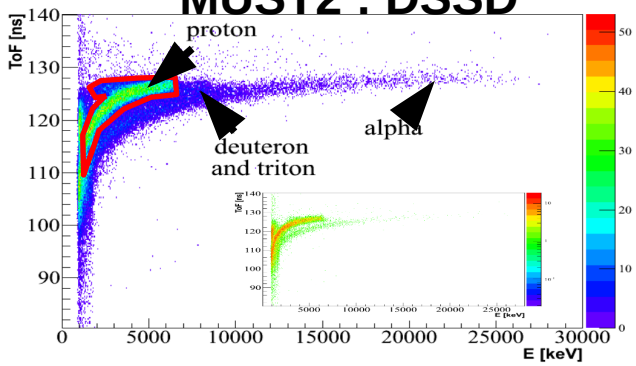

S1 : DSSD

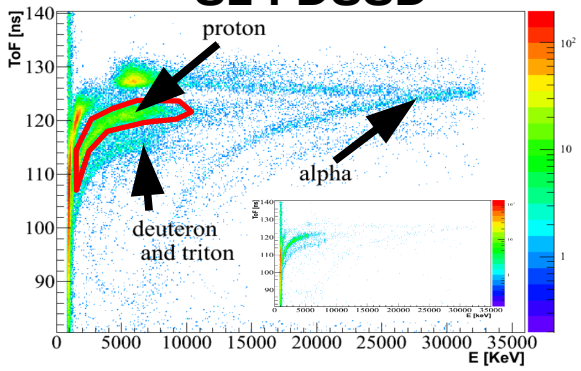

Experimental set-up

Beam reconstruction
In the target plane

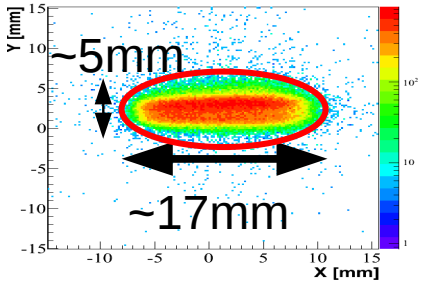

MUST2 : Si(Li)

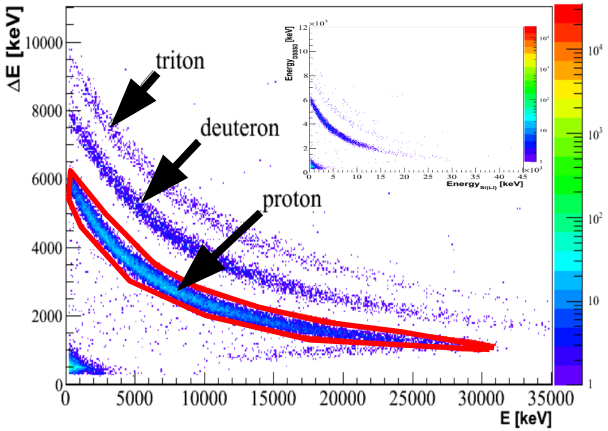

Plastic

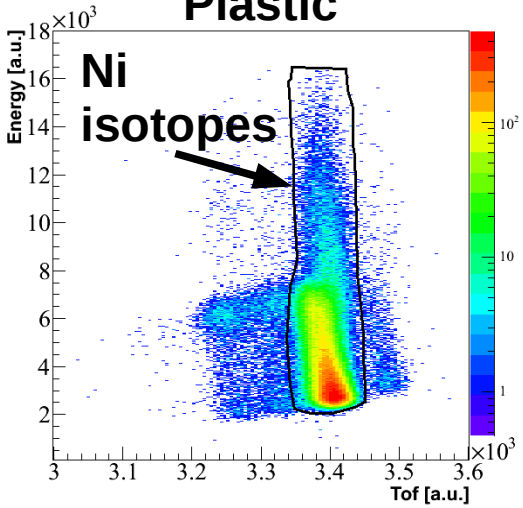

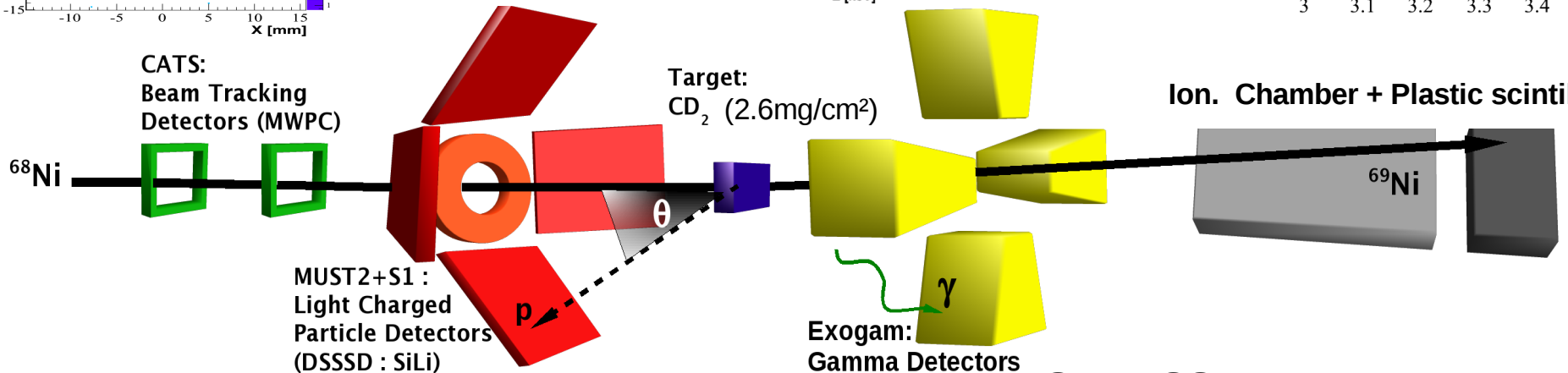

MUST2 : DSSD

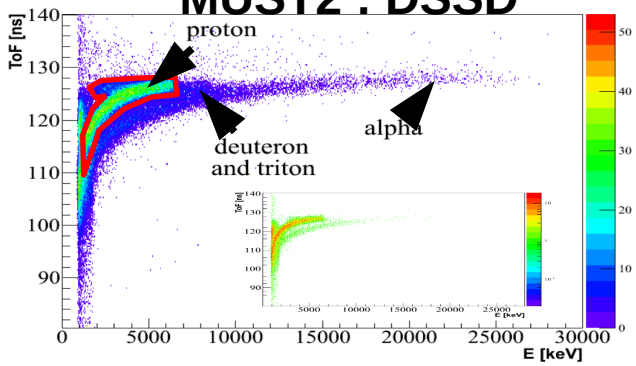

S1 : DSSD

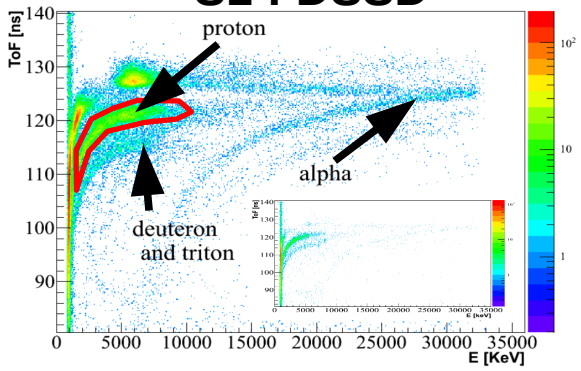

Excitation energy spectrum

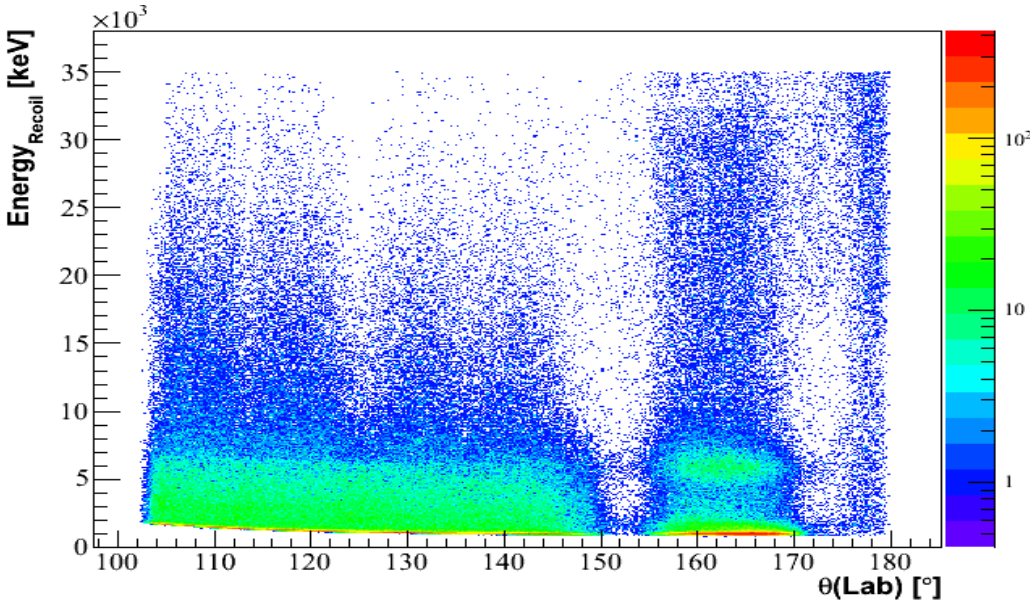

Excitation energy spectrum

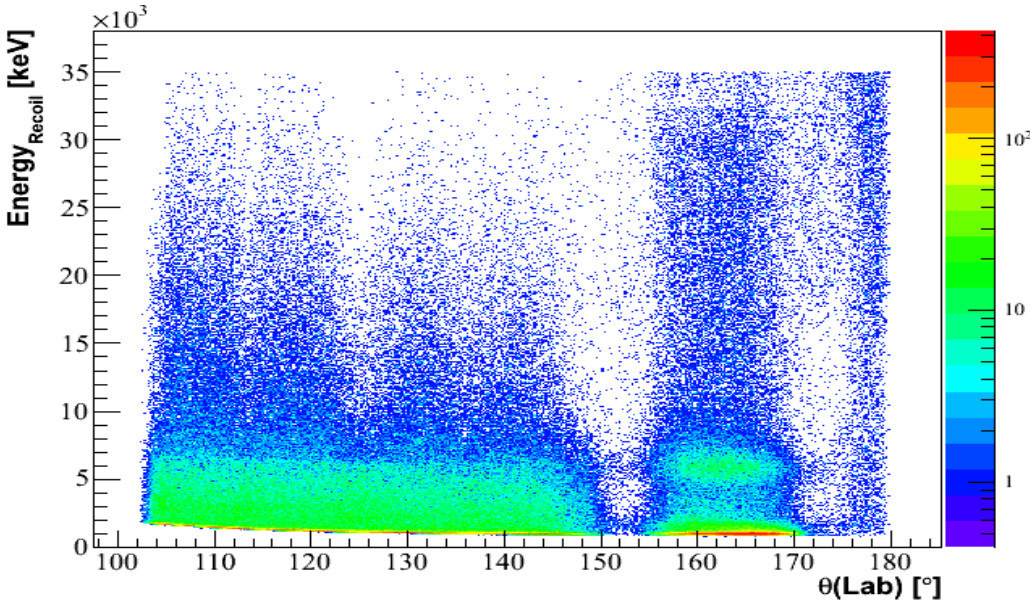

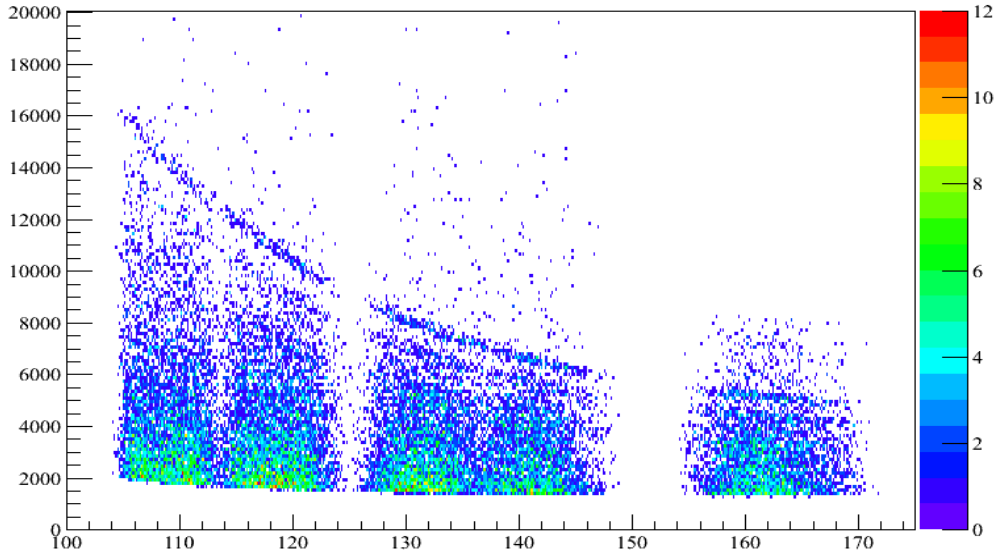

Excitation energy spectrum

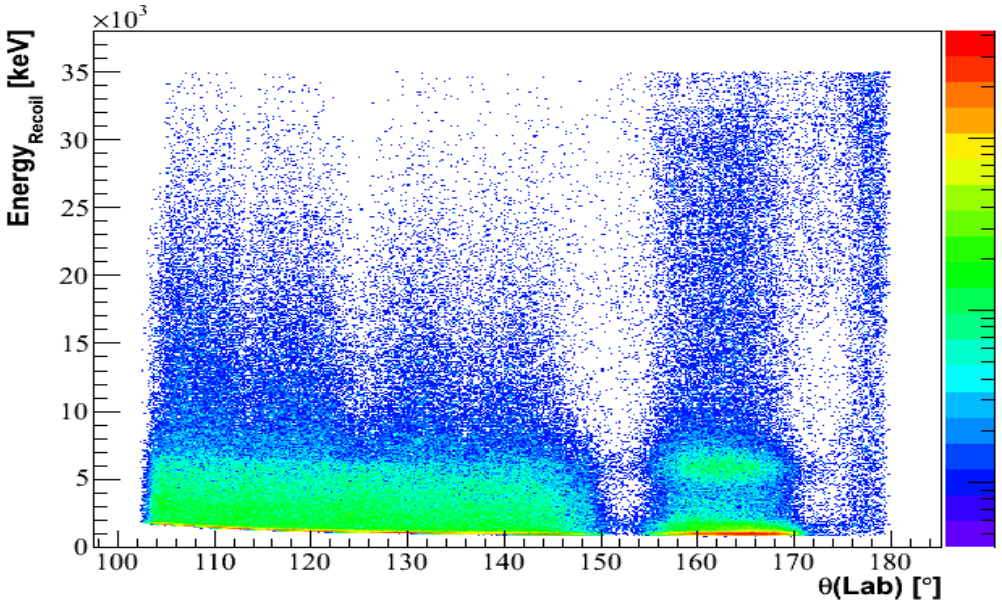

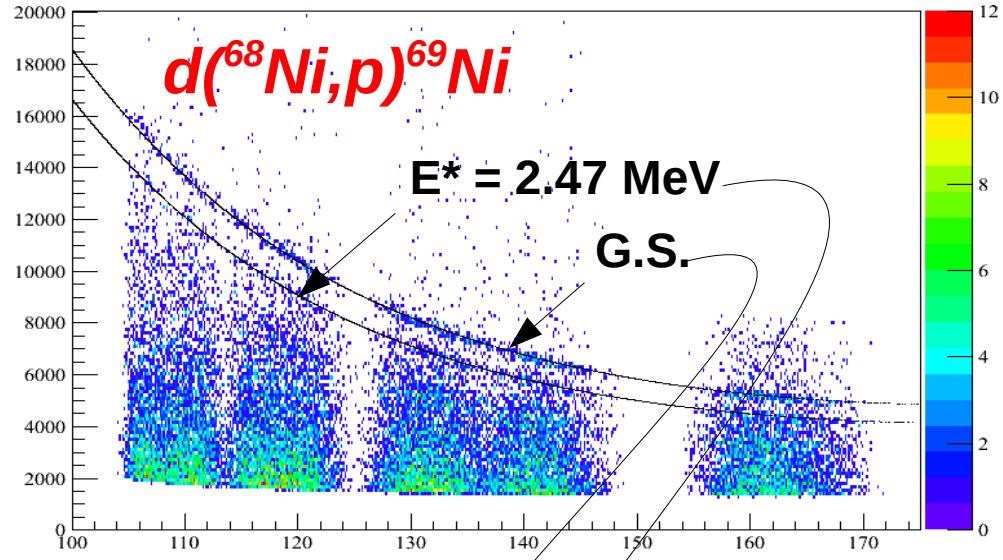

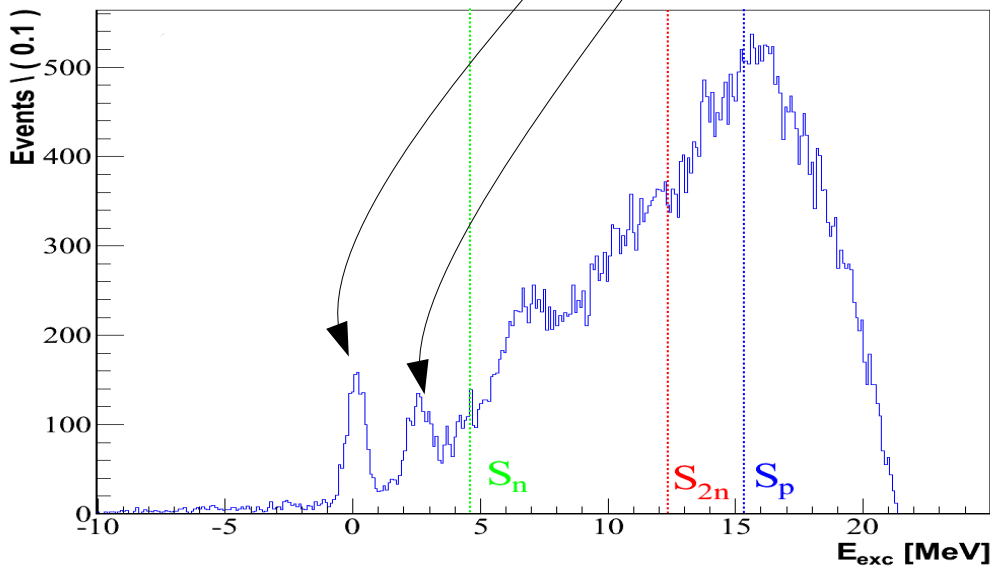

- Pronounced G.S.
- 1st excited state at ~ 2.5 MeV
- Structures ~ 4 MeV
  and 6−7 MeV (> S_n)

Excitation energy spectrum

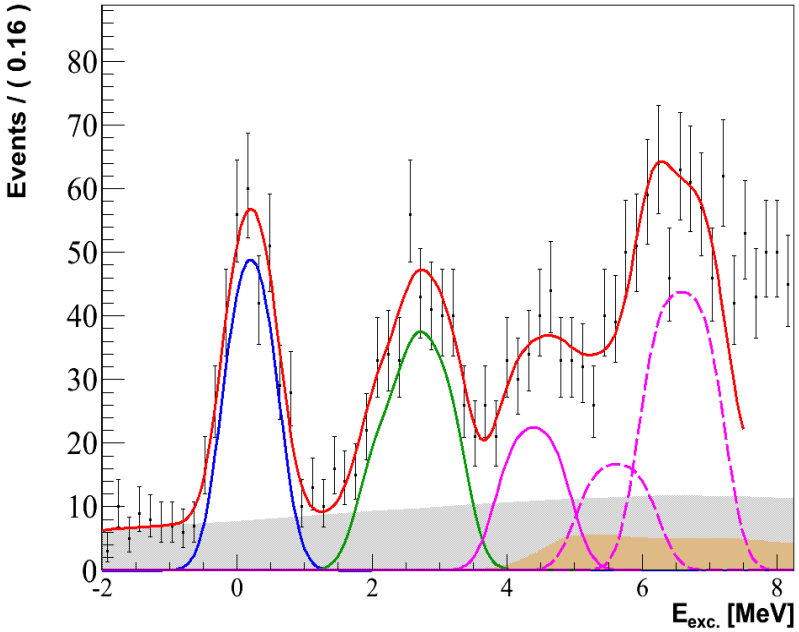

- **Energy reference : S1**
  - 3 bound states
  - 2 resonances
  - Background reactions

Excitation energy spectrum

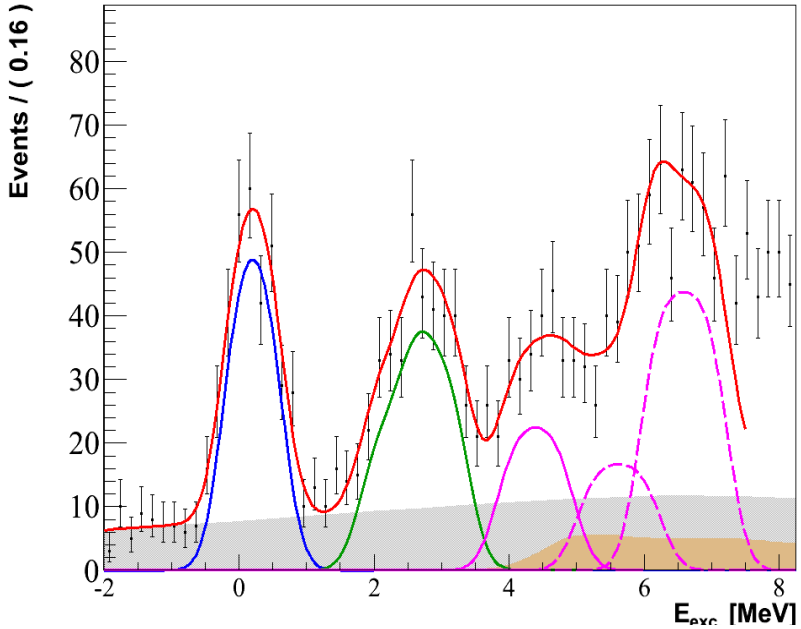

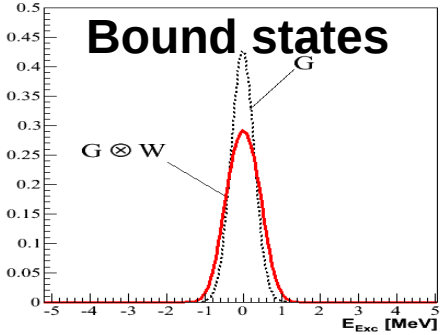

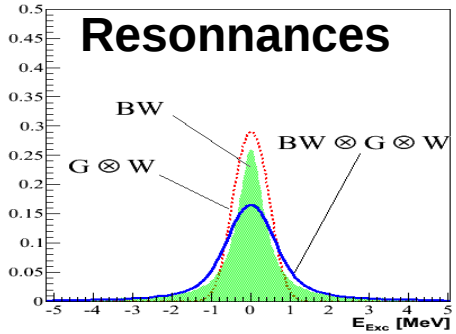

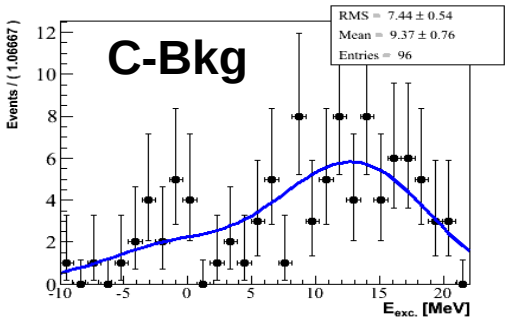

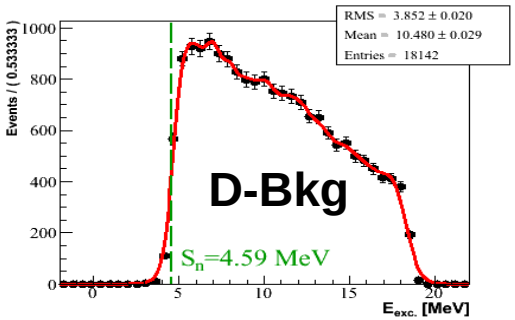

- **Energy reference : S1**
  - 3 bound states
  - 2 resonances
  - Background reactions

- CD2 Target : 2.6mg/cm^2
  $\Rightarrow$ Window function ≡ W
- Bound states : G⊗W
- Resonnances : BW⊗G⊗W

- Carbon Bkg. : pure C Target
- Deuton Bkg. : Simulation
  - Phase-space calculation
- « Kernel estimation » method

Excitation energy spectrum

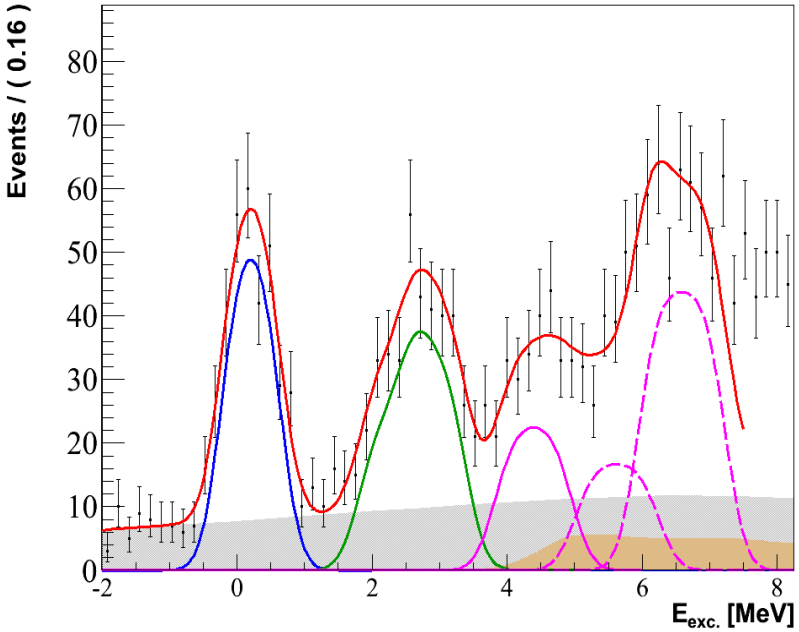

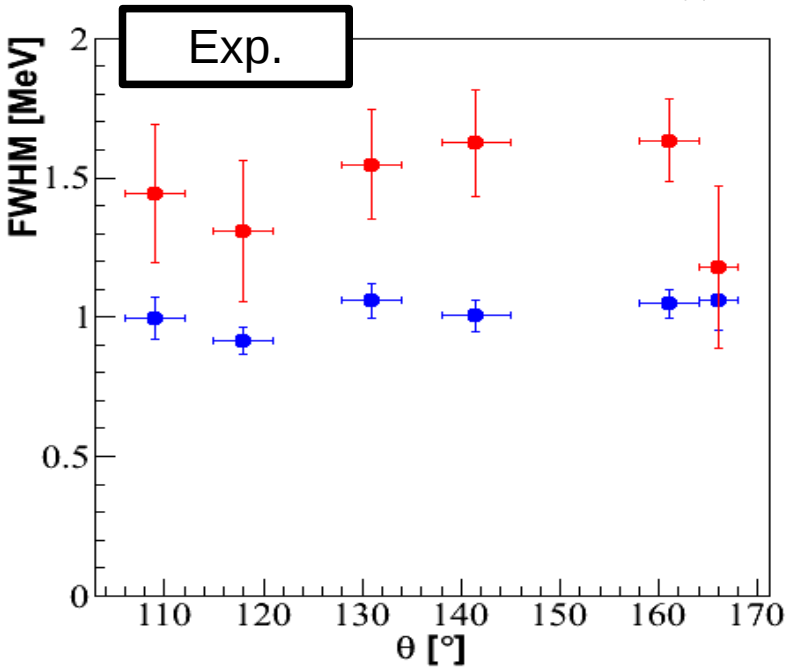

- **Energy reference : S1**
  - 3 bound states
  - 2 resonances
  - Background reactions

Excitation energy spectrum

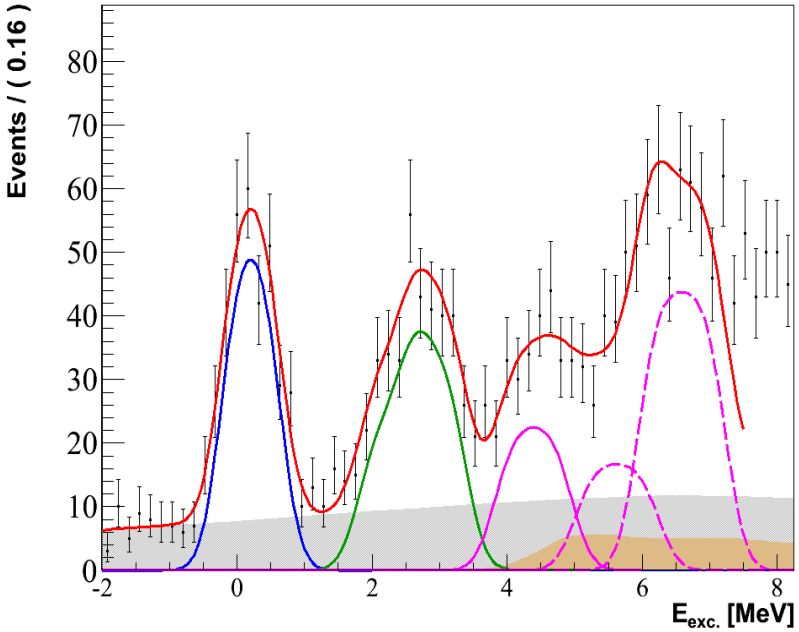

- **Energy reference : S1**
  - 3 bound states
  - 2 resonances
  - Background reactions

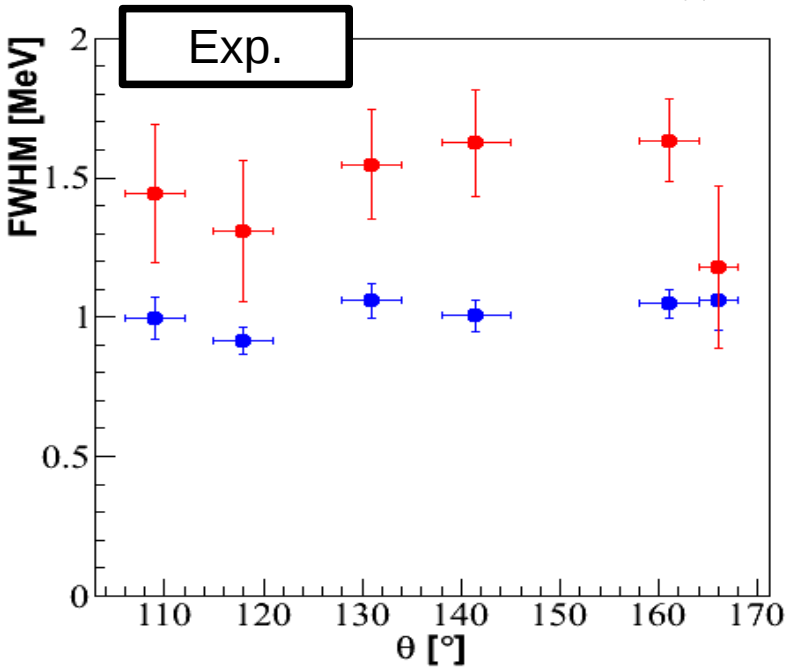

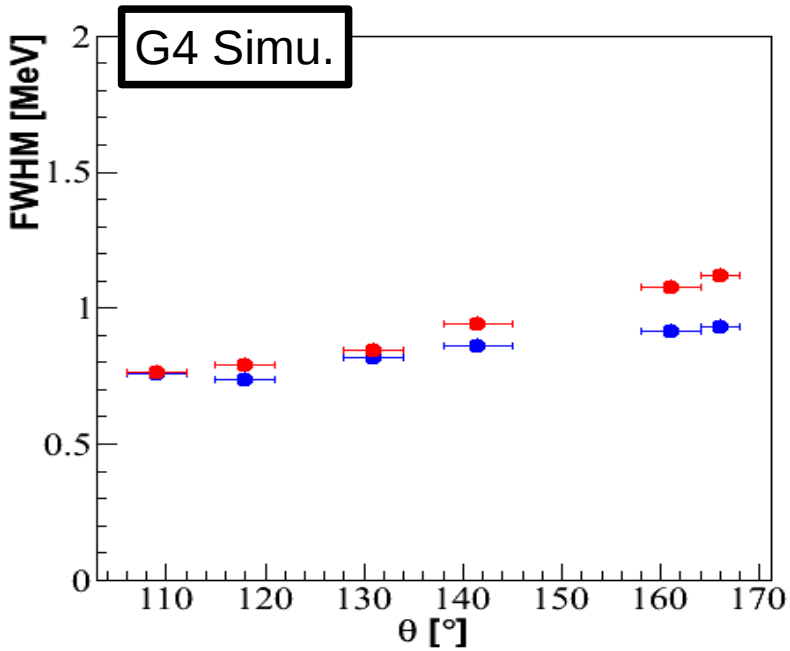

Excitation energy spectrum

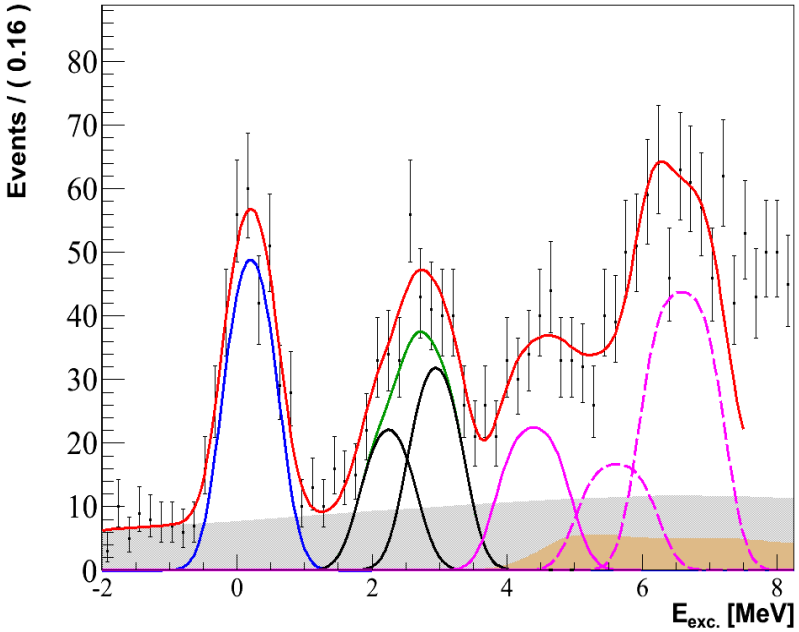

- **Energy reference : S1**
  - 3 bound states
  - 2 resonances
  - Background reactions

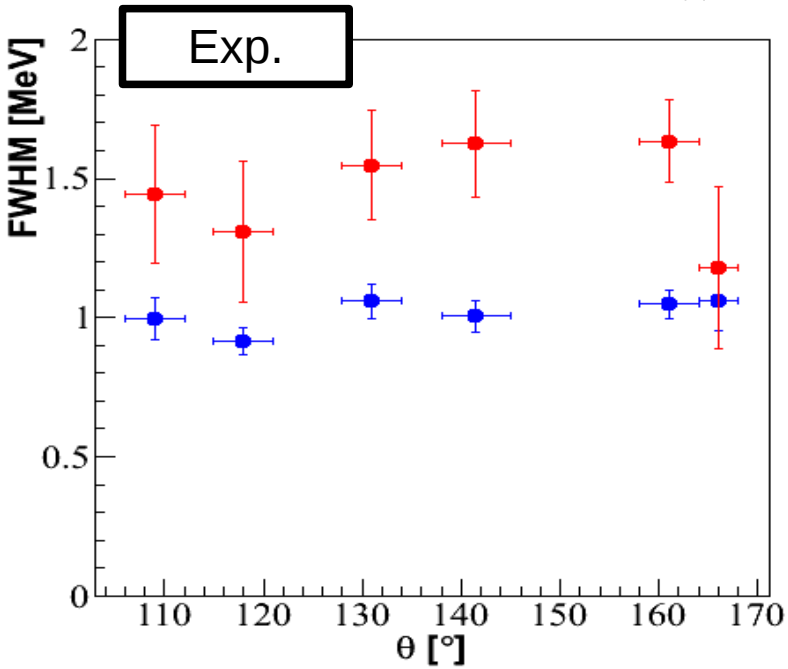

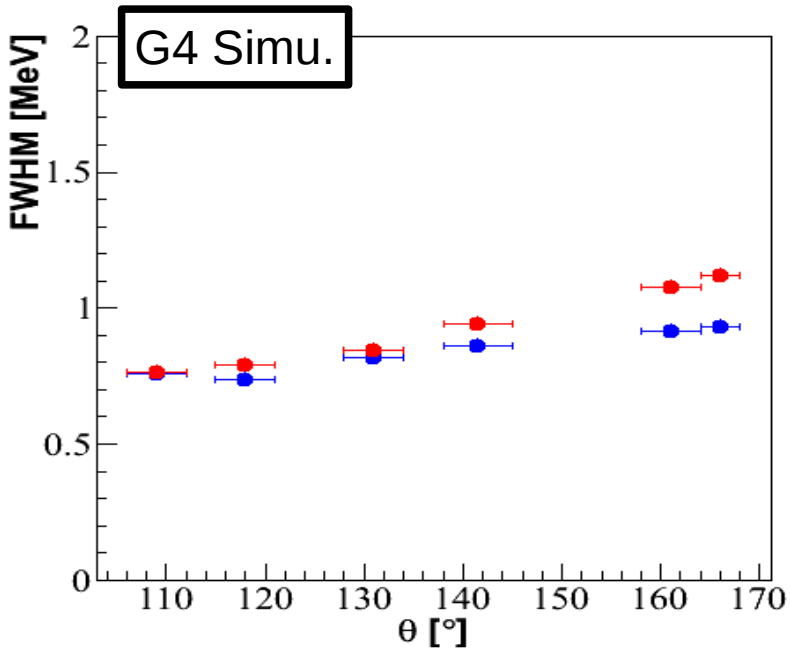

Angular efficiency

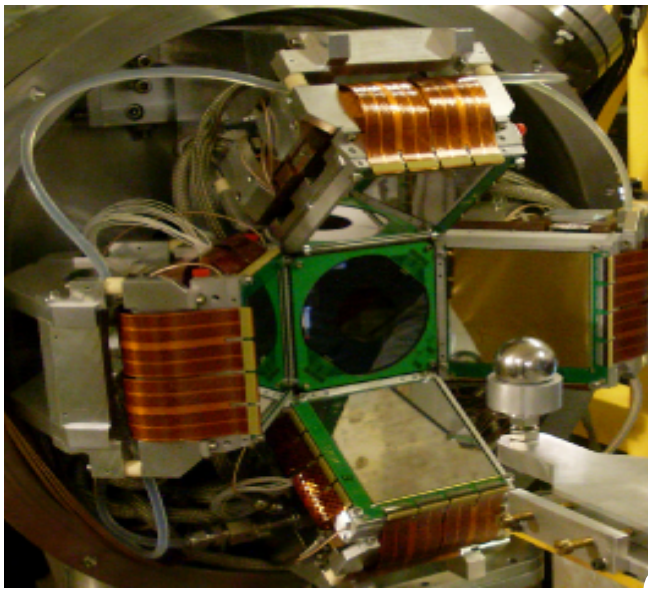

Angular efficiency :

- Detec. Geometry
- Operational strips
- Analysis method

  ⇒ Simulation

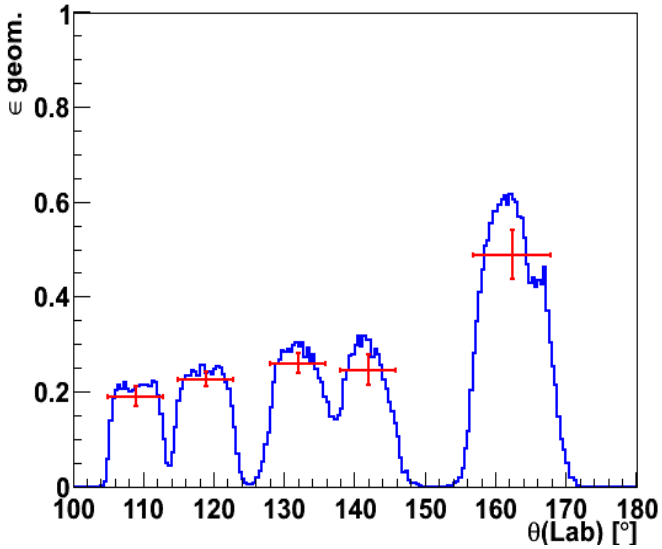

Angular efficiency

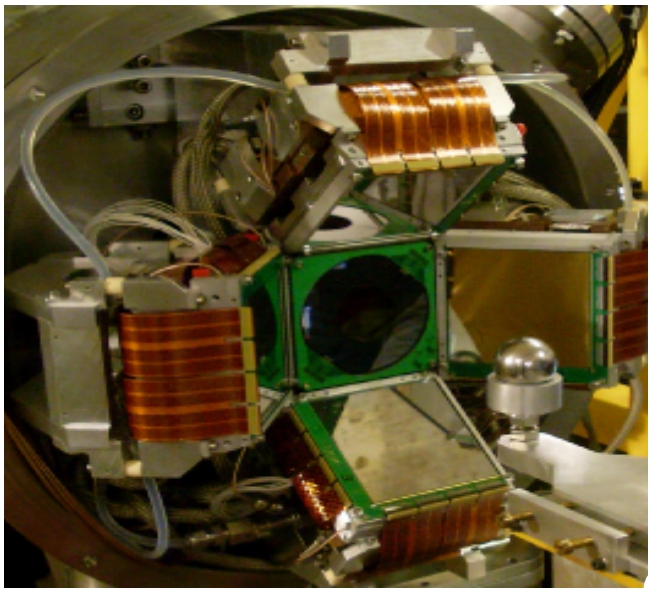

Angular efficiency :
- Detec. Geometry
- Operational strips
- Analysis method
  ⇒ Simulation

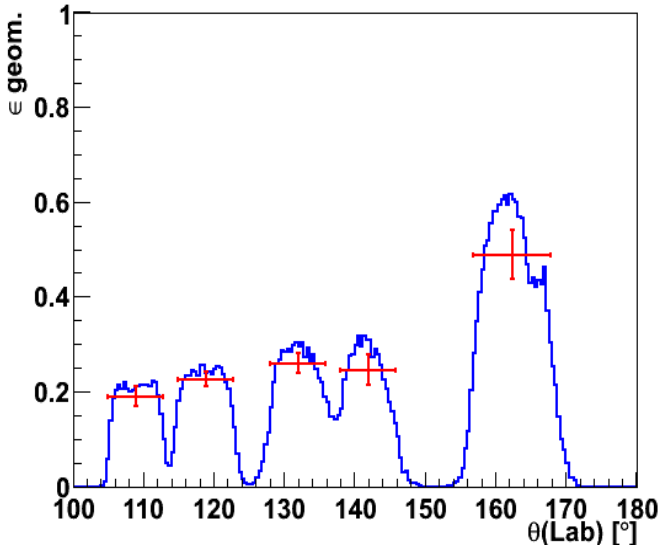

$$\frac{d\sigma}{d\Omega}(\theta_{Lab}) = \frac{N_{det}(\theta_{Lab})\ (1+\epsilon_{temps\,mort})}{N_{faisceau}\ N_{Cible}\ \Delta\Omega(\theta_{Lab})\ \epsilon_{MUST2,S1}}$$

$$\frac{d\sigma}{d\Omega}(\theta_{CM}) = Jacob.(\theta_{Lab})\ \frac{d\sigma}{d\Omega}(\theta_{Lab})$$

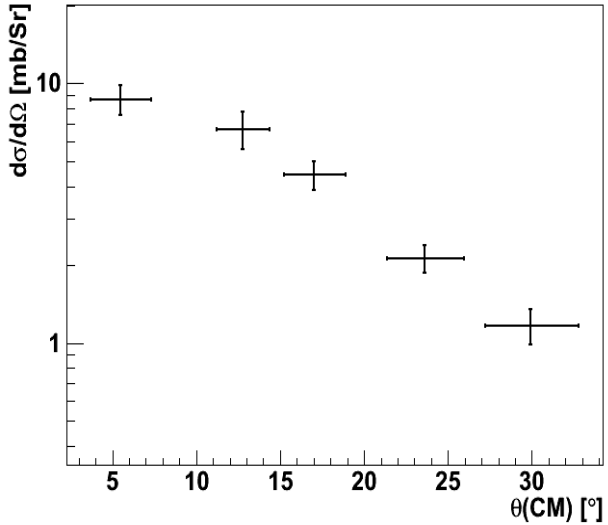

Analysed differential cross sections

CH89 (ADWA) ⊗ KD03

SF = 0.53 ± 0.13

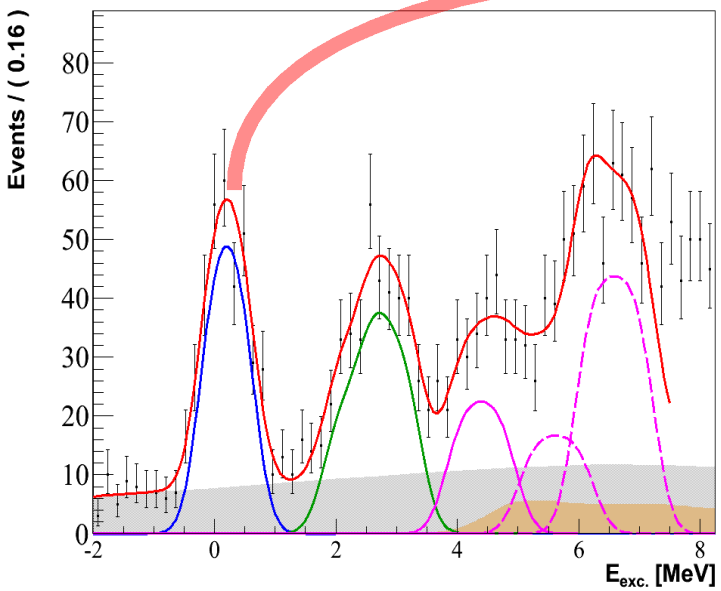

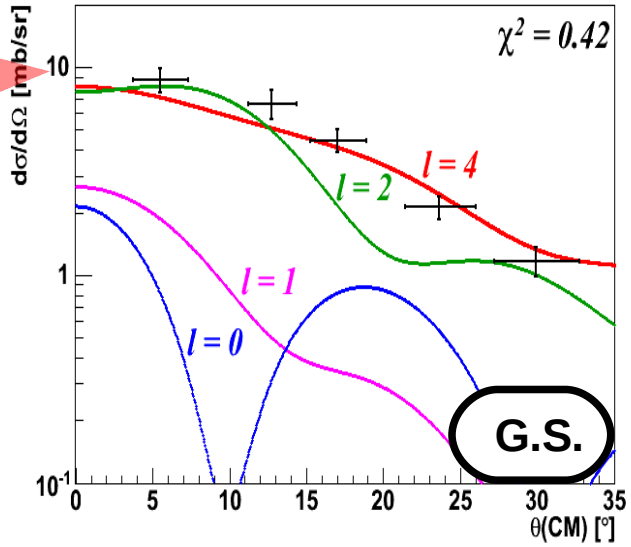

Analysed differential cross sections

CH89 (ADWA) ⊗ KD03

SF = 0.53 ± 0.13
SF = 0.86 ± 0.22

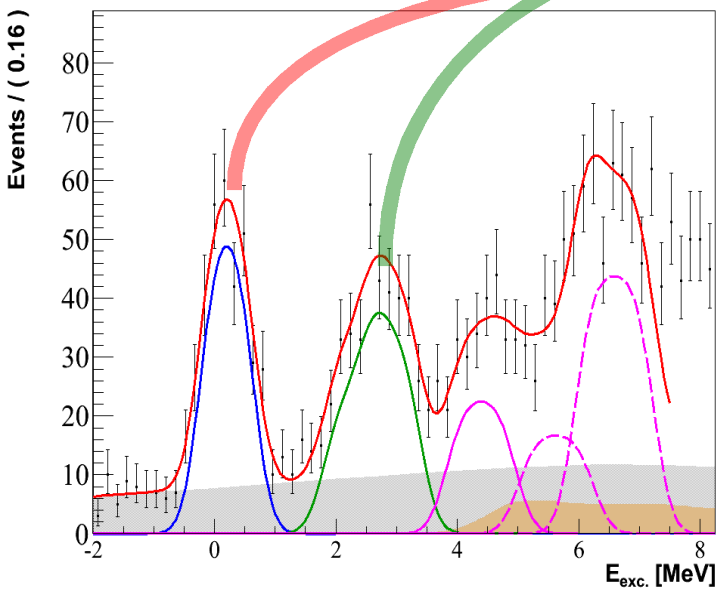

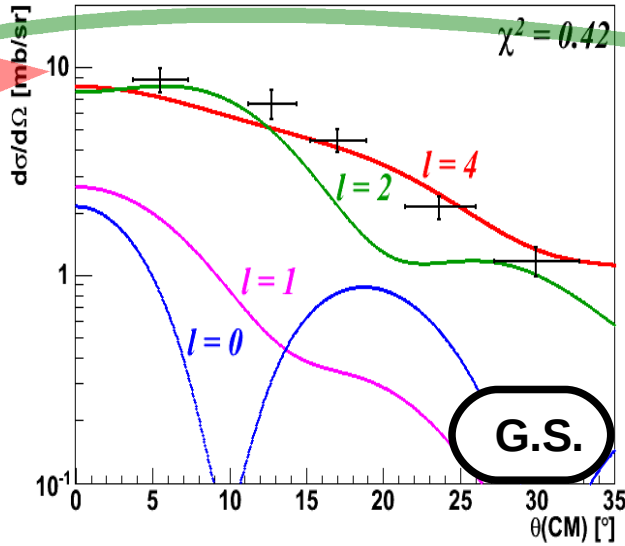

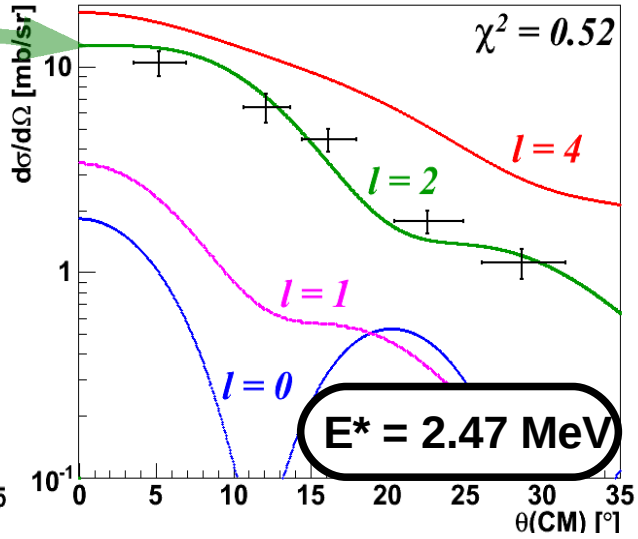

Analysed differential cross sections

CH89 (ADWA) ⊗ KD03

SF = 0.53 ± 0.13
SF = 0.86 ± 0.22

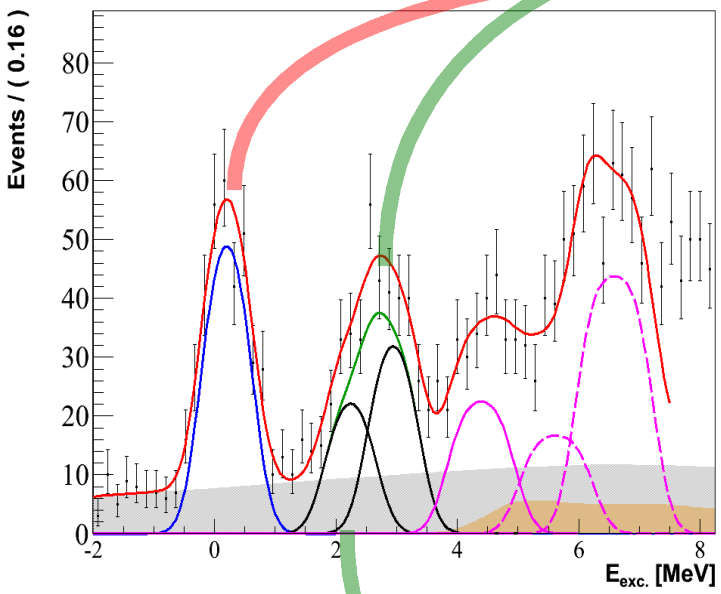

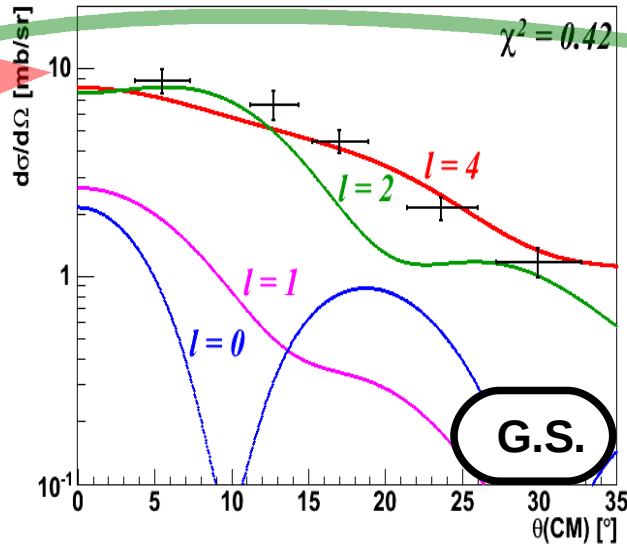

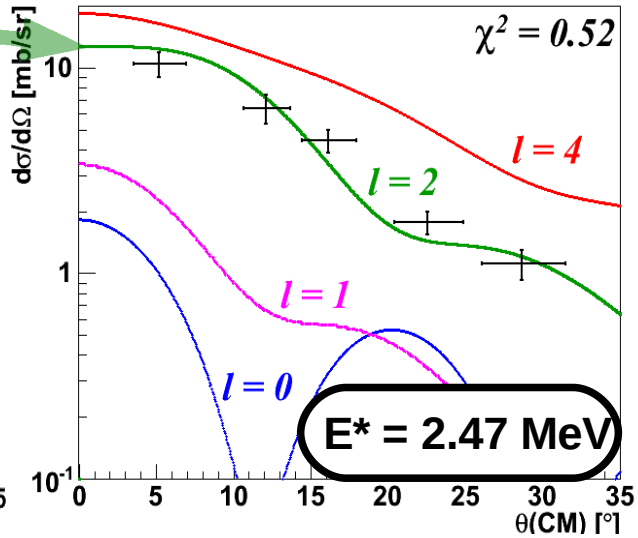

SF = 0.32 ± 0.10

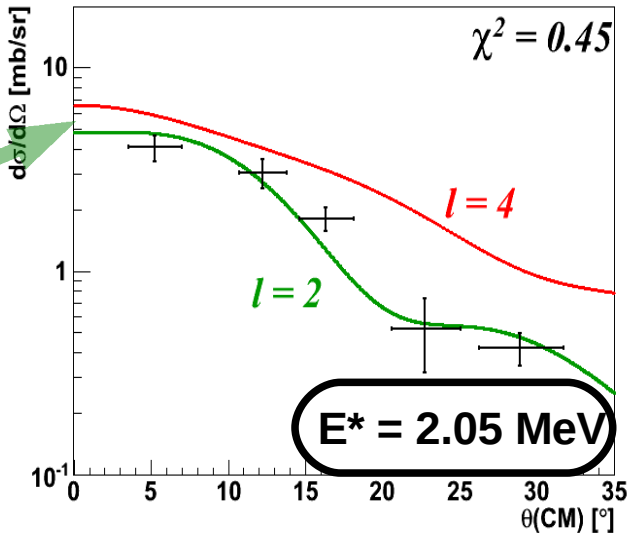

Analysed differential cross sections

CH89 (ADWA) ⊗ KD03

SF = 0.53 ± 0.13
SF = 0.86 ± 0.22

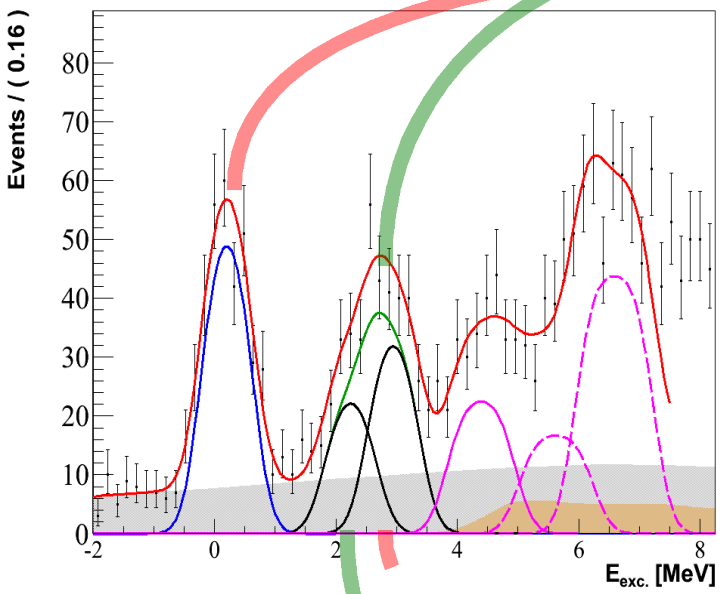

SF = 0.32 ± 0.10
SF = 0.21 ± 0.06

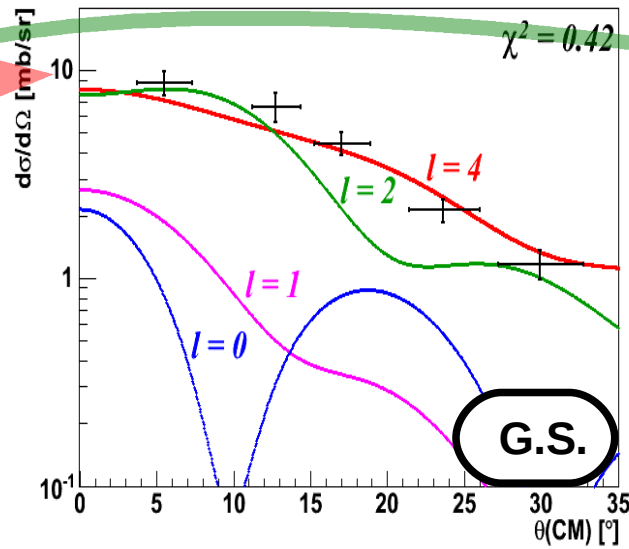

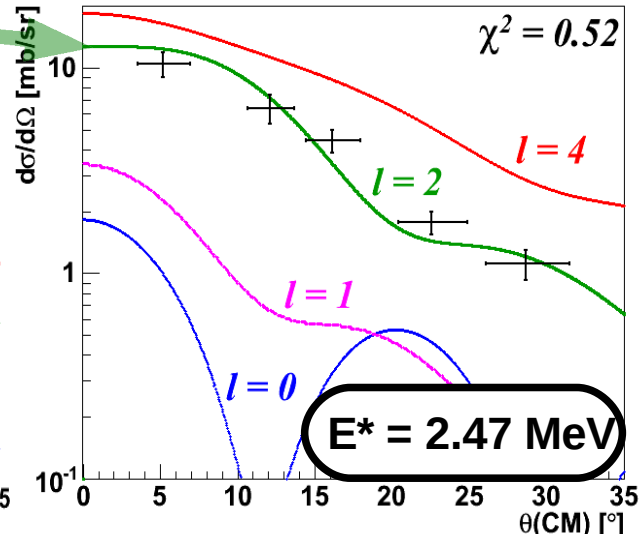

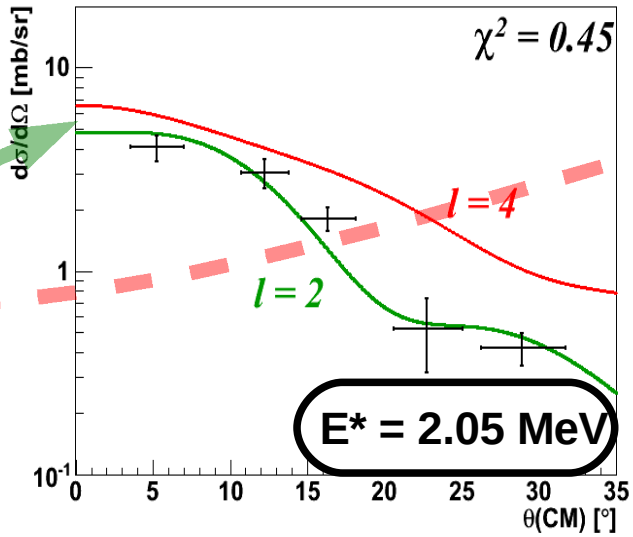

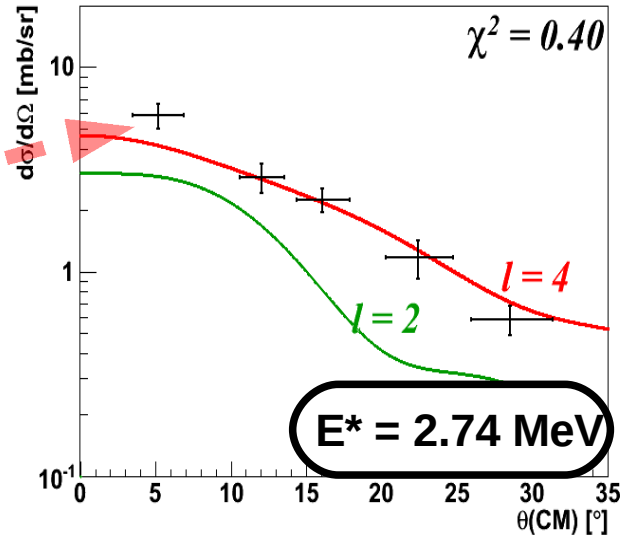

Analysed differential cross sections

CH89 (ADWA) ⊗ KD03

SF = 0.53 ± 0.13
SF = 0.86 ± 0.22

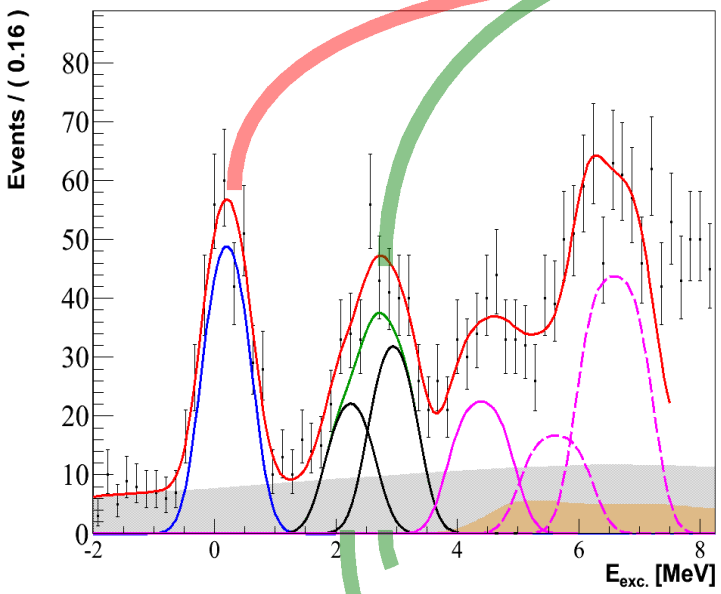

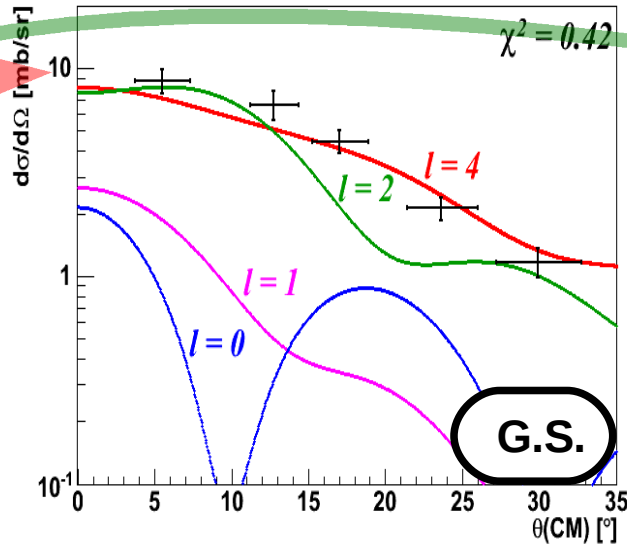

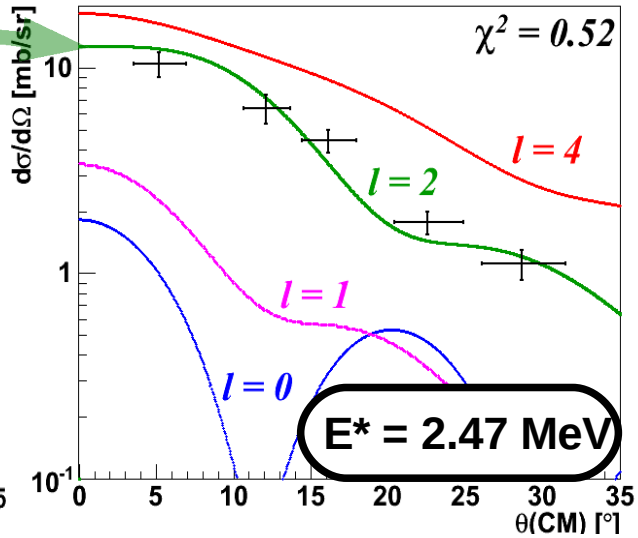

SF = 0.32 ± 0.10
SF = 0.44 ± 0.13

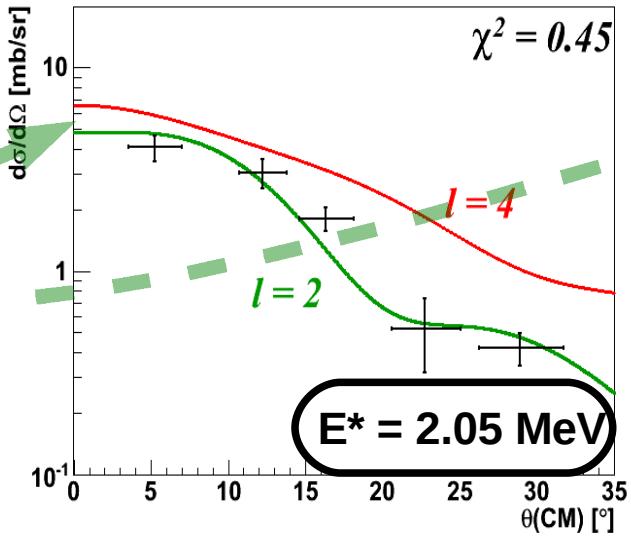

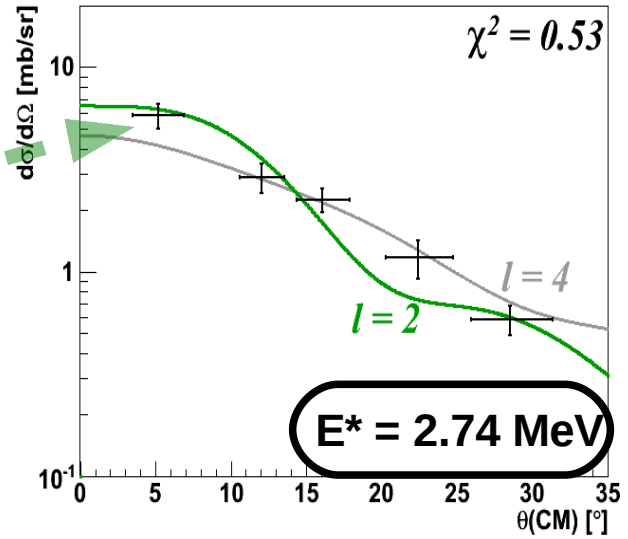

Shell-model calculations

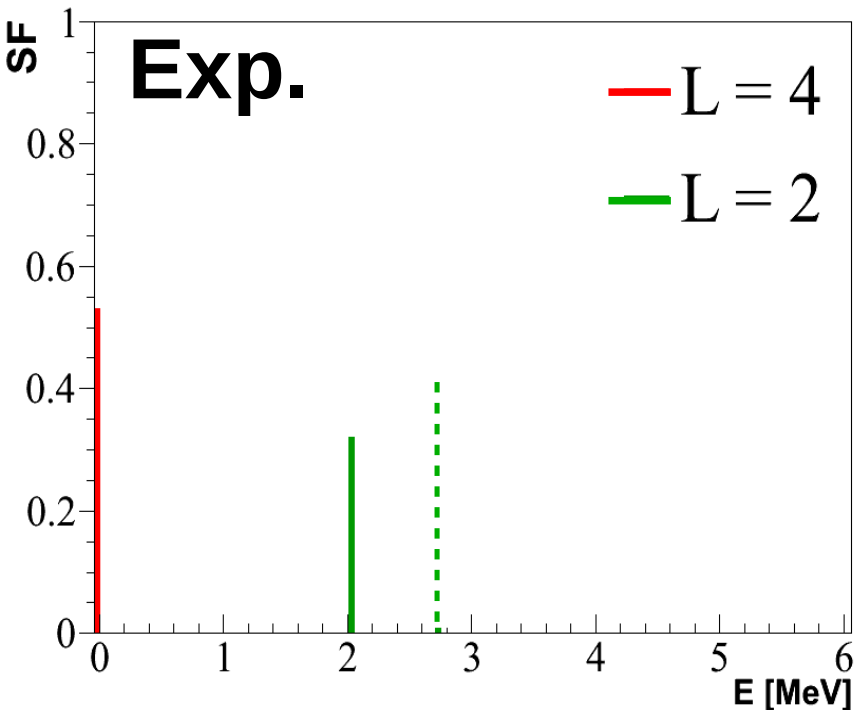

- Interaction LNPS
  Lenzi et al., PRC 82, 054301, 2010
- fp shell + {$1g_{9/2}$,$2d_{5/2}$}

Shell-model calculations

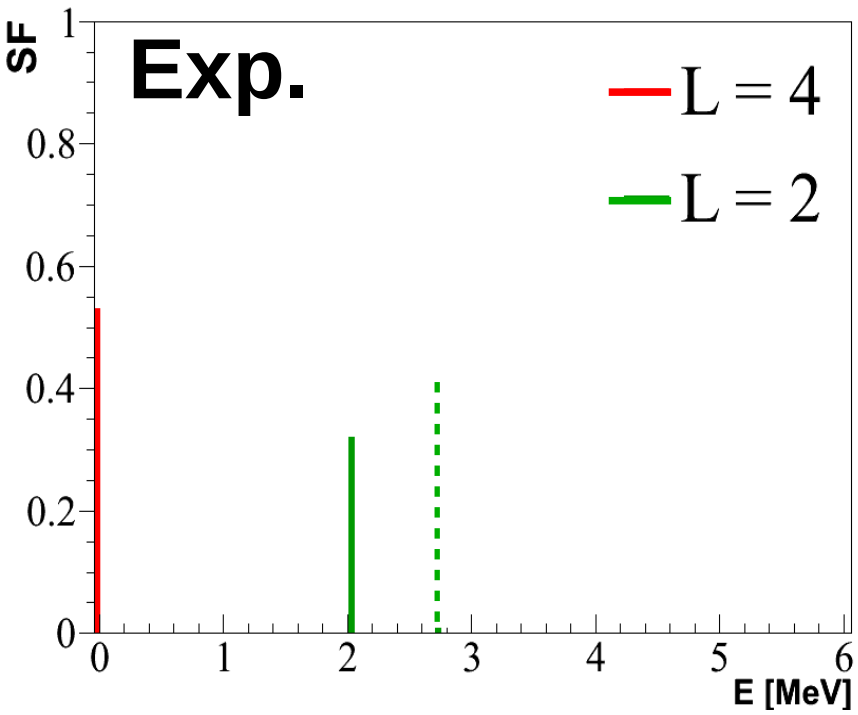

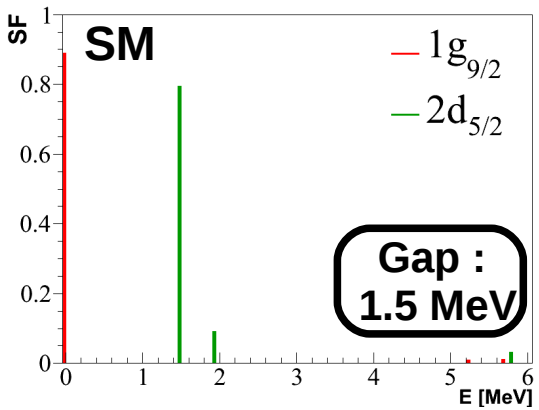

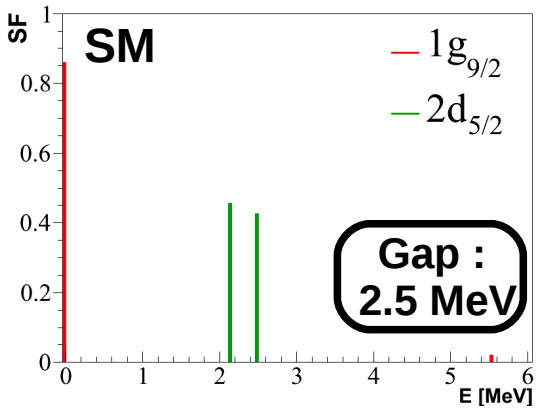

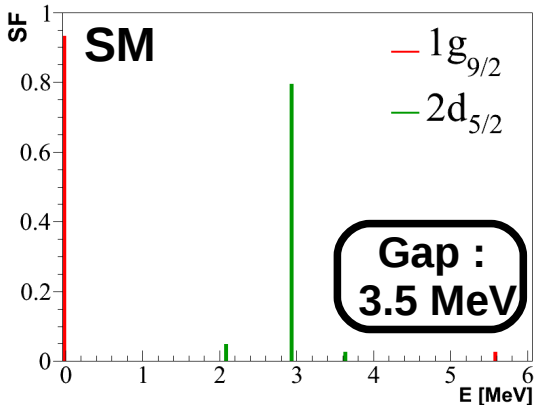

- Interaction LNPS
  Lenzi et al., PRC 82, 054301, 2010
- fp shell + {$1g_{9/2}$,$2d_{5/2}$}

Shell-model calculations

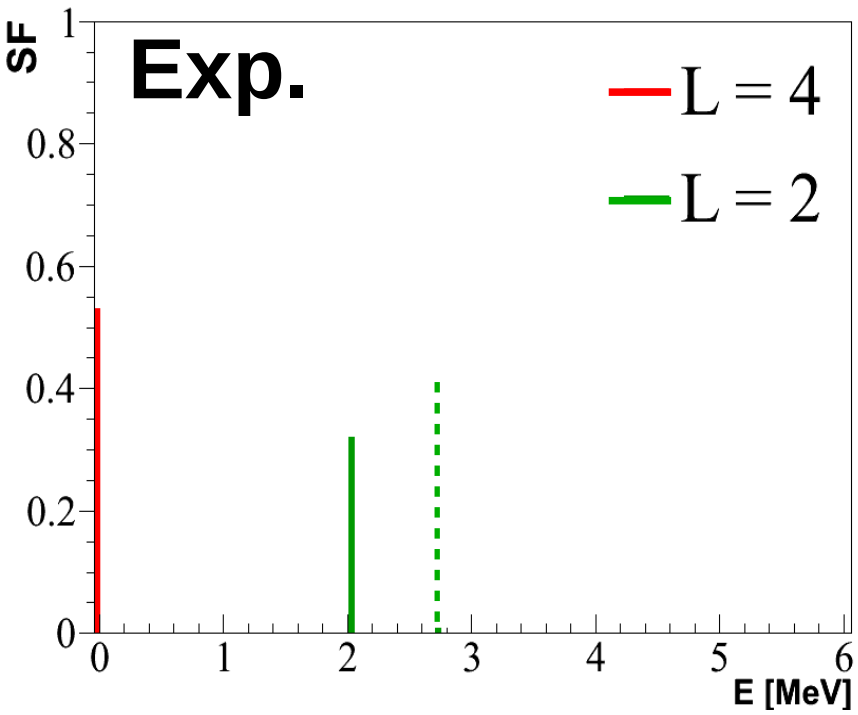

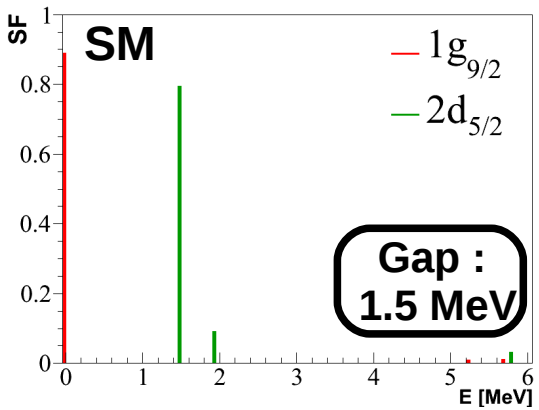

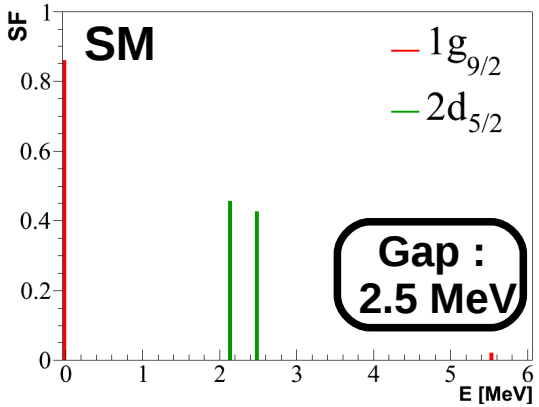

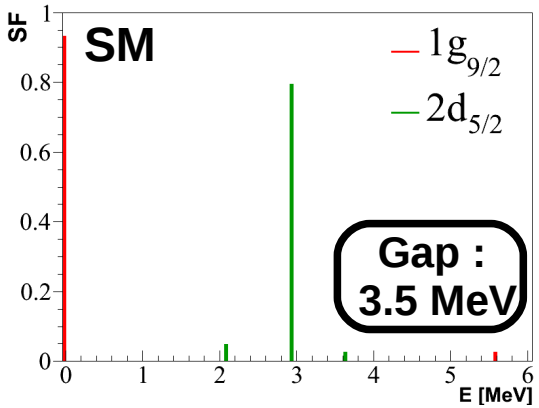

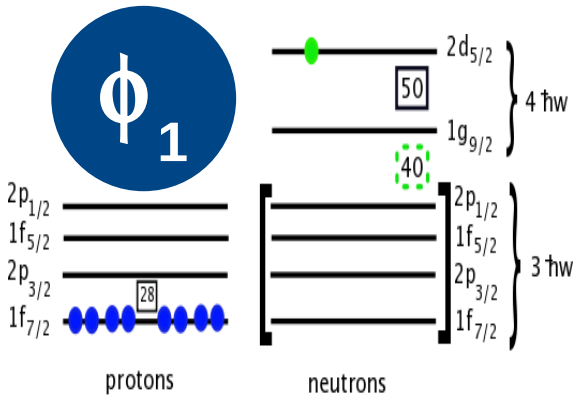

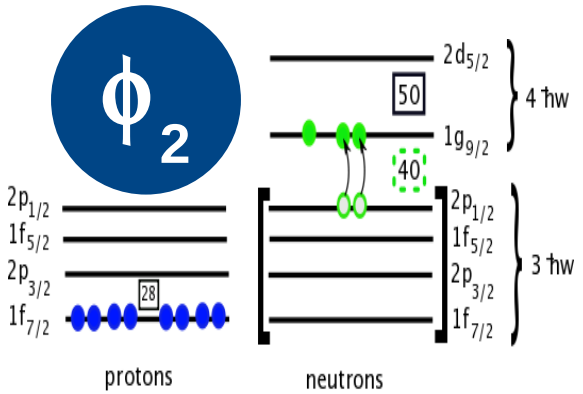

- Interaction LNPS
  Lenzi et al., PRC 82, 054301, 2010
- fp shell + {$1g_{9/2}$,$2d_{5/2}$}

$$\Psi_1 \sim \alpha\,\phi_1 + \beta\,\phi_2$$
$$\Psi_2 \sim -\beta\,\phi_1 + \alpha\,\phi_2$$

Conclusion

- Search for the $2d_{5/2}$ neutron orbital in the ^{69}Ni nucleus,
- Study of the d(^{68}Ni,p)^{69}Ni transfer reaction at GANIL,
- Experimental set-up : CATS/MUST2-S1/Plastic,
- Spin and parity assignement $9/2^+$ for the G.S. and $5/2^+$ for the doublet at 2.47 MeV, with an important spectroscopic factor,
- Identification of a neutron state at E* = 4.2 MeV and two resonances E* > 5 MeV.

- Good agreement with the shell model calculations,
- Validation of the hypothesis on the small energy difference between the $1g_{9/2}$ and $2d_{5/2}$, orbitals playing a major role in **the island of inversion at N = 40.**

- **Data analysis of gamma rays (EXOGAM) for more accurate determination of the excitation energies.**

Collaborators

G. Duchêne, D. Curien, F. Didierjean, Ch. Finck, F. Haas, F. Nowacki, J. Piot, K. Sieja
(IPHC - Strasbourg, France)

D. Beaumel, S. Giron, F. Hammache, N. de Séréville, S. Franchoo, J. Guillot, Y. Matea, A. Matta, L. Perrot, E. Pllumbi, J. A. Scarpaci, I. Stefan
(IPN - Orsay, France)

G. Burgunder, L. Caceres, E. Clement, B. Fernandez, S. Grevy, J. Pancin, R. Raabe, O. Sorlin, C. Stoedel, J.C. Thomas
(GANIL - Caen, France)

F. Flavigny, A. Gillibert, V. Lapoux, L. Nalpas, A. Obertelli
(SPhN - Saclay, France)

J. Gibelin
(LPC - Caen, France)

K. Kemper
(Florida State University, USA)

M. Harakeh
(GSI - Darmstadt, Germany)

Back up

Island of inversion at N = 40 : Deformation in Fe

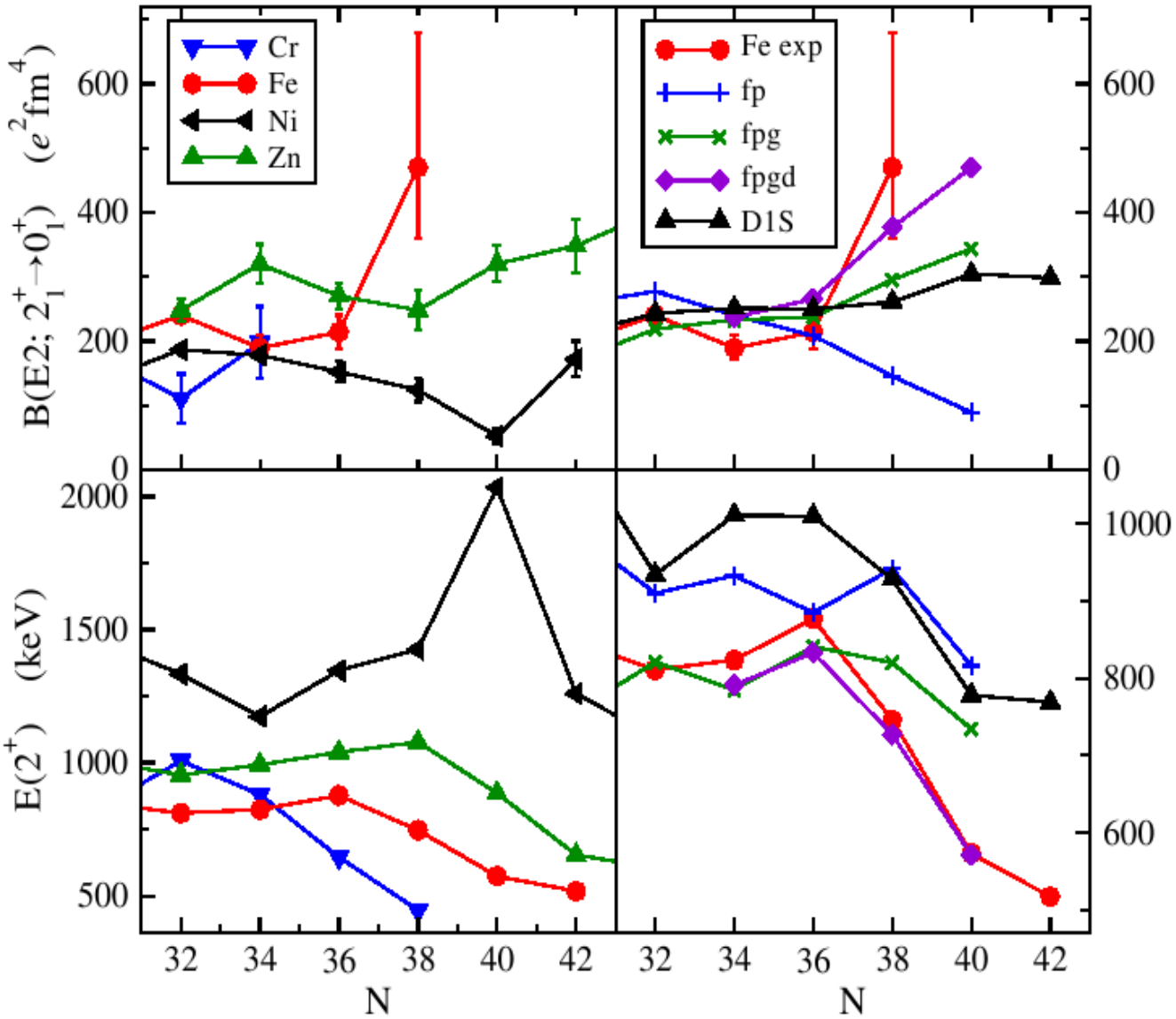

Ljungval et al. Physical Review C 81 (2010) 061301

- **fp**
- **fp + 1g9/2**
- **fp + 1g9/2 + 2d5/2**

Island of inversion - N=20 and N=40

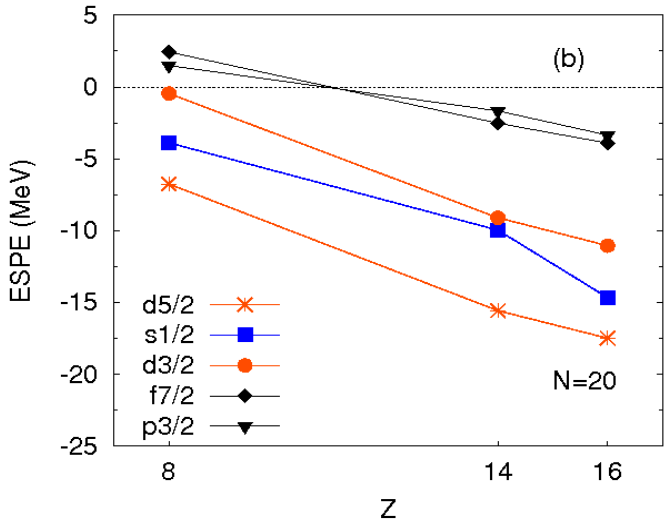

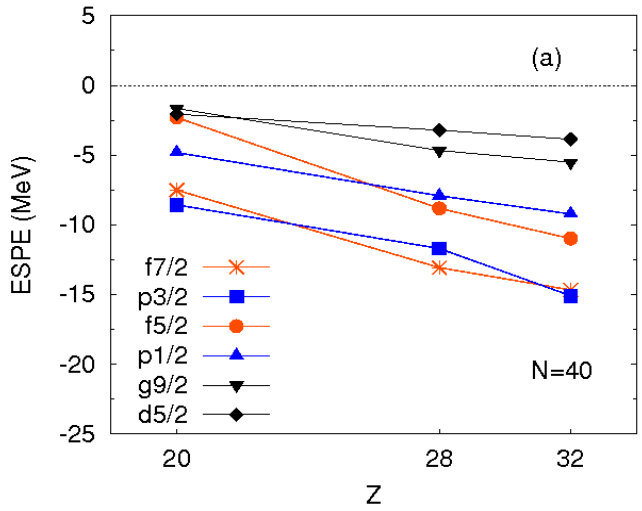

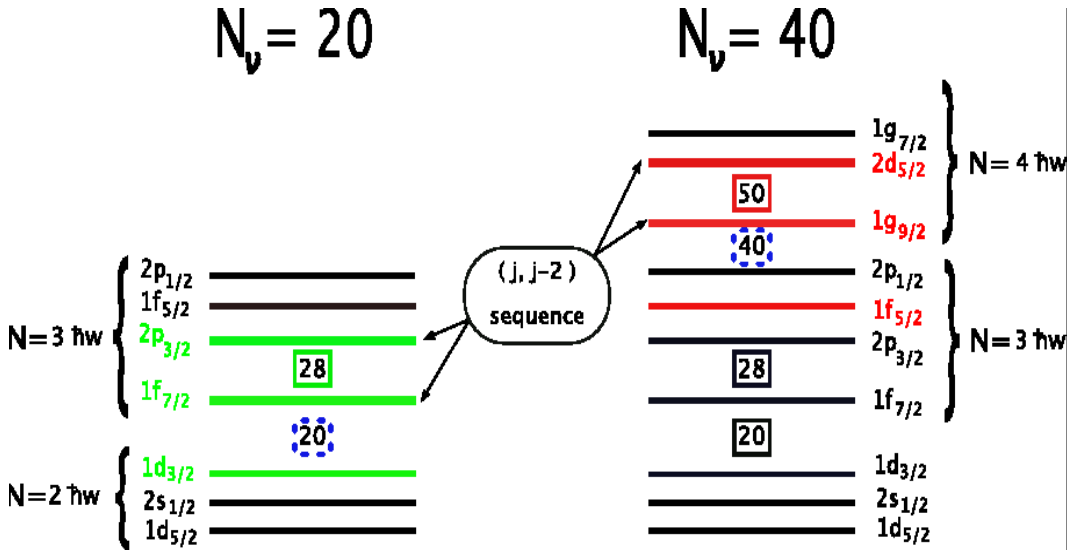

Experimental setup : Inverse kinematics

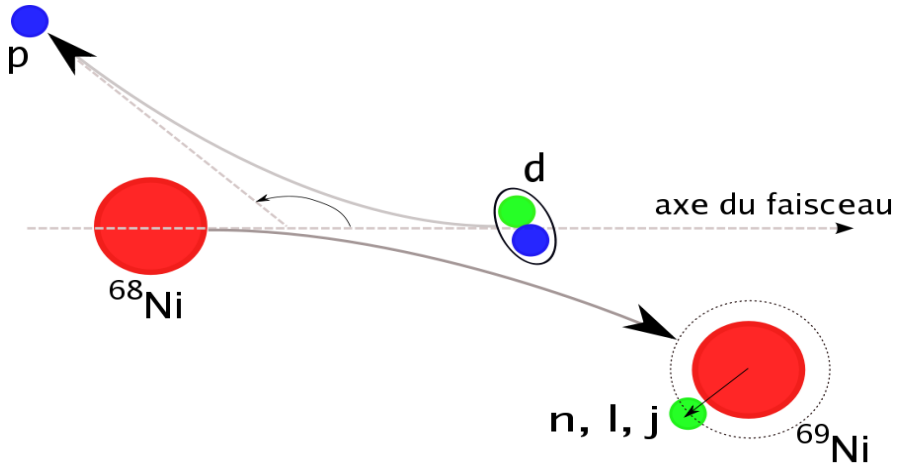

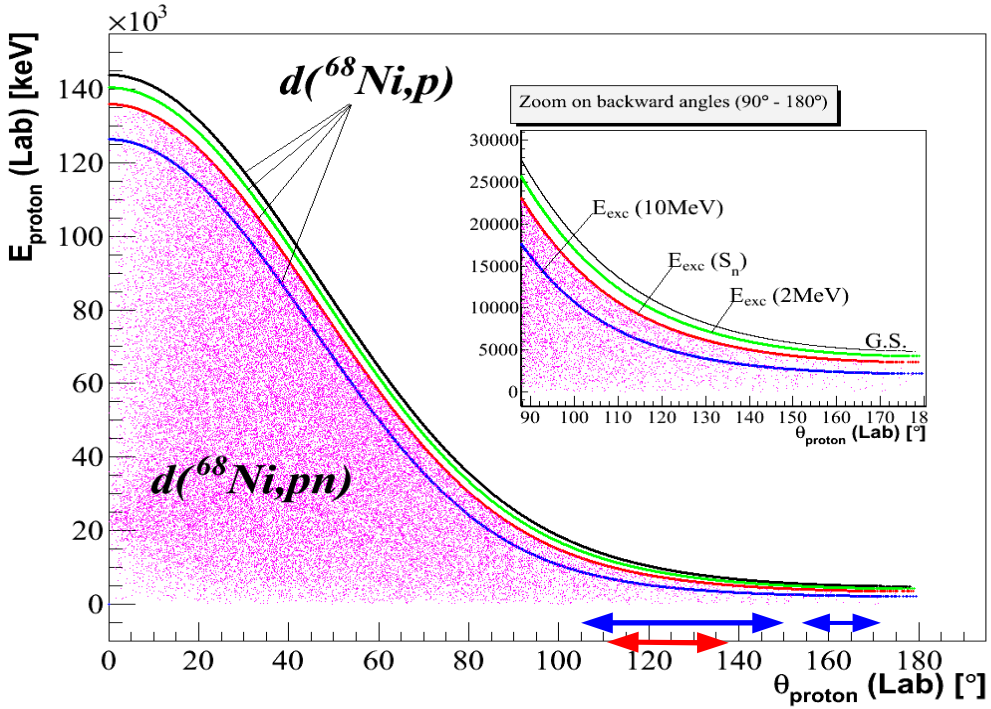

^{68}Ni (T = 29s)

⇒ Inverse kinematics

Forward CM angles

⇔

Backward lab angles

Interesting angular range :

12° - 30° (CM) ⇔ 110° - 140° (Lab.)

Kinematic lines

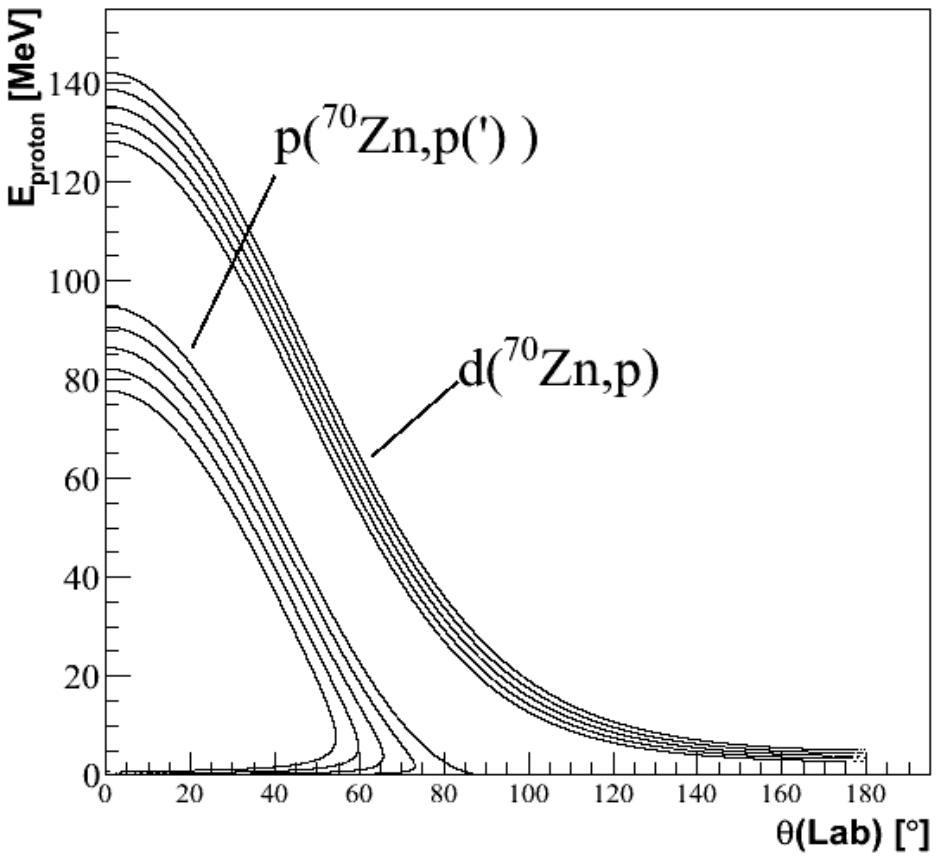

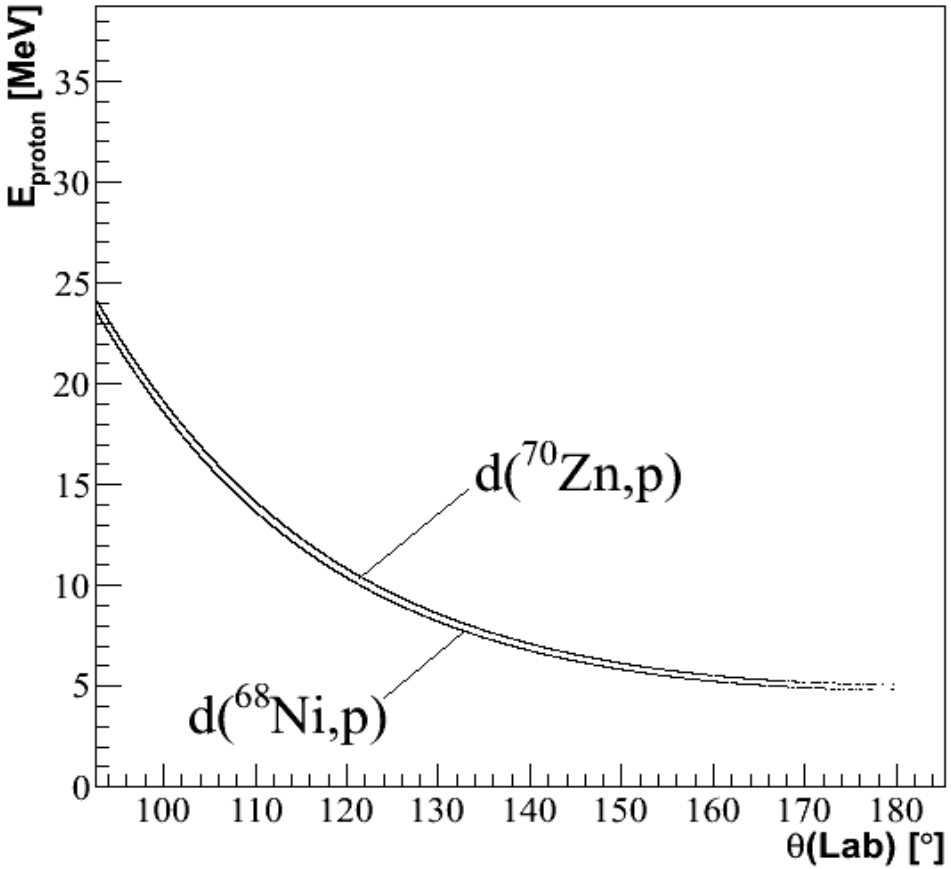

Variation of E_{exc} with respect to proton's energy and angle of emission

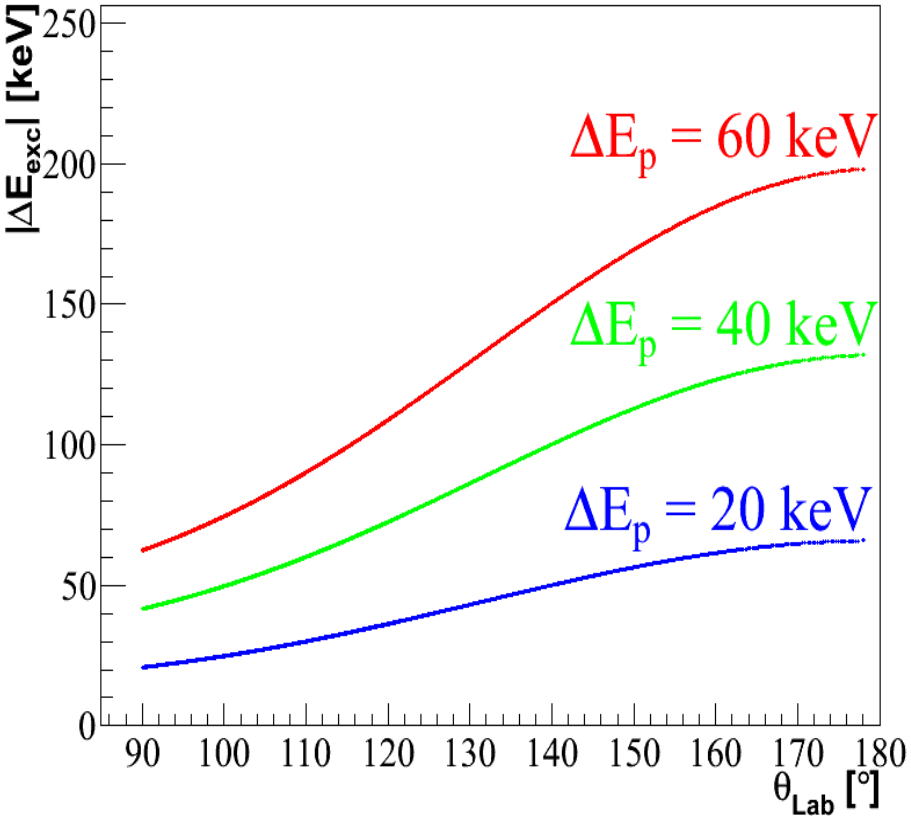

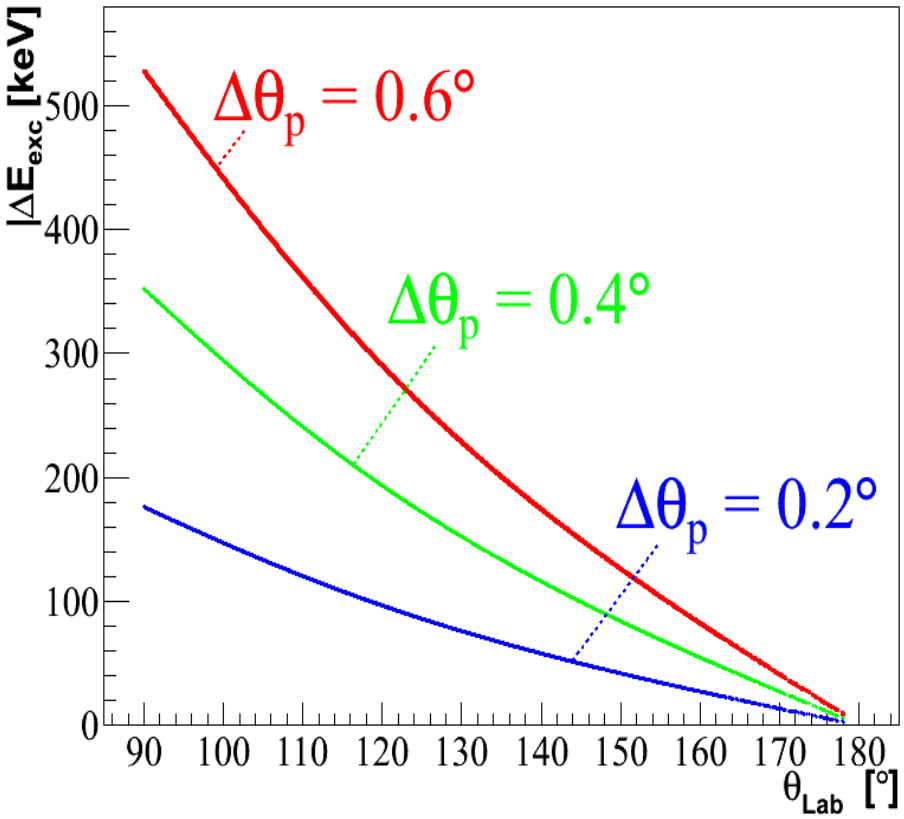

Beam trackers : CATS

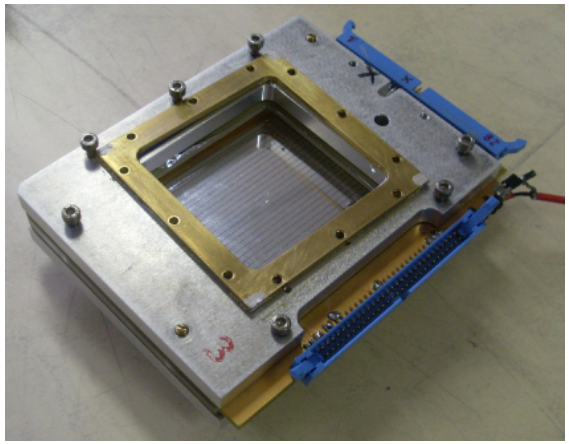

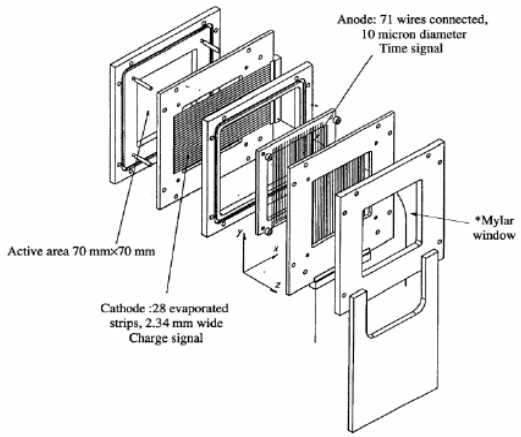

(Ottini-Hustache et al., NIM A, 431, 476, 1999)

- Event by event Reconstruction
- Reconstruction algorithms:
  - Center of gravity
  - **Analytical fit**
- Uncert. ~ 0.65mm (X)
  ~ 0.40 mm (Y)
- Uncert. on incidence angle
  ~ 0.1°
- CATS2 : Time of flight stop signal

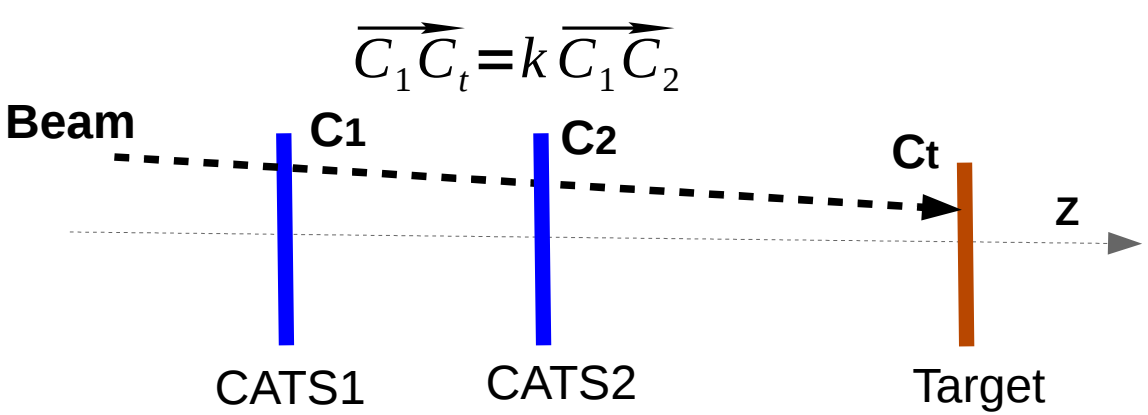

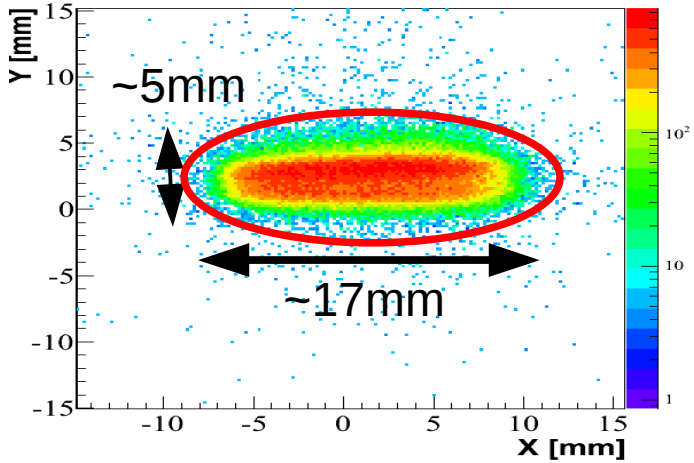

Beam reconstruction
In the target plane

(Ottini-Hustache et al., NIM A, 431, 476, 1999)

Light charged particle detectors : MUST2 and S1

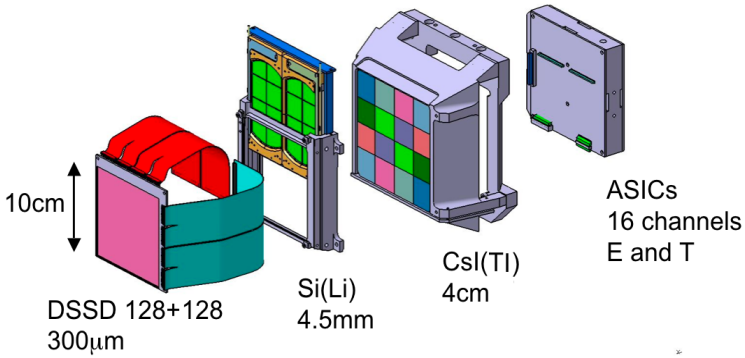

Pollaco et al., NIM A, 25, 287, 2005

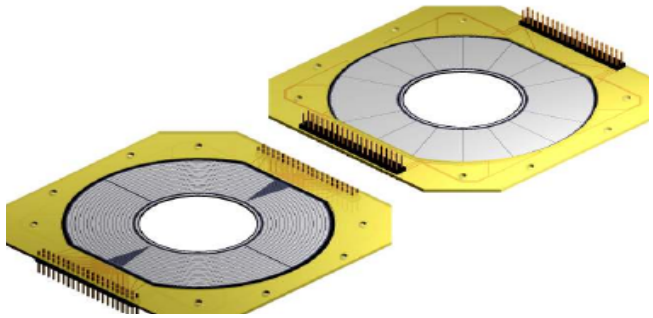

Micron semi-conductors

- DSSD (300 μm)and Si(Li) (4.5 mm)
- Active surface: 100mm*100mm
- 128 strips in X and Y (0.76 mm)

- DSSD (500 μm)
- Active surface : 53mm²
- 64 strip θ, 16 sectors ϕ

MUST2 : DSSD

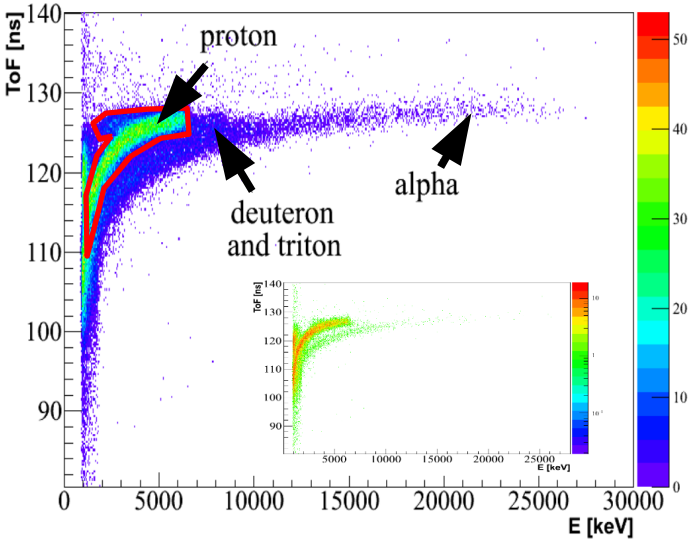

MUST2 : Si(Li)

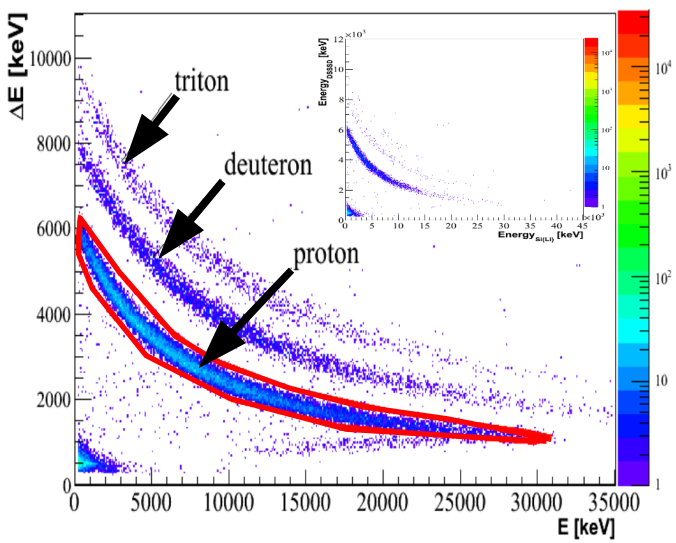

S1: DSSD

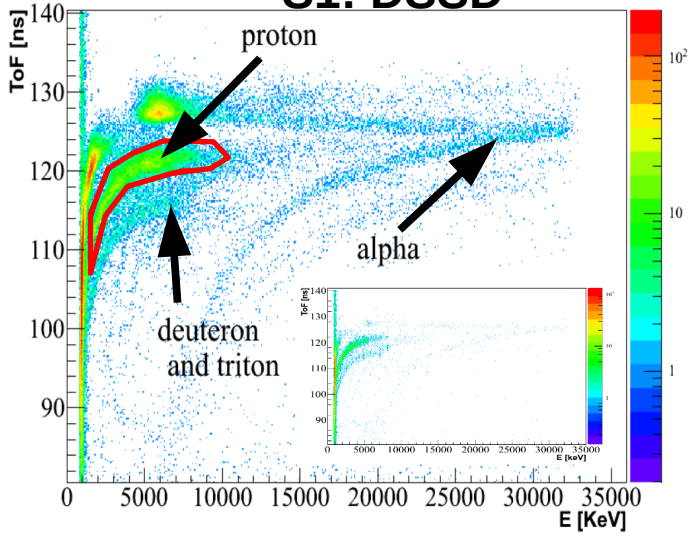

Heavy residue detector

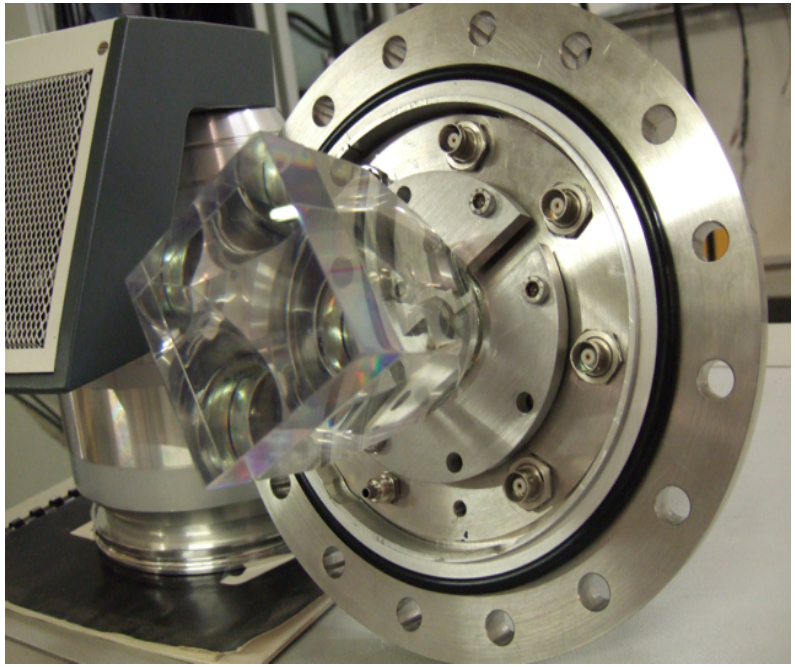

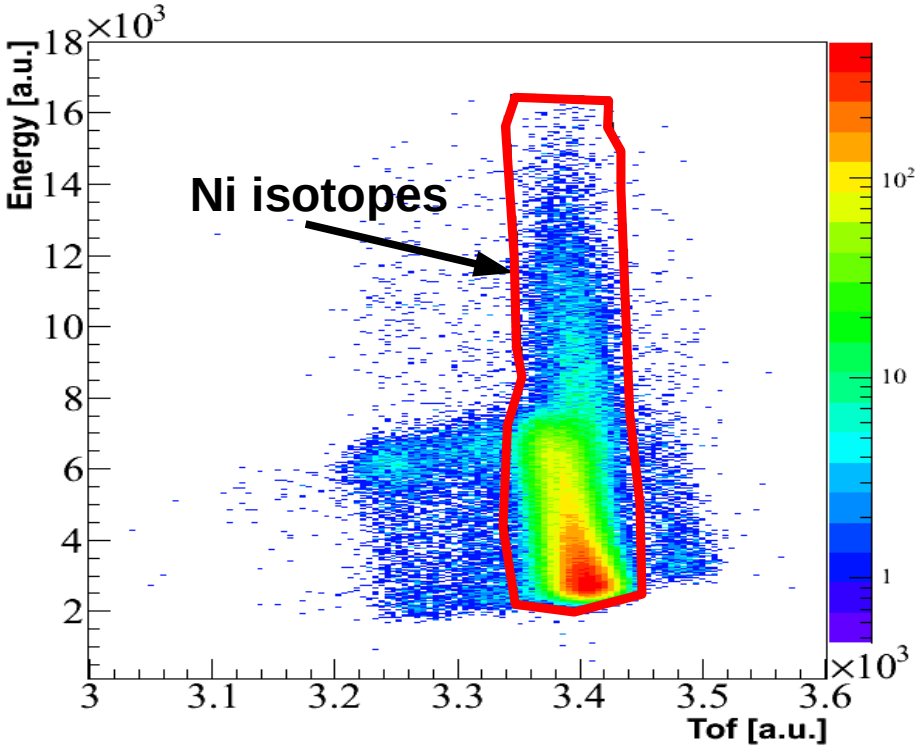

- Plastic scintillator
- Active surface : 60mm*60mm
- Energy and time (ToF)

LISE (D4) beam identification

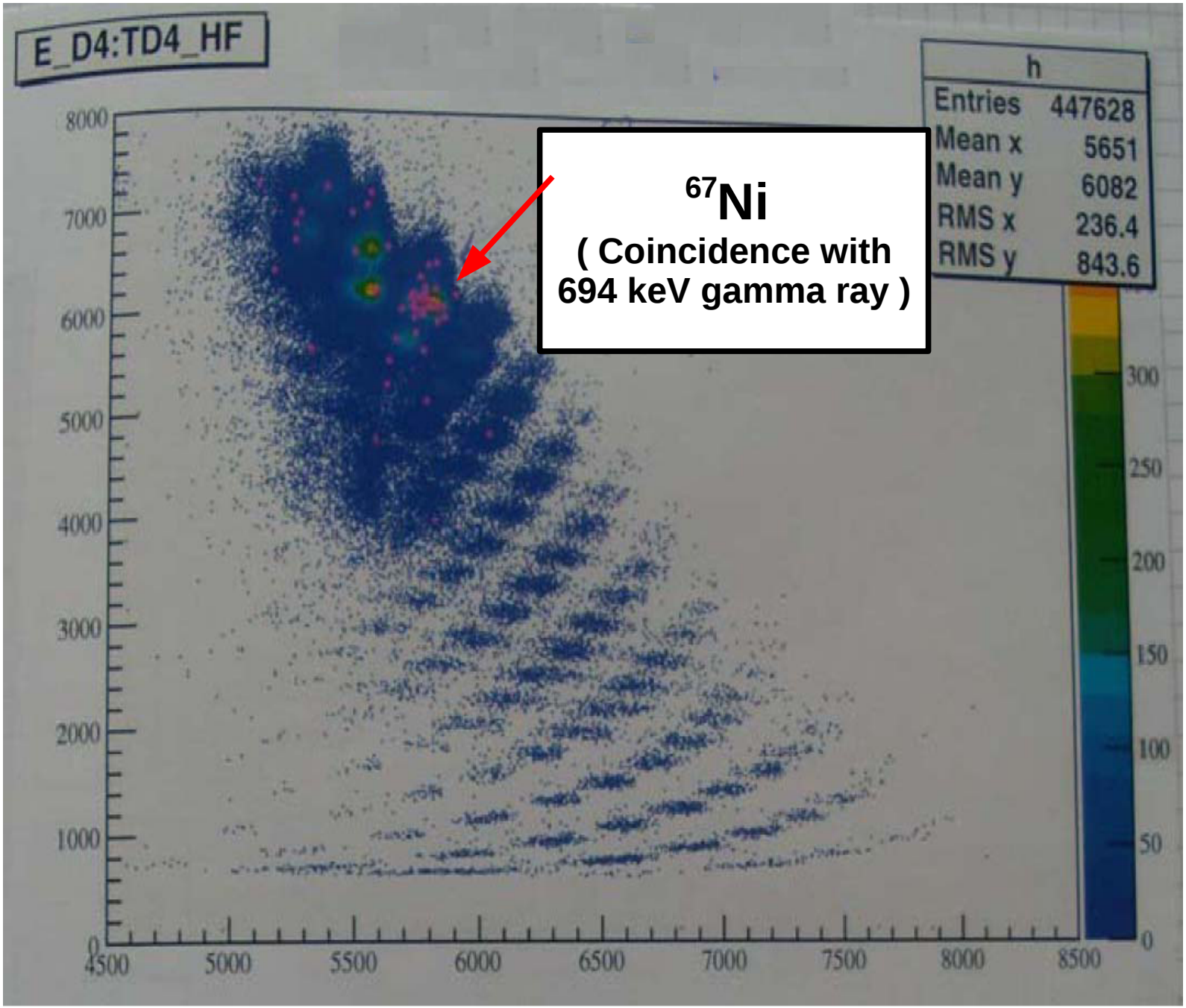

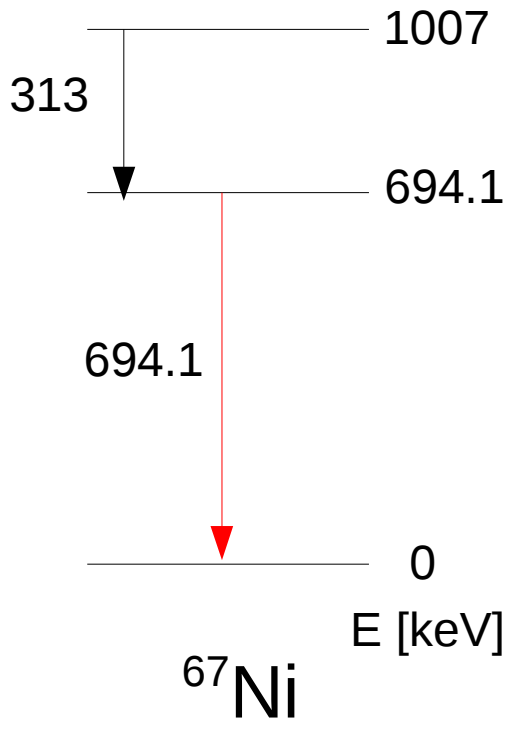

Beam tracker : CATS

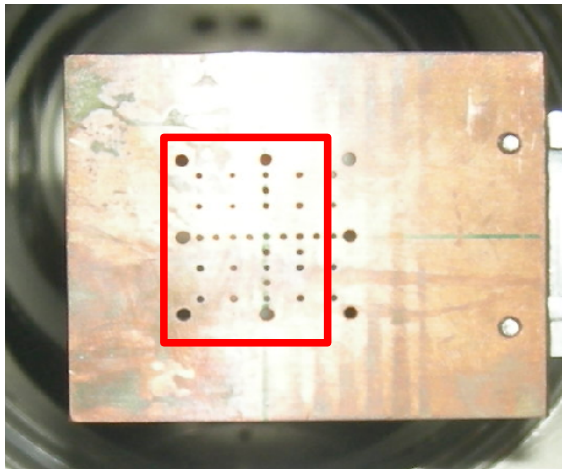

CATS1 mask

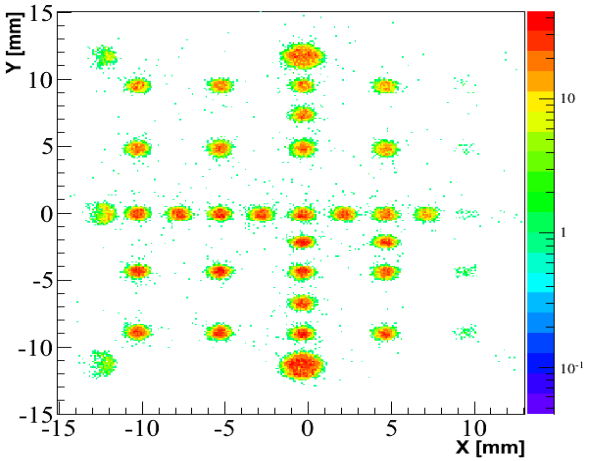

Analytical method :
(Hyperbolic secant squared)

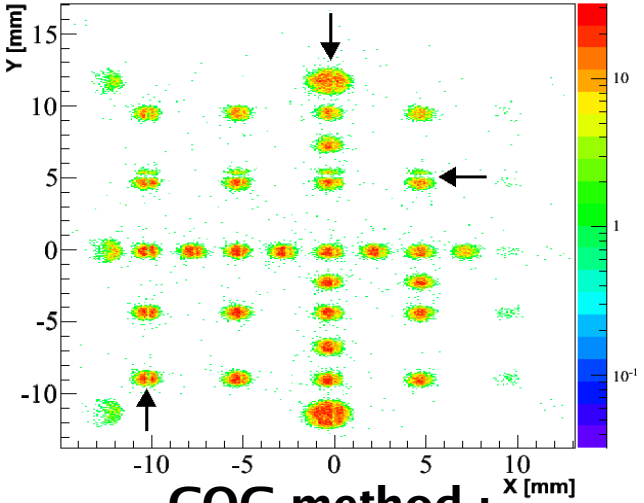

COG method :
(3 strips)

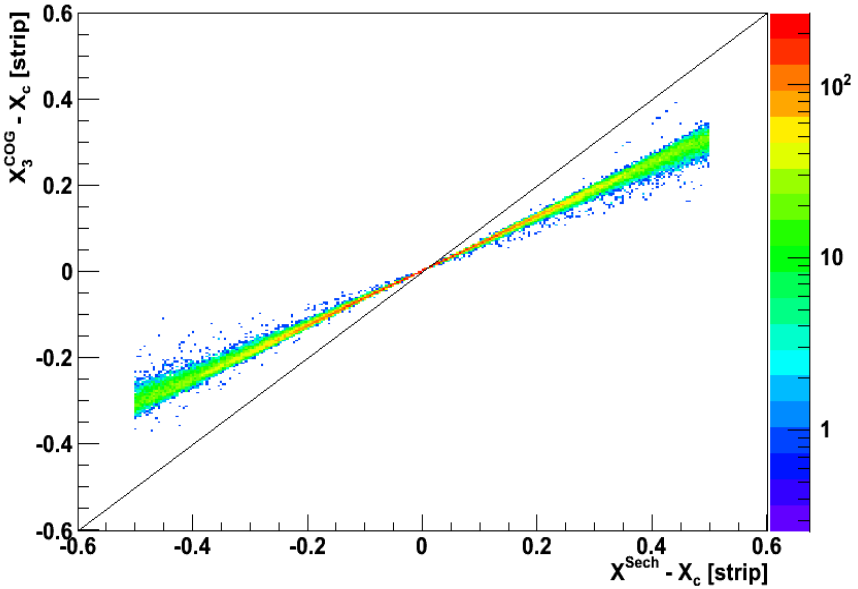

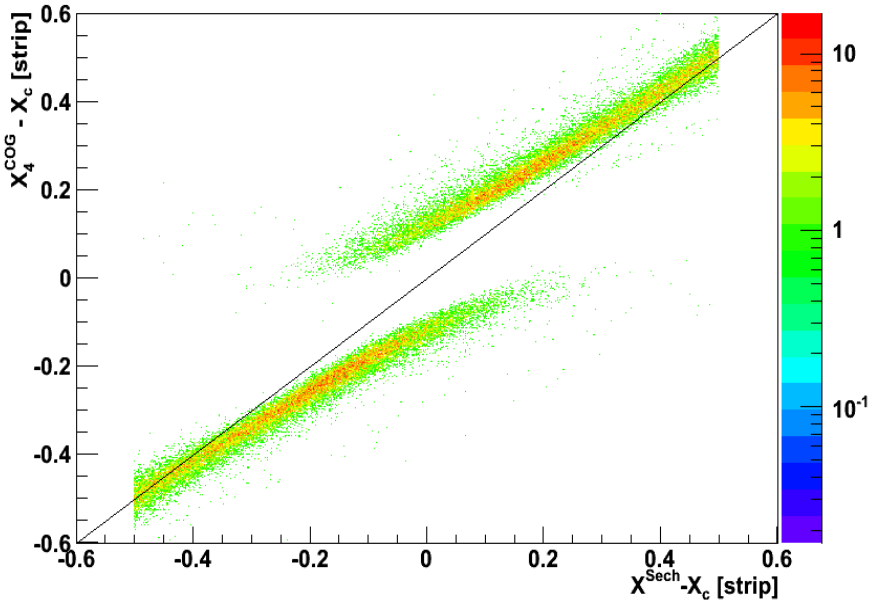

Beam tracker : CATS

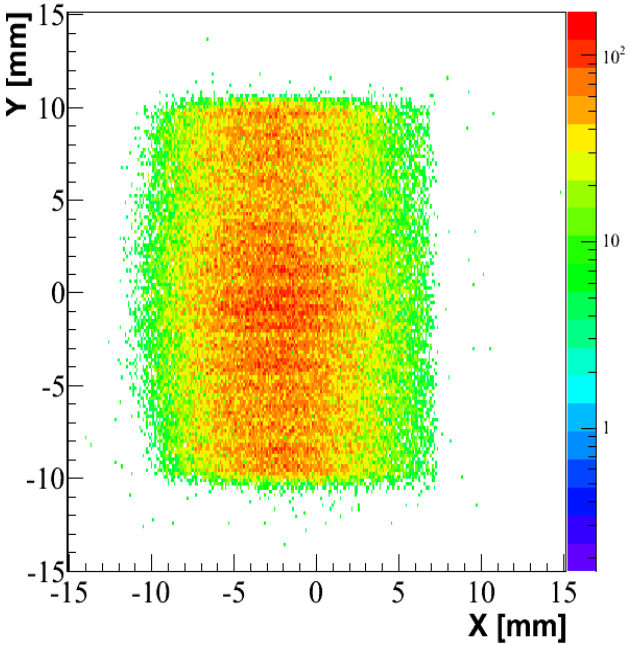

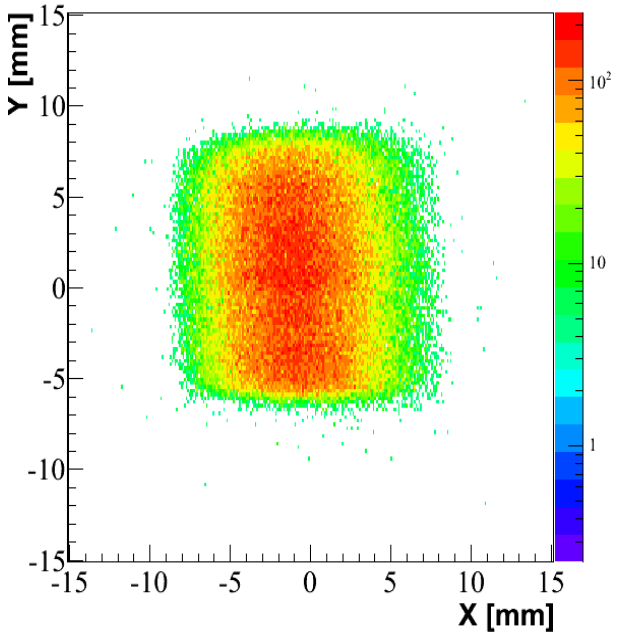

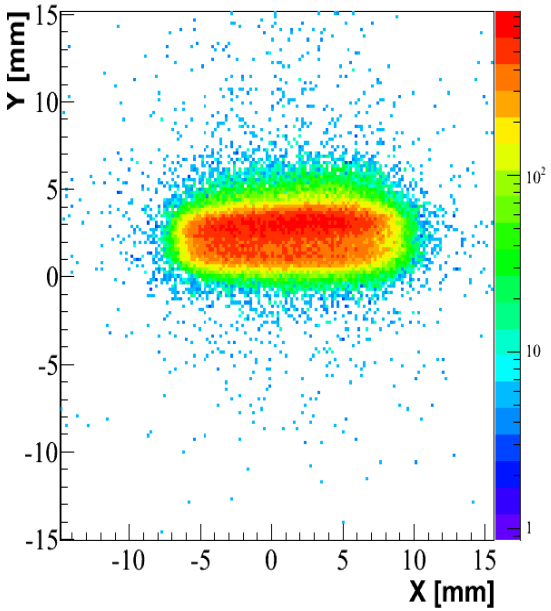

Construction with CATS : systematic errors

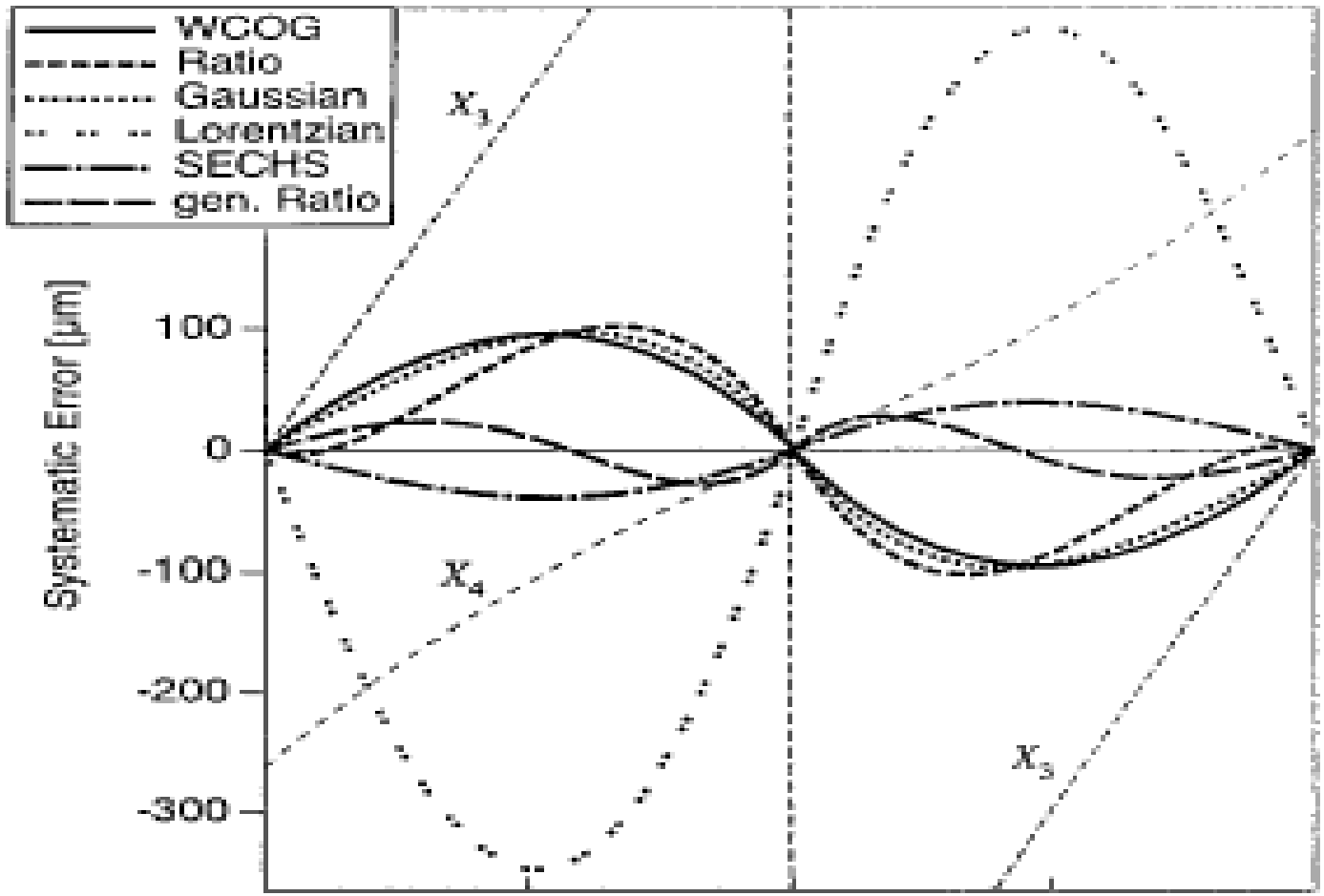

Strip (n) center

Strip (n+1) center

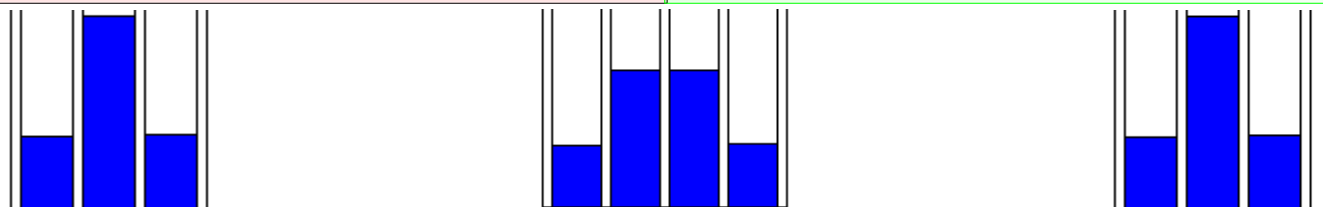

Plastic deterioration

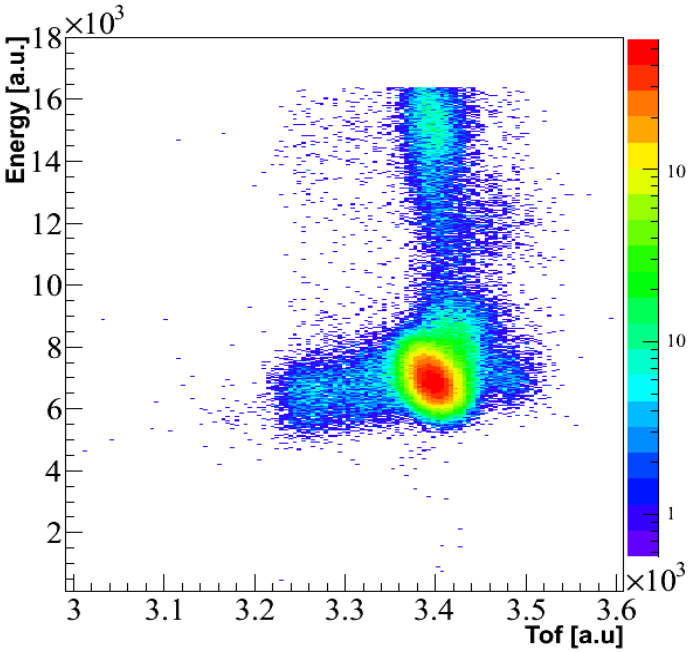

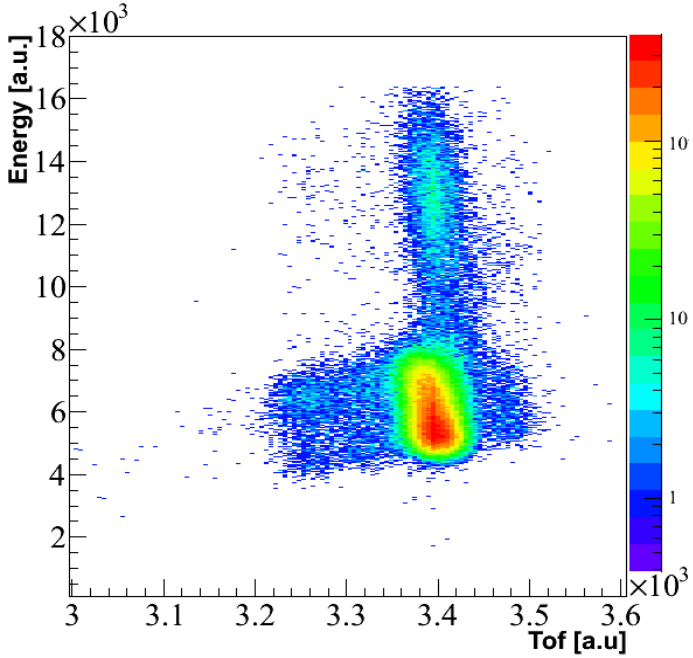

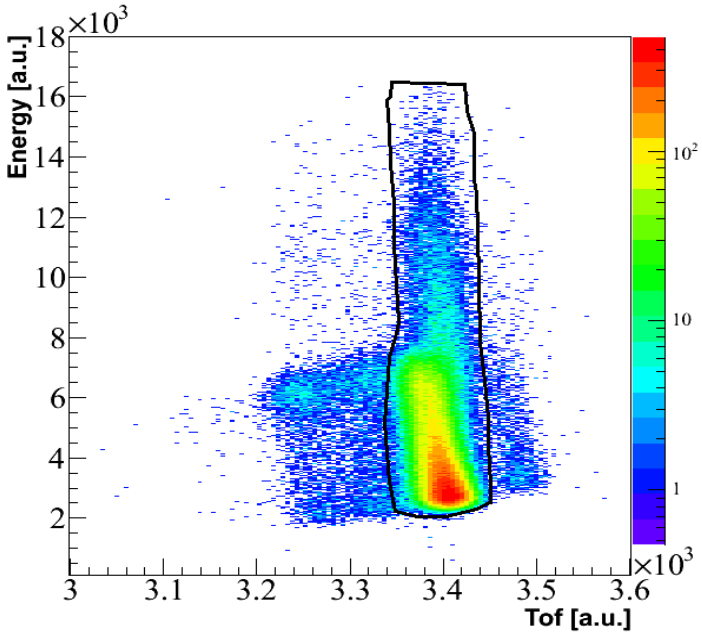

Calculated parameters

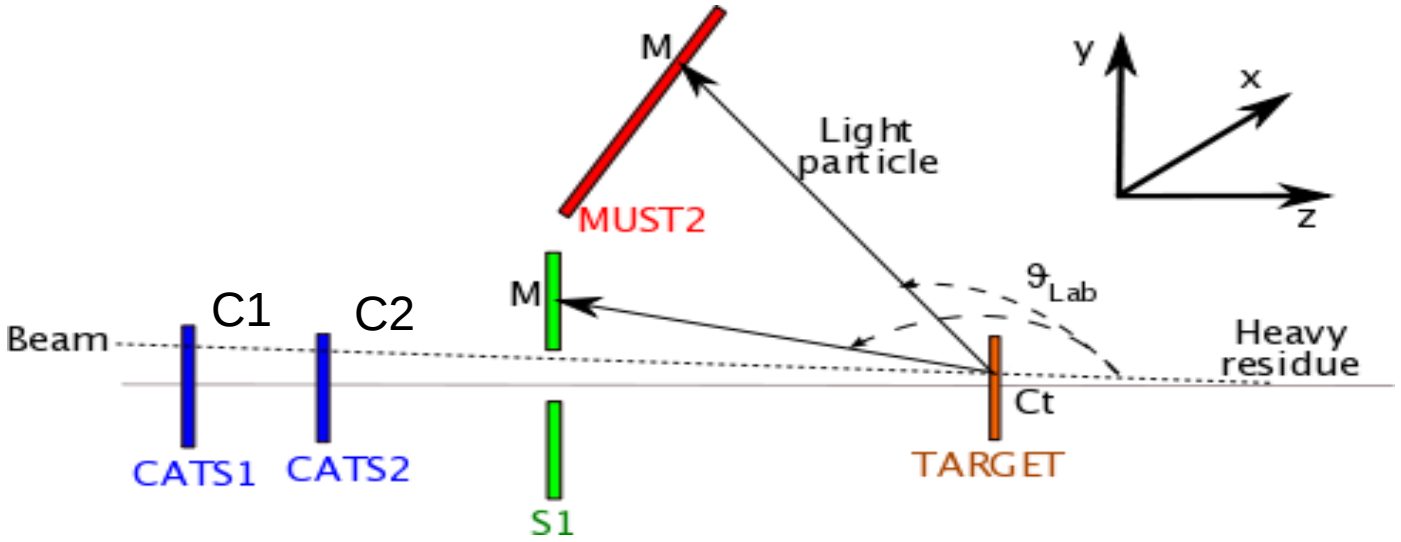

- Reconstruction of angle of emission θ(Lab) (uncert. ~ 0.5°)
- Beam energy correction taking into account the energy losses in the:
  - Beam trackers CATS
  - Target
- Proton energy correction taking into account the energy losses in the :
  - Target
  - Detector dead layers
- Reconstruction of excitation energy using missing mass method

Background reactions : Carbon background

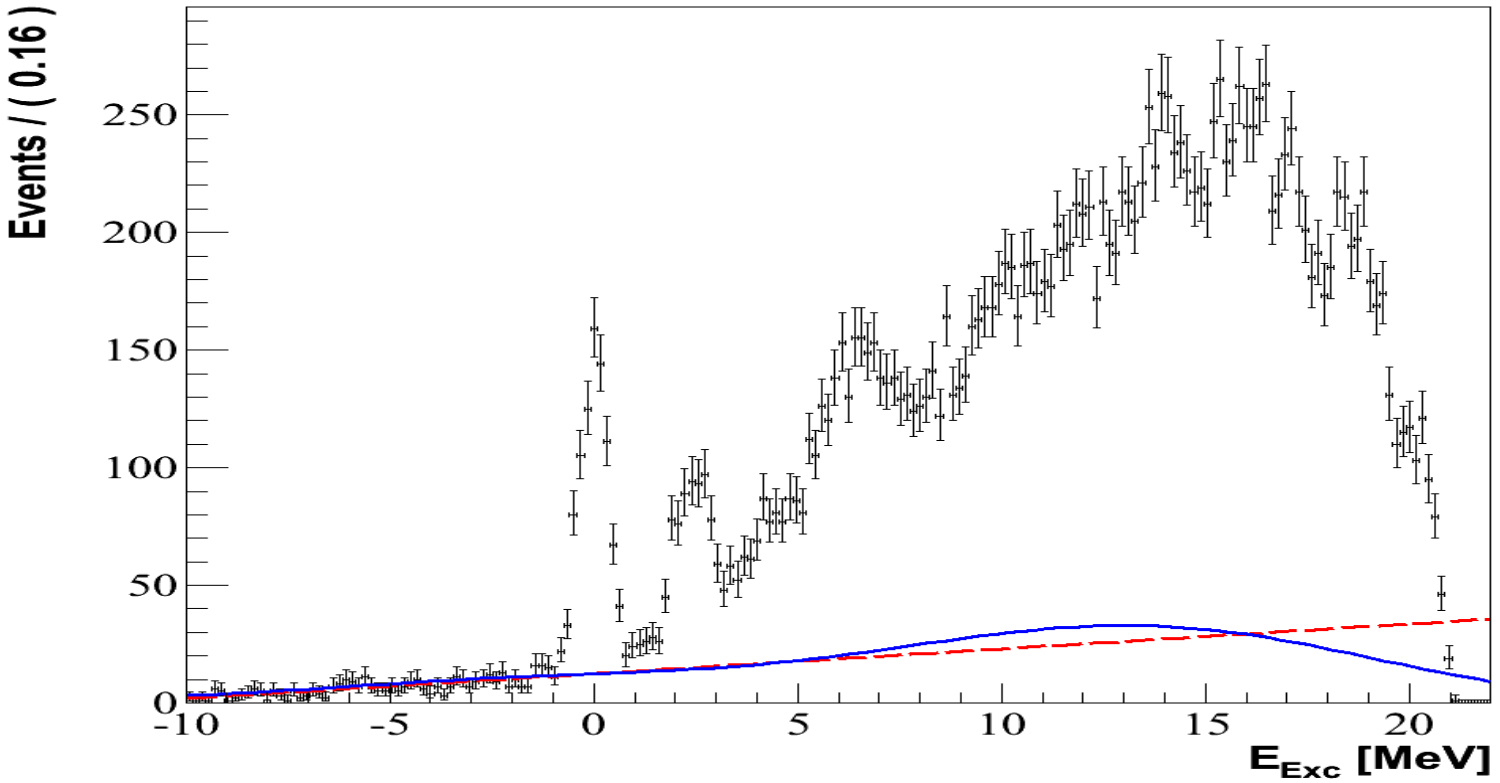

- CD_2 Target ⇒ Carbon background
- Poor statistics
- Estimated with:
  - → Linear back-ground
  - → **« Kernel estimation»**

Excitation energy spectrum : no cuts

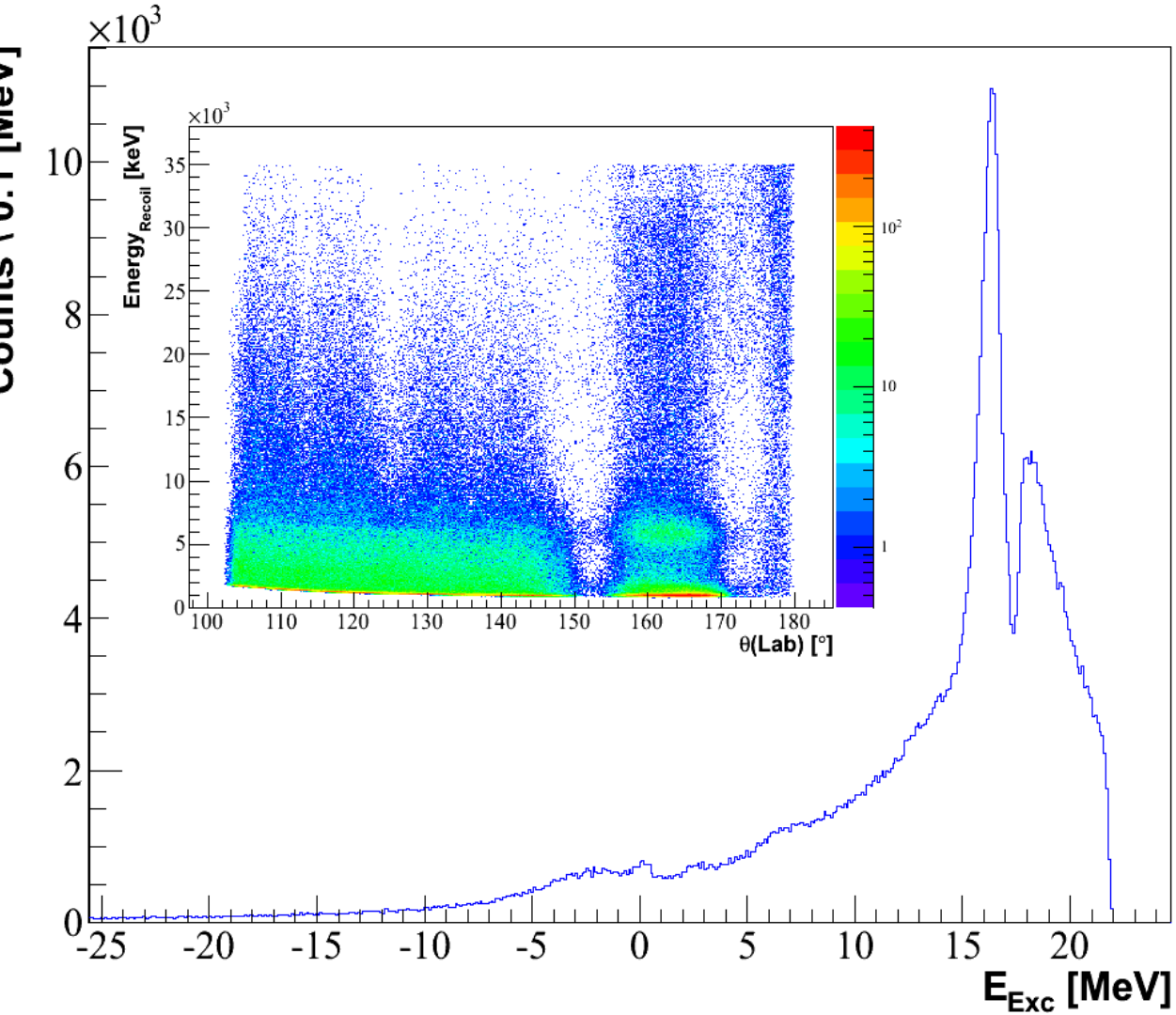

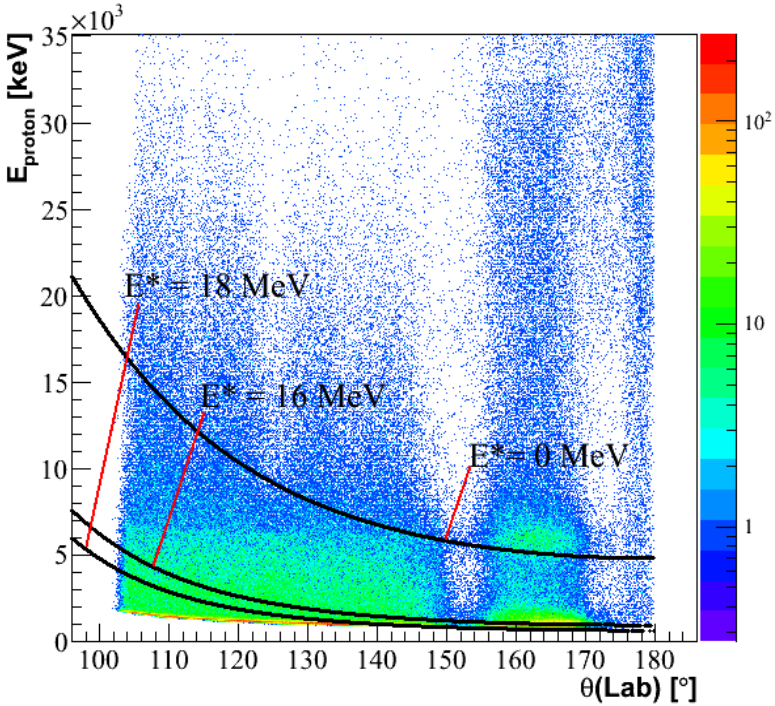

Excitation energy spectrum : gated

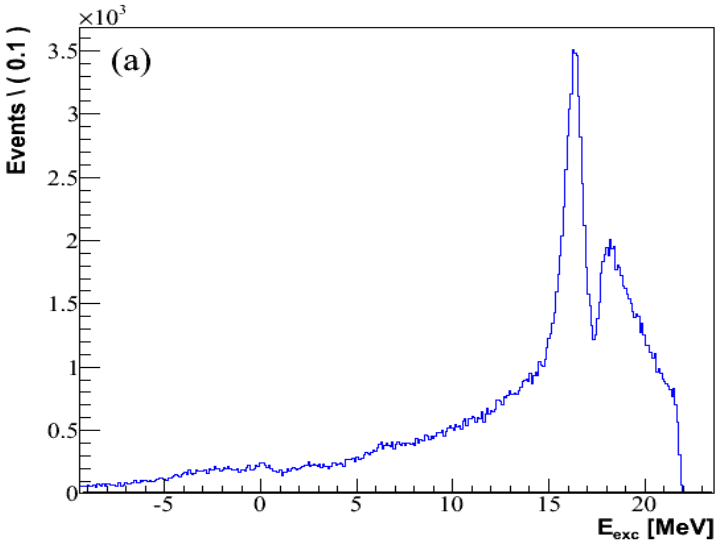

Target gate

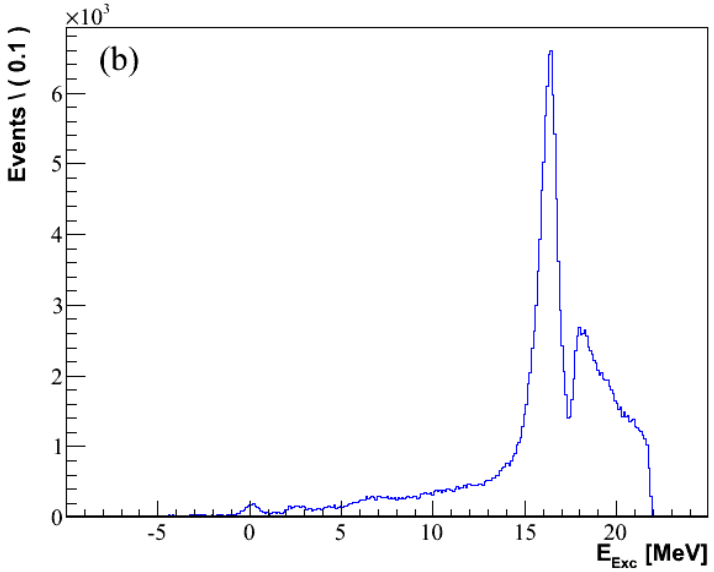

Heavy residue gate

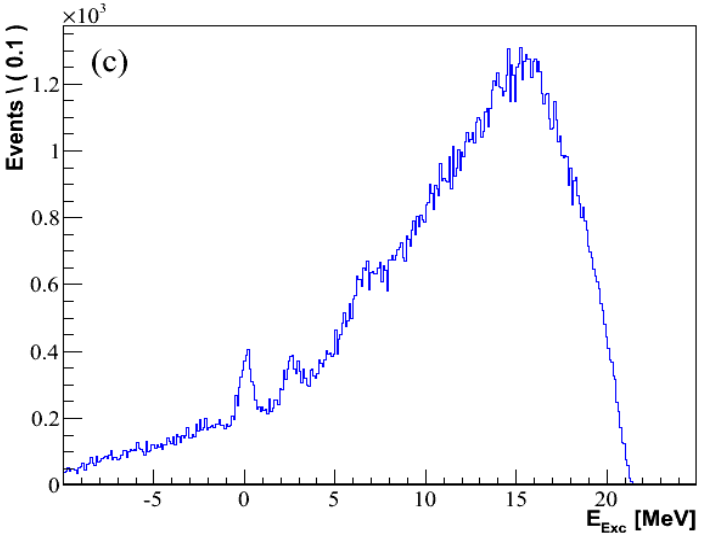

Proton gate

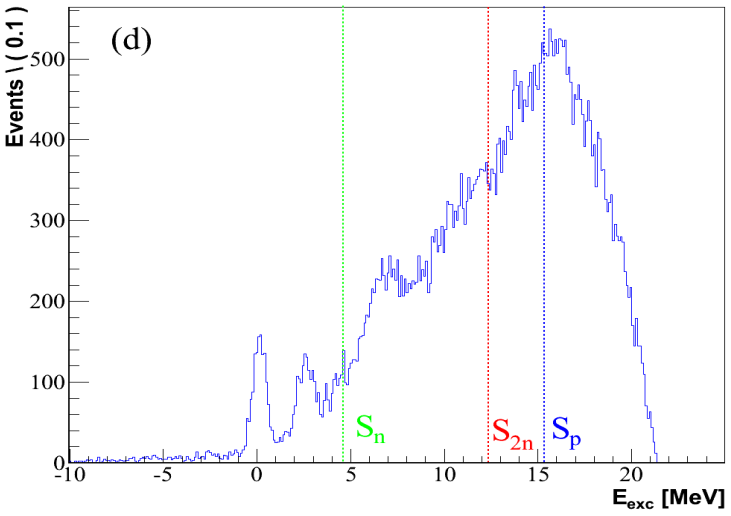

All gates

Efficacité angulaire simulée

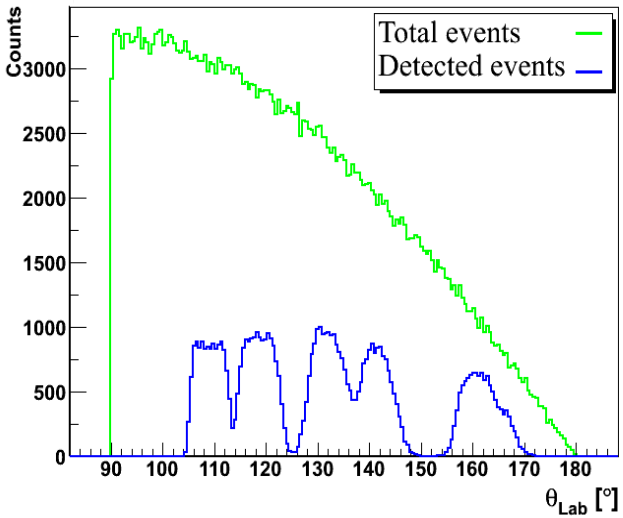

⇒

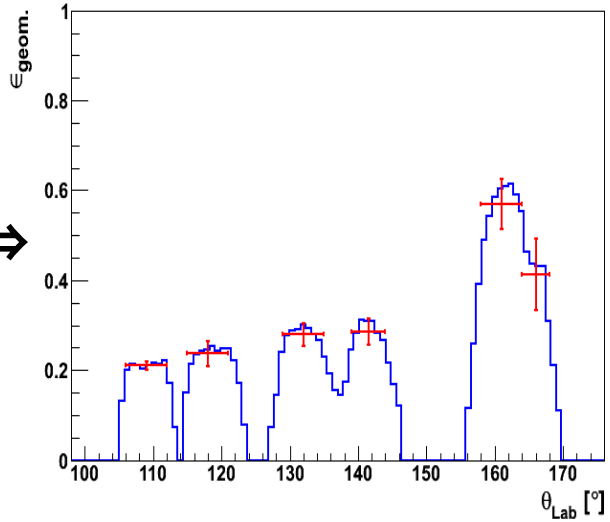

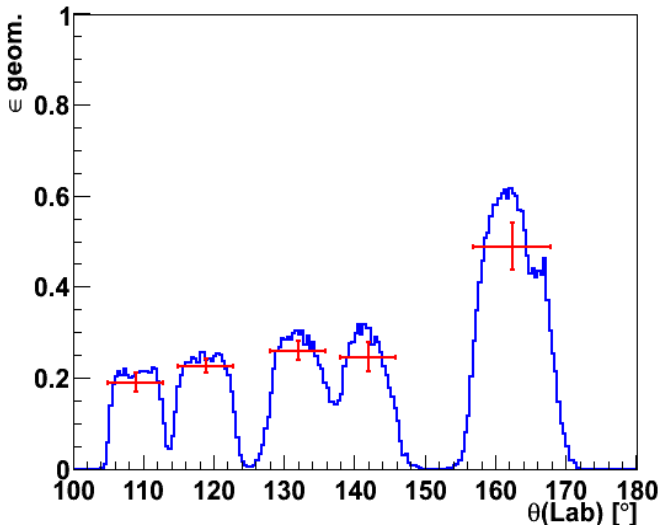

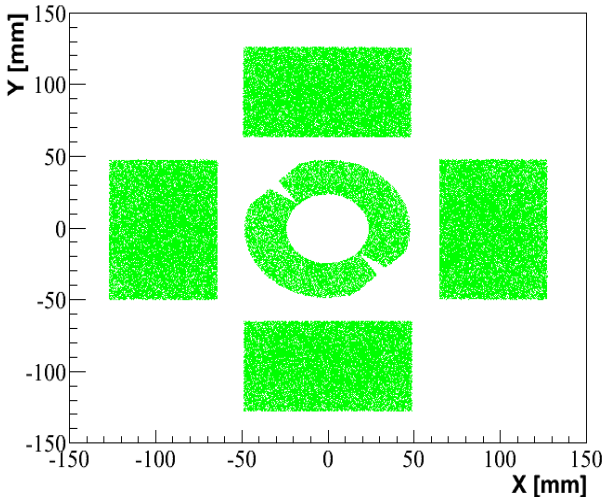

Détecteur parfait

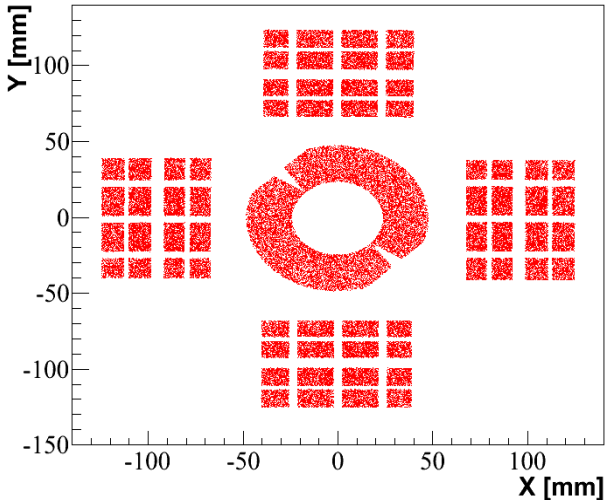

+ matching

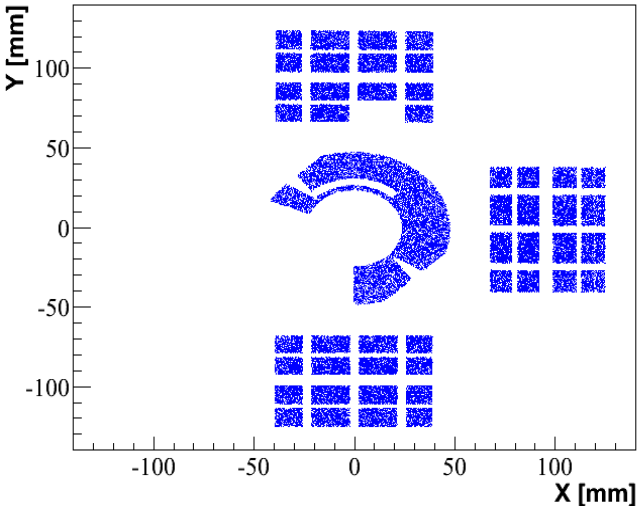

+ pistes manquantes

Excitation energy spectrum

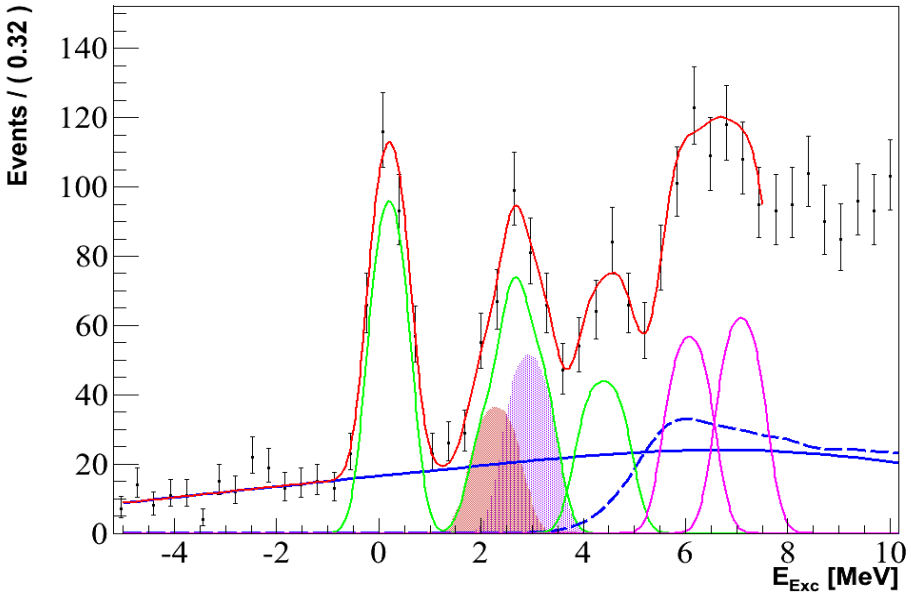

Pic #	Energy [MeV]	FWHM [MeV]
G.S	0.00	1.04
1	2.47	**1.43**
2	4.19	1.27
3	5.88	1.39
4	6.89	1.39

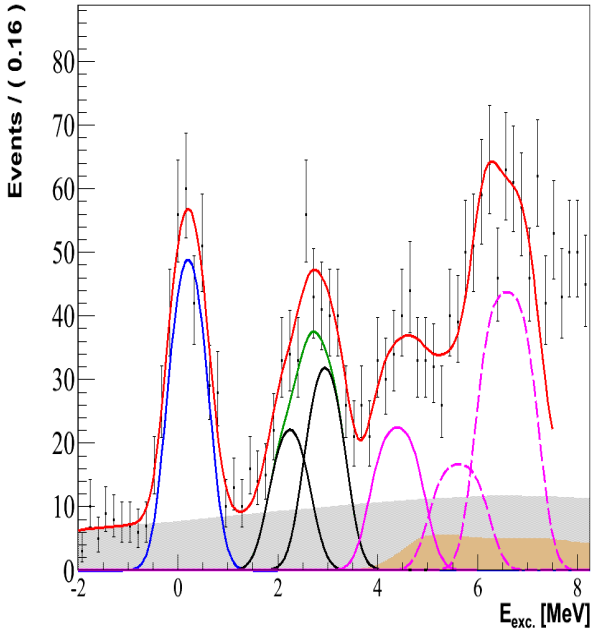

Pic #	Energy [MeV]	FWHM [MeV]
G.S	0.000(27)	1.032(42)
1	2.478(49)	**1.474(100)**
2	4.195(91)	1.257(34)
3	5.427(190)	1.346(32)
4	6.391(46)	1.401(31)

Deuteron break-up

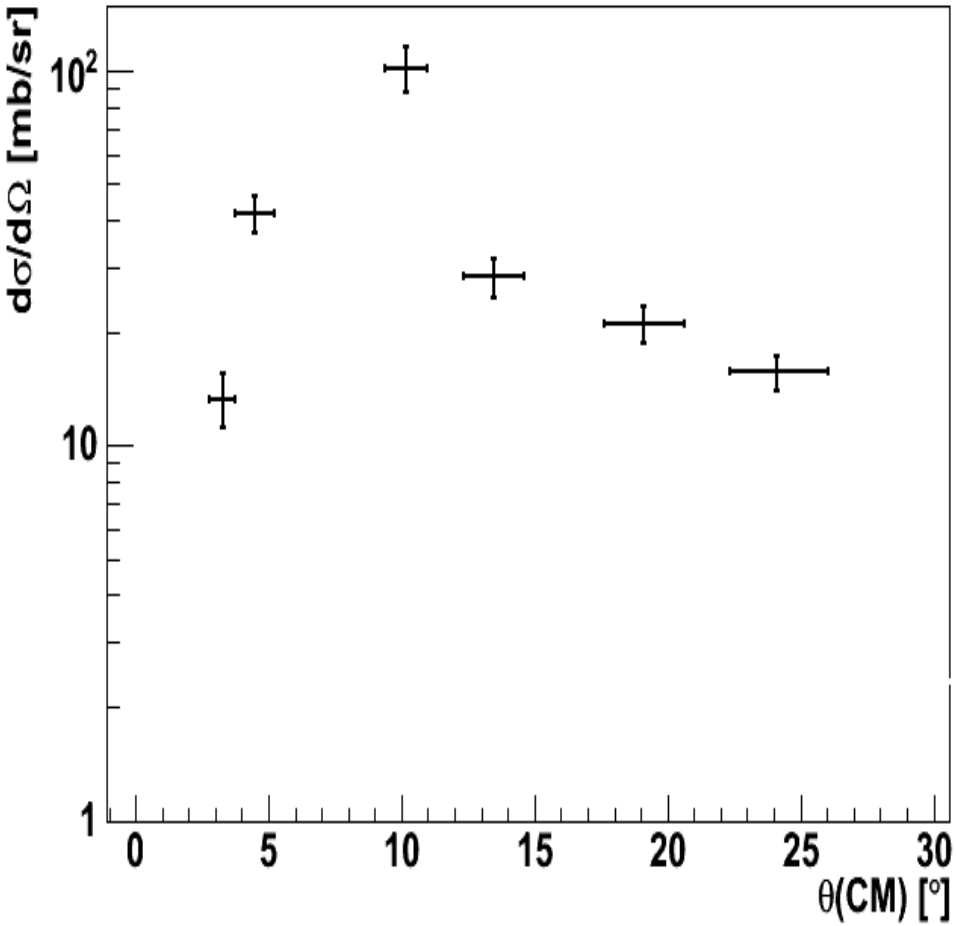

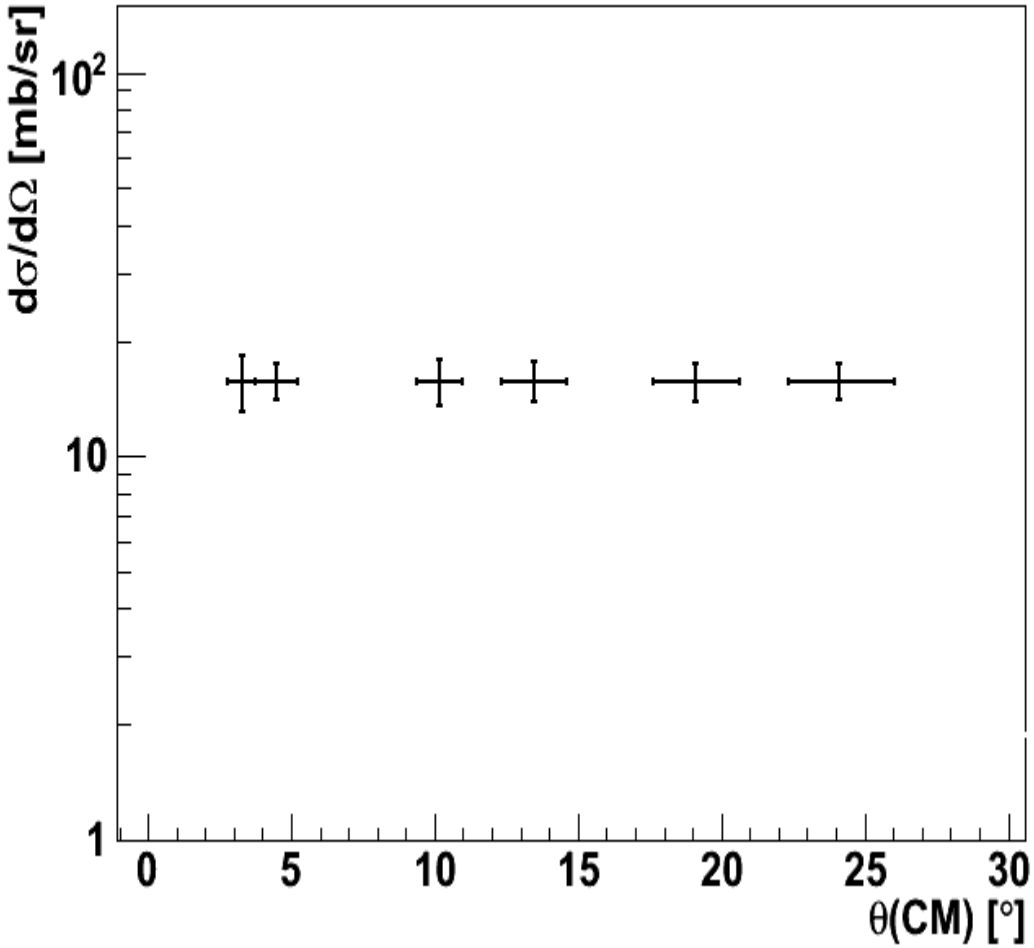

Excitation energy : spectra analysis

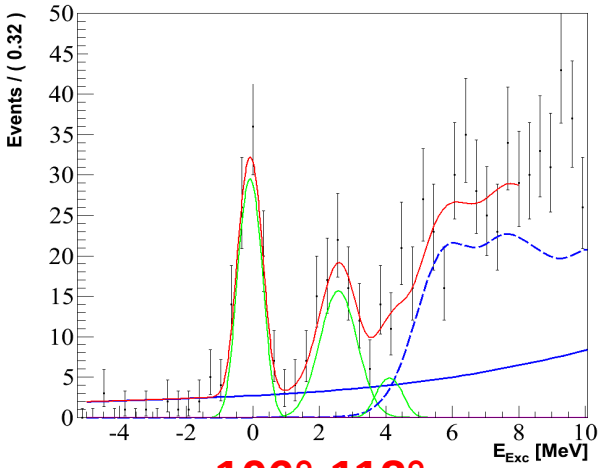

106°-112°

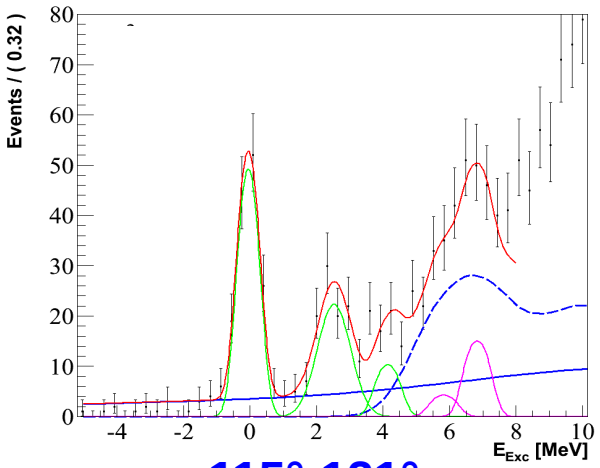

115°-121°

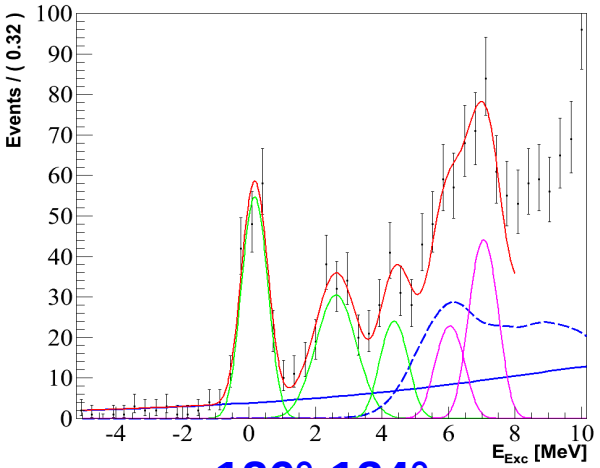

126°-134°

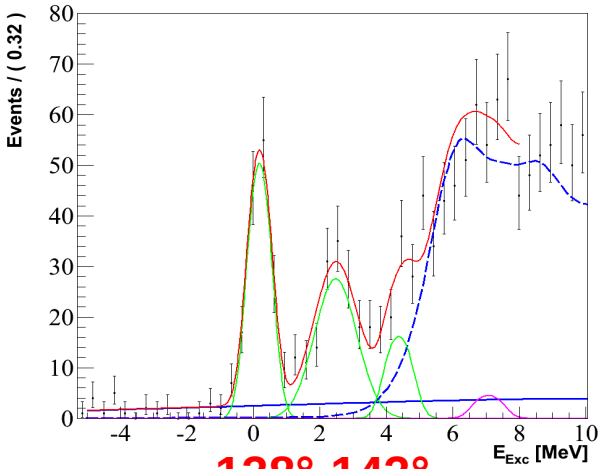

138°-143°

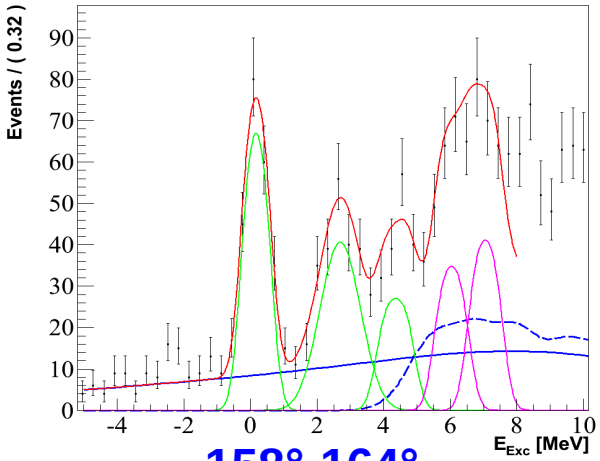

158°-164°

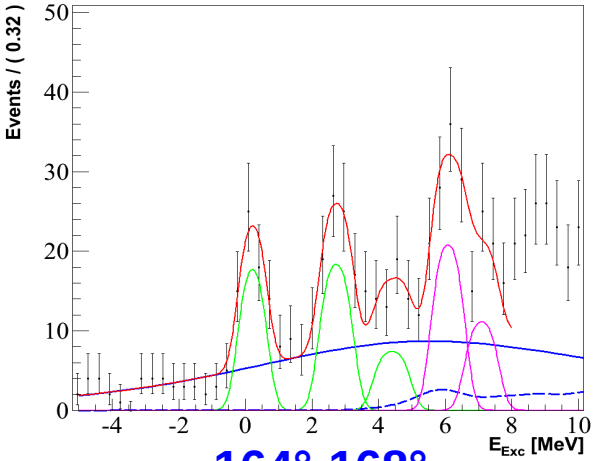

164°-168°

Excitation energy : spectra analysis

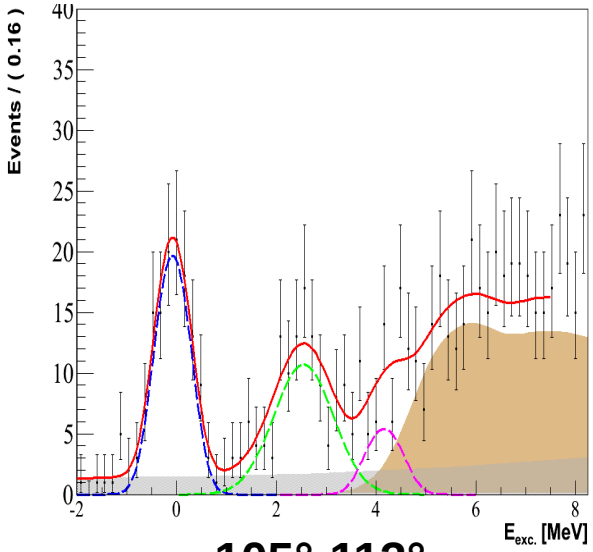

105°-113°

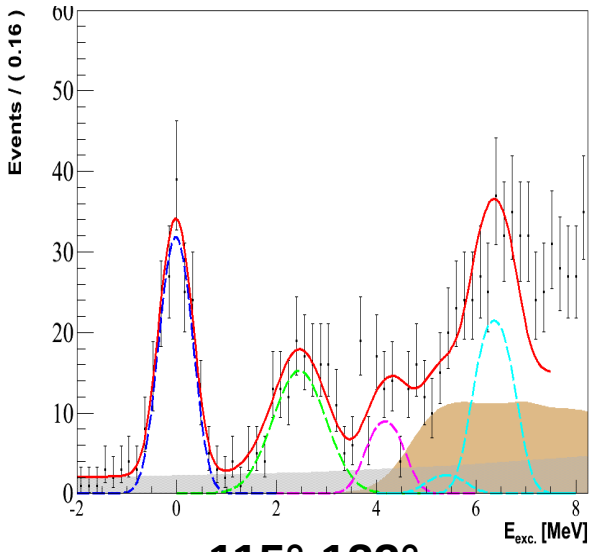

115°-123°

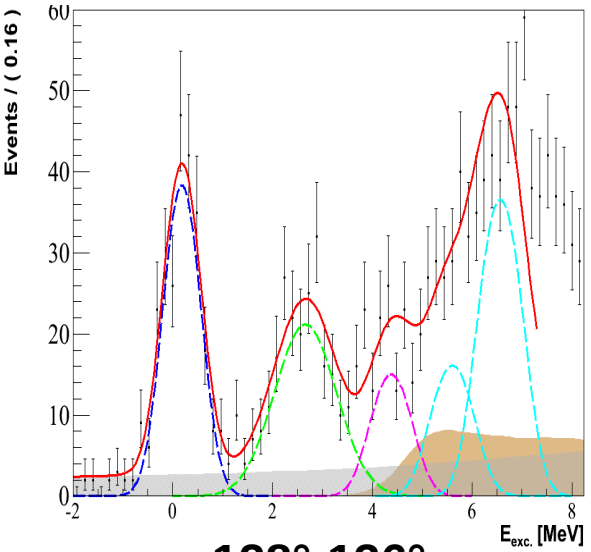

128°-136°

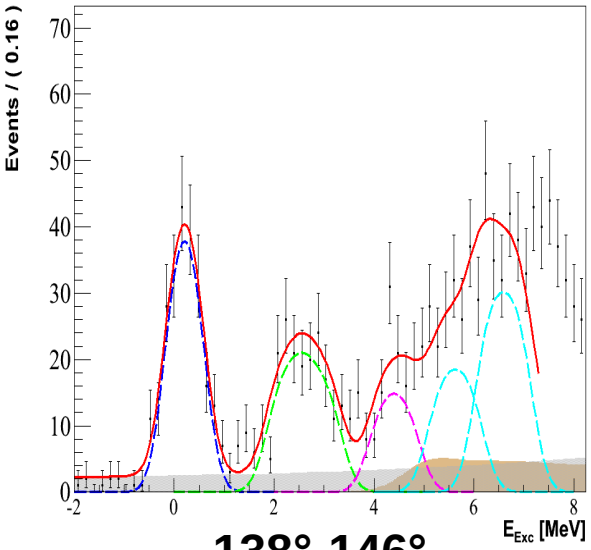

138°-146°

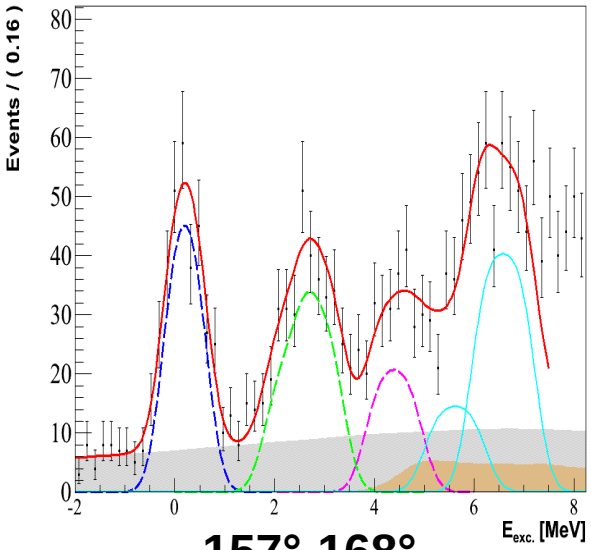

157°-168°

Excitation energy : spectra analysis (split)

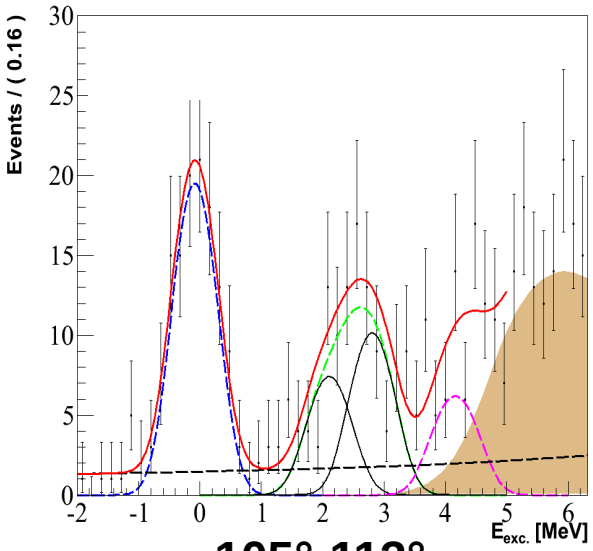

105°-113°

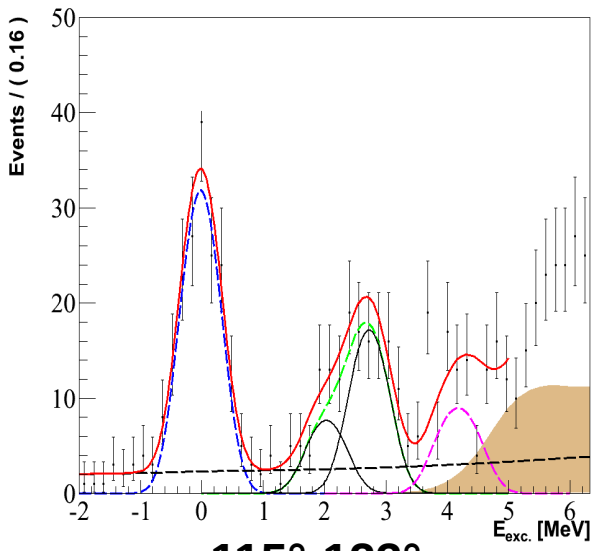

115°-123°

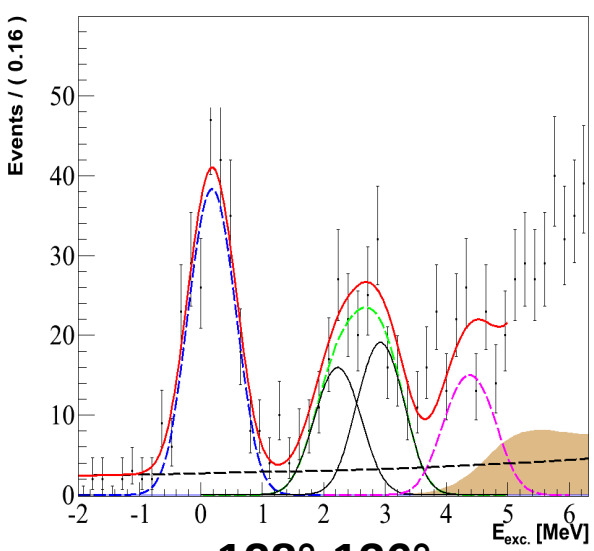

128°-136°

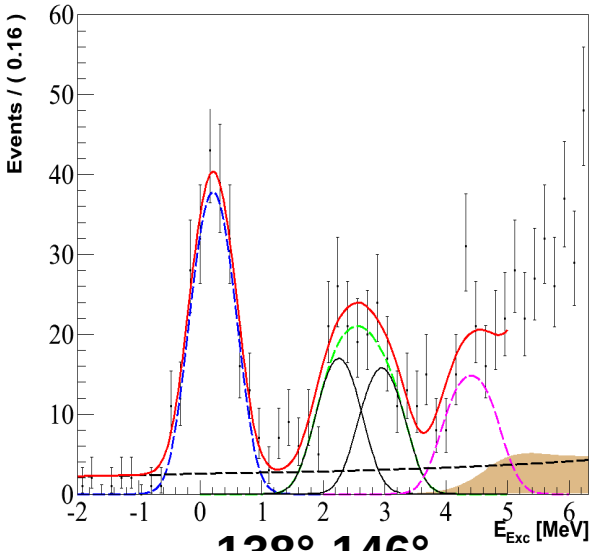

138°-146°

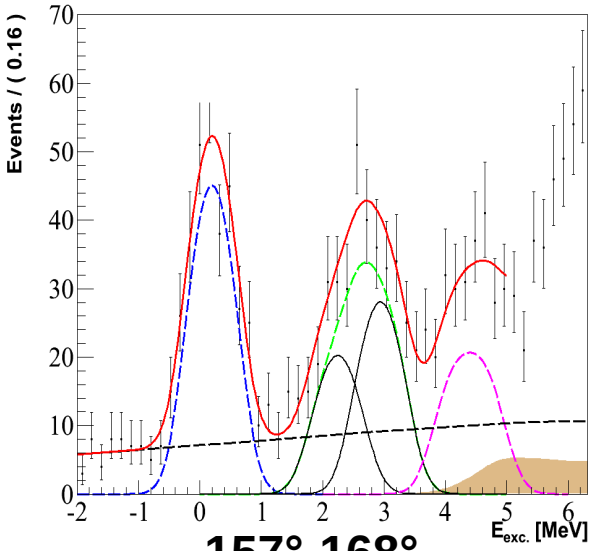

157°-168°

Differential cross sections

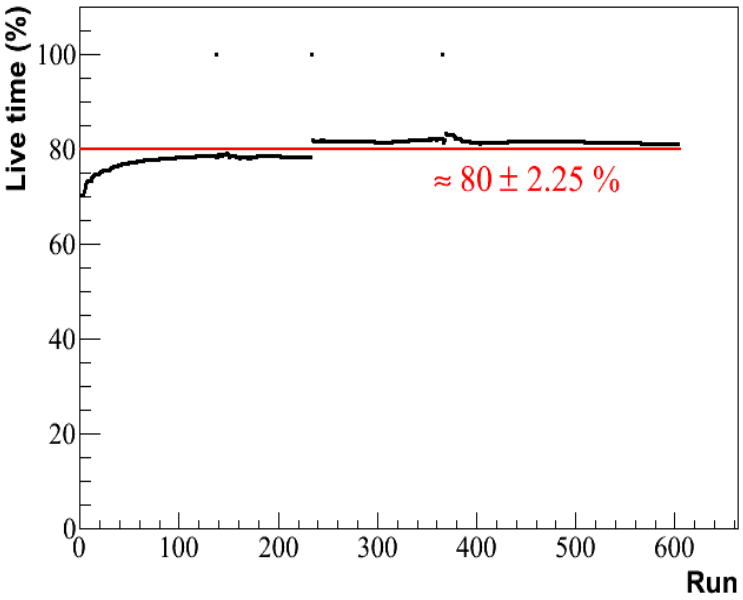

$$\frac{d\sigma}{d\Omega}(\theta_{Lab}) = \frac{N_{det}(\theta_{Lab})\ \ (1+\epsilon_{temps\,mort})}{N_{faisceau}\ \ N_{Cible}\ \ \Delta\Omega(\theta_{Lab})\ \ \epsilon_{MUST2,S1}}$$

$$\frac{d\sigma}{d\Omega}(\theta_{CM}) = Jacob.(\theta_{Lab})\ \ \frac{d\sigma}{d\Omega}(\theta_{Lab})$$

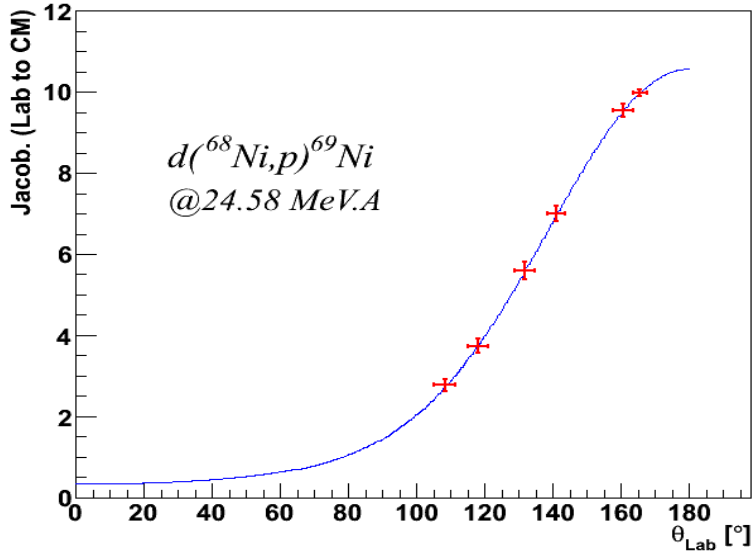

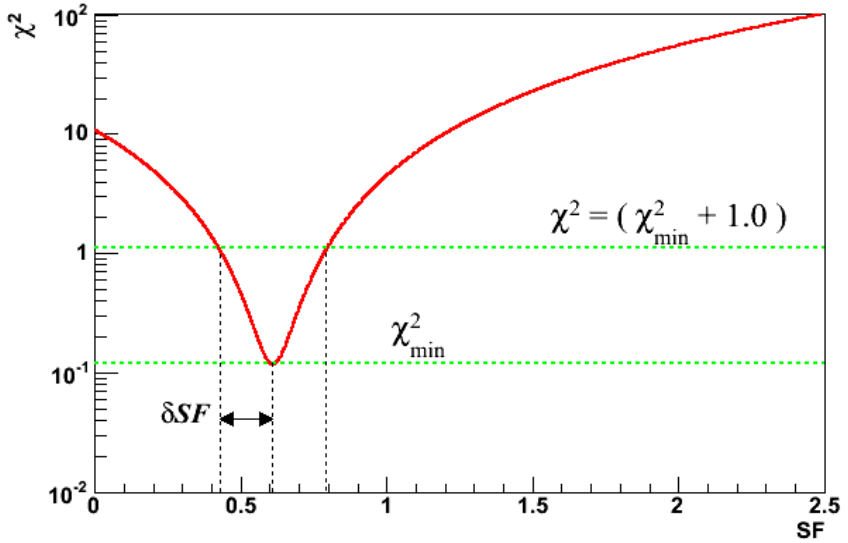

Distorted Wave Born Approximation

- **Code DWUCK4, Zero-Range approximation**
- **Pas de mesure de diffusion élastique ^{68}Ni + d et ^{69}Ni +p ⇒ Potentiels optiques globaux**
  - **^{68}Ni + d :**
    - **DWBA** : 27 < A < 238, 12 MeV < E_d < 90 MeV

      Daehnick et al. PRC, 21, 2253, 1981
    - **ADWA** : $V = V_p + V_n + V_{pn}$ ($E_n = E_p = E_d/2$)

      pour le break-up deuton quand E_d > 20 MeV

      Johnson and Soper, PRC, 1, 976, 1970
  - **^{69}Ni + p :**
    - KD03 : 24 < A < 209, 1 keV < E_p < 200 MeV

      Koning and Delaroche. Nucl. Phys. A, 713, 231, 2003

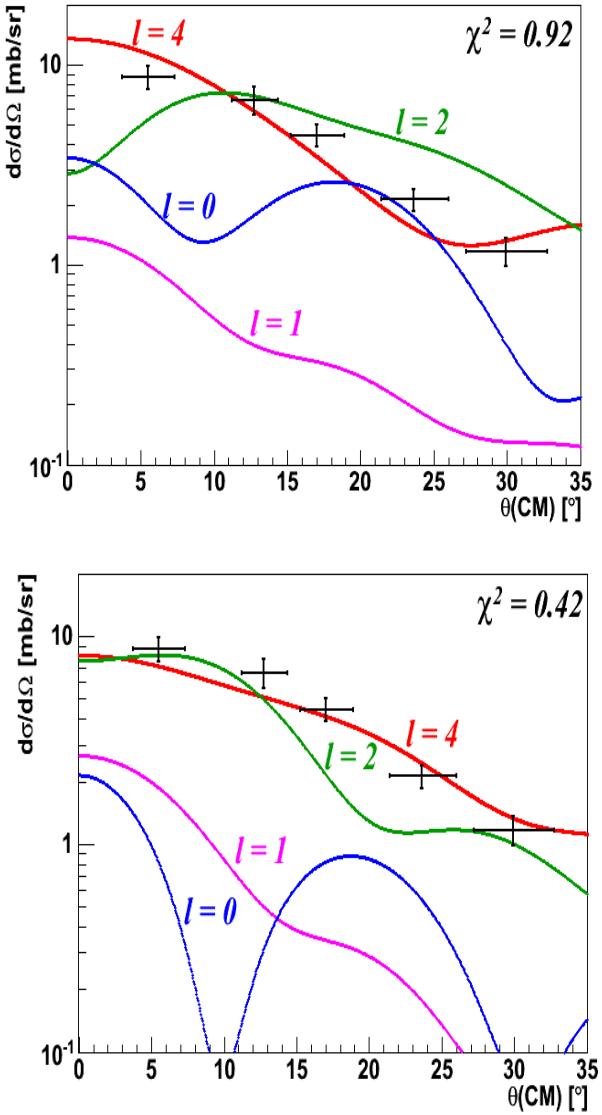

Analysed differential cross sections

CH89 (ADWA) ⊗ KD03

G.S.

- **L = 4, SF = 0.52 ± 0.17**
- **L = 4, SF = 0.61 ± 0.15**

1st Excited (2.47 MeV)

- **L = 2, SF = 0.76 ± 0.24**
- **L = 2, SF = 0.86 ± 0.22**

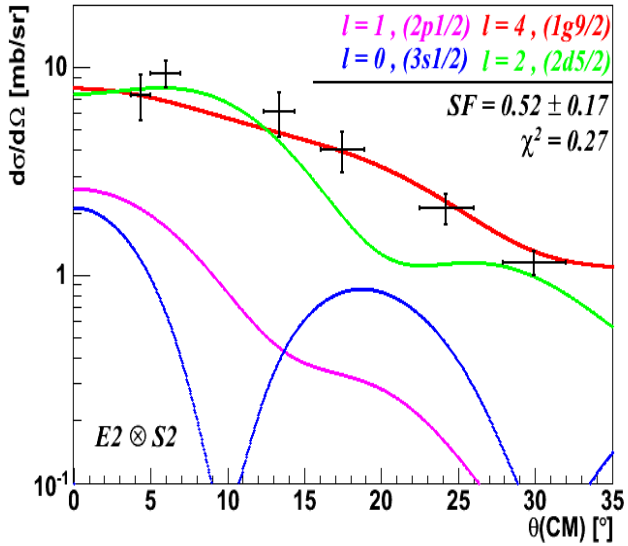

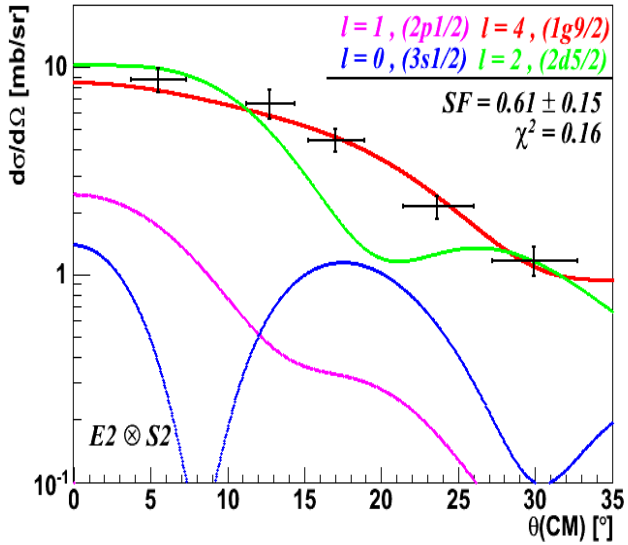

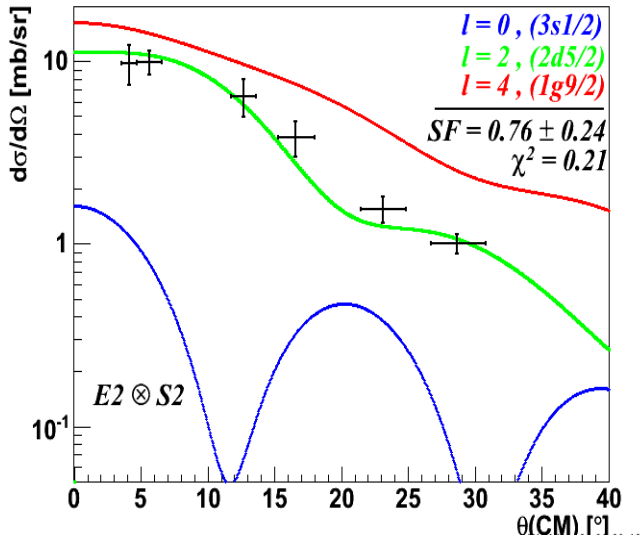

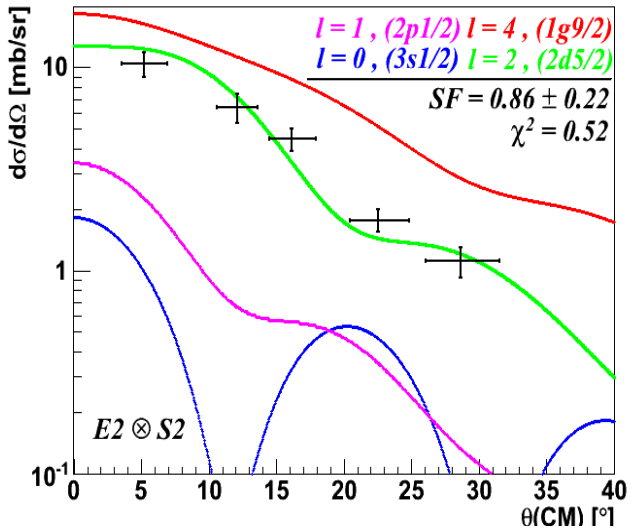

Analysed differential cross sections : 1st excited state

- E_{exc} = 2.11 MeV
  - **L = 2, SF = 0.36 ± 0.12**
- E_{exc} = 2.76 MeV
  - **L = 2, SF = 0.37 ± 0.13**

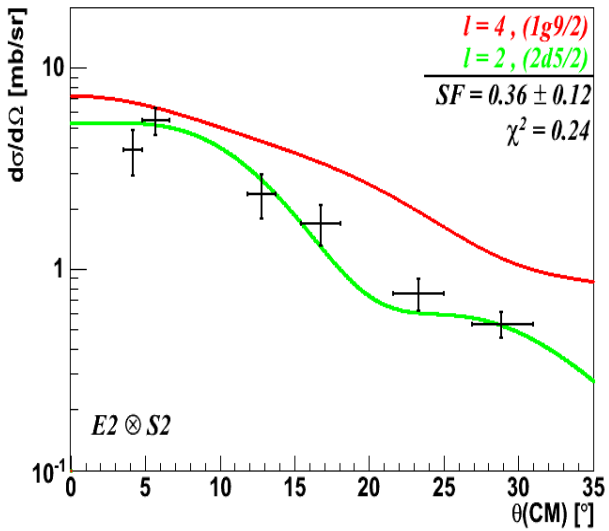

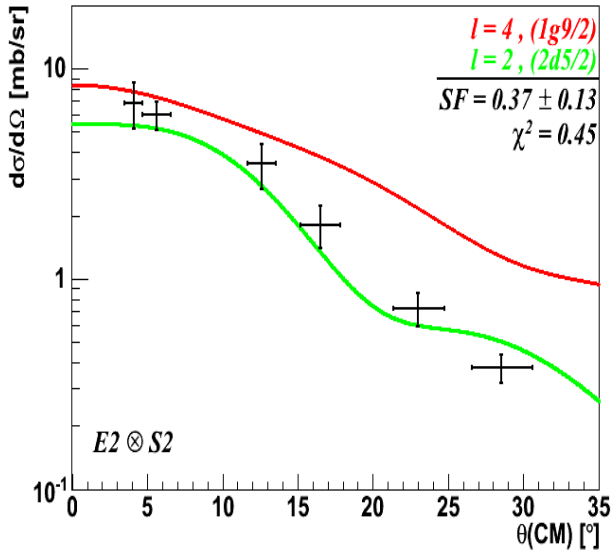

- E_{exc} = 2.05 MeV
  - **L = 2, SF = 0.32 ± 0.10**
- E_{exc} = 2.74 MeV
  - **L = 2, SF = 0.44 ± 0.13**

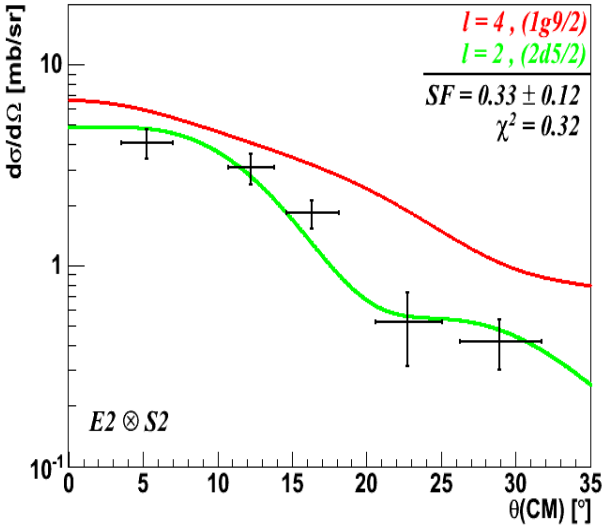

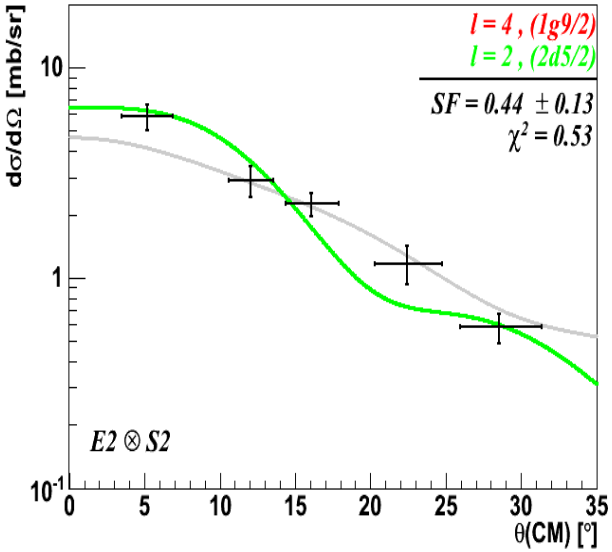

Diff. cross sections analysis : state ~ 2.5 MeV

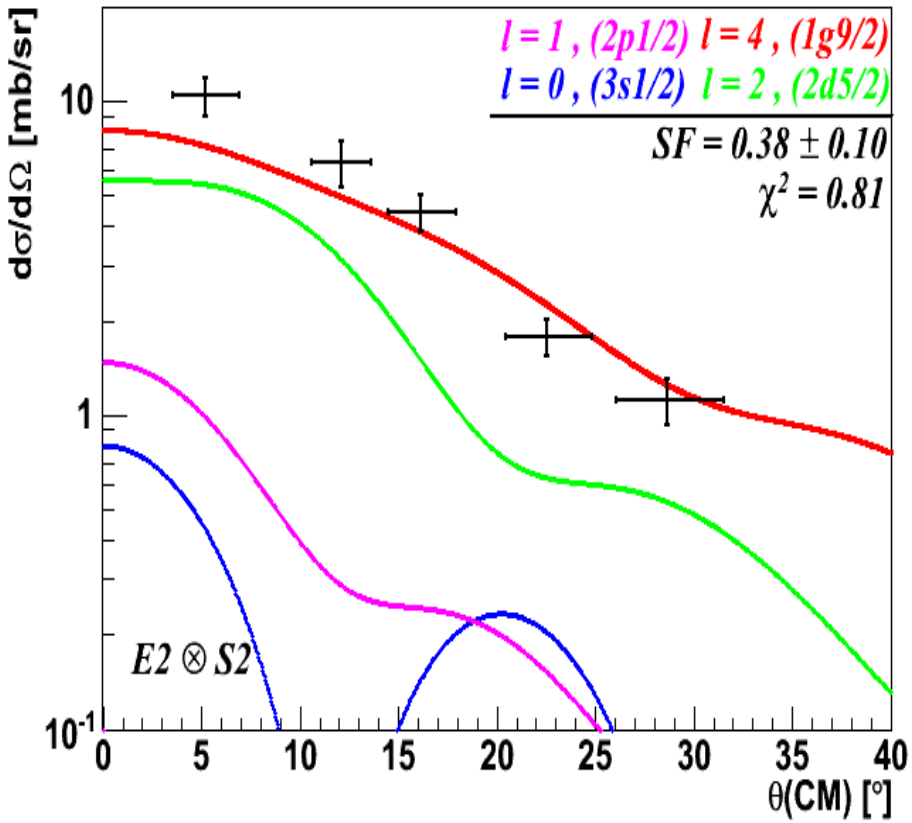

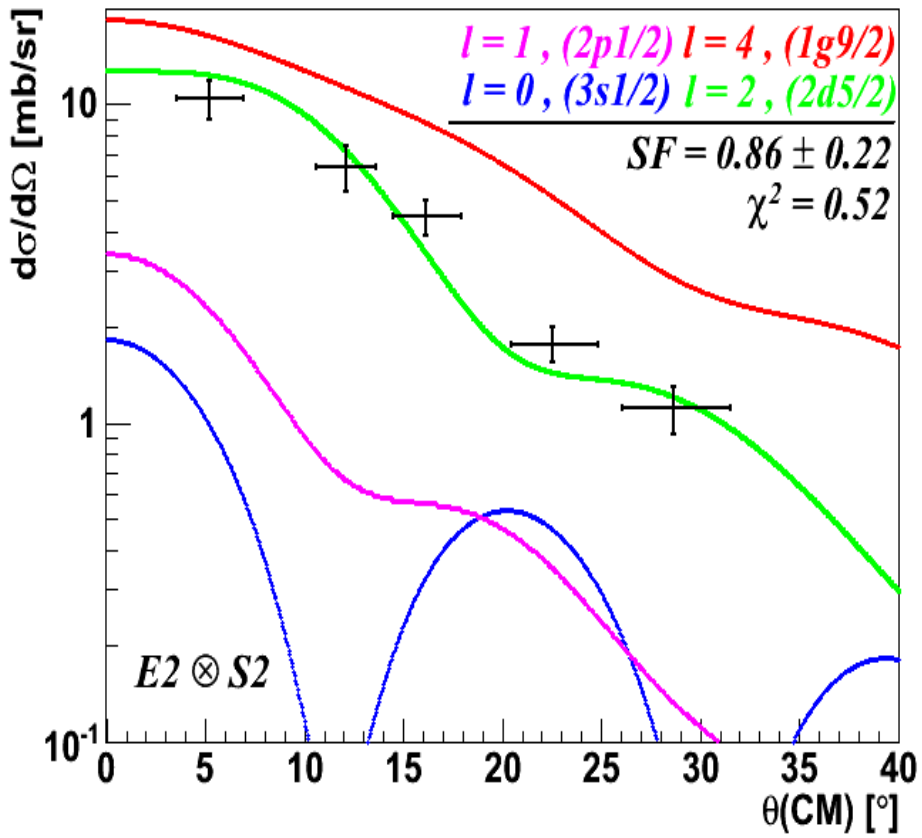

Diff. cross sections analysis : states ~ 2.5 MeV (old)

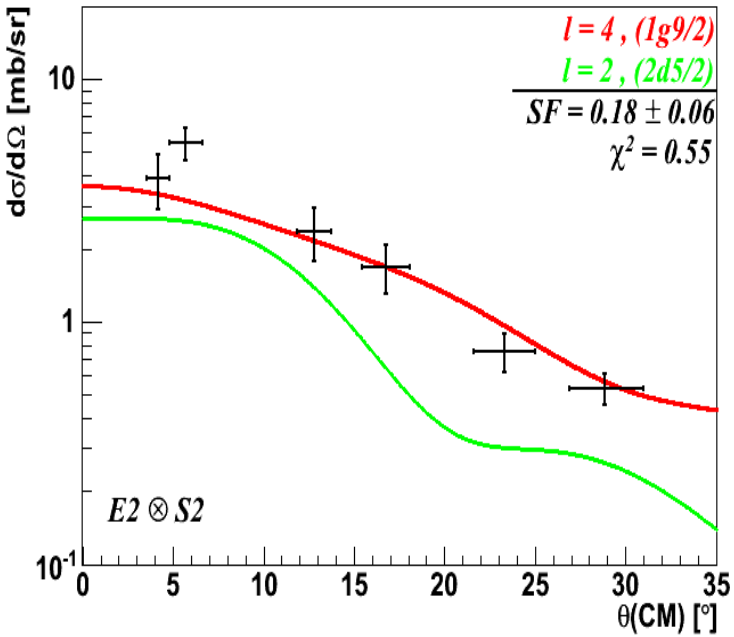

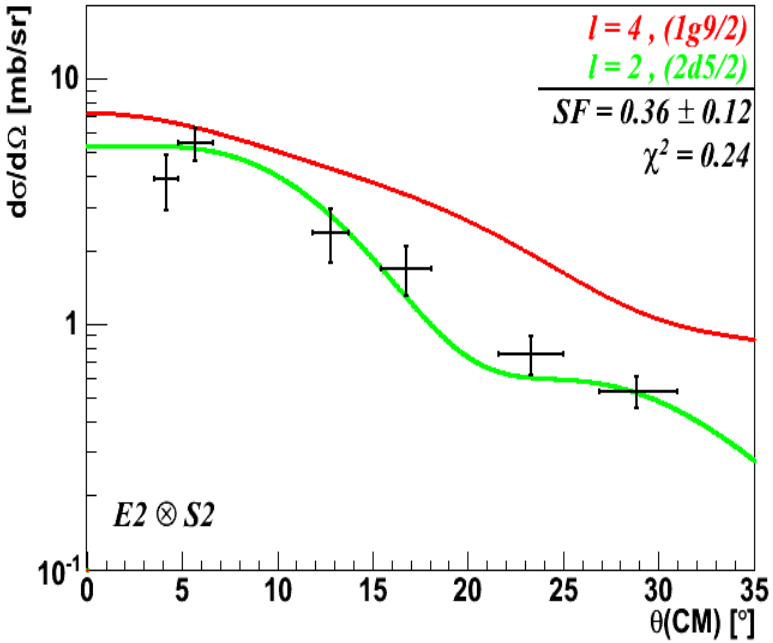

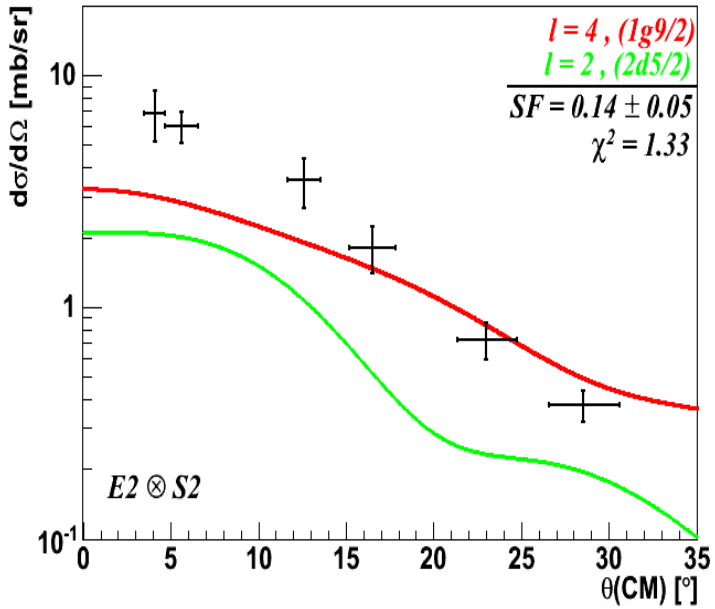

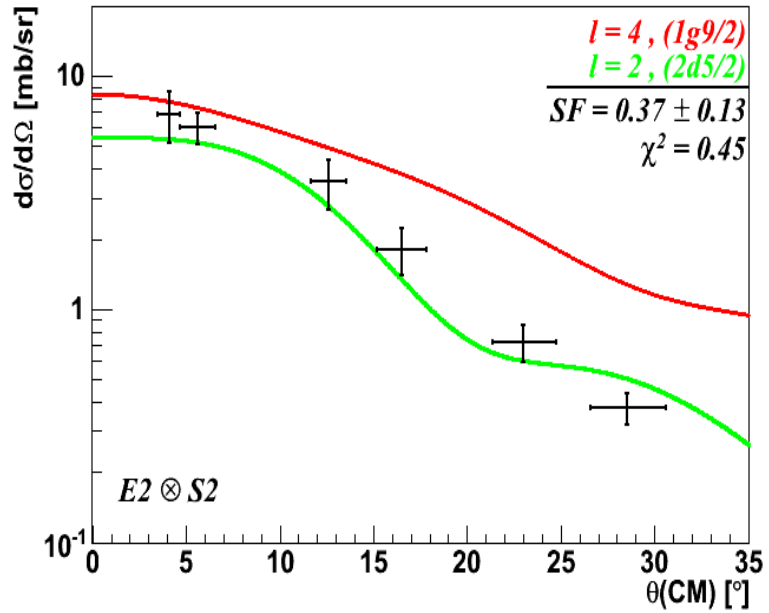

Diff. cross sections analysis : states ~ 2.5 MeV (new)

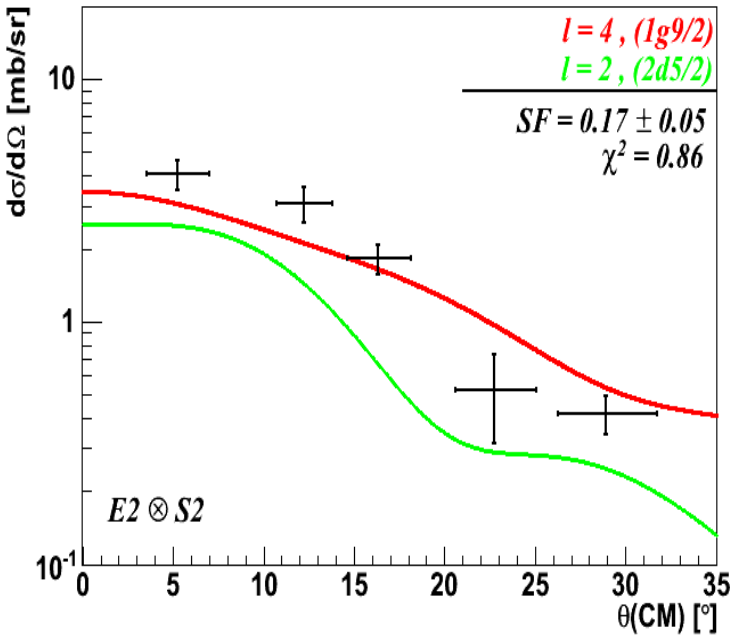

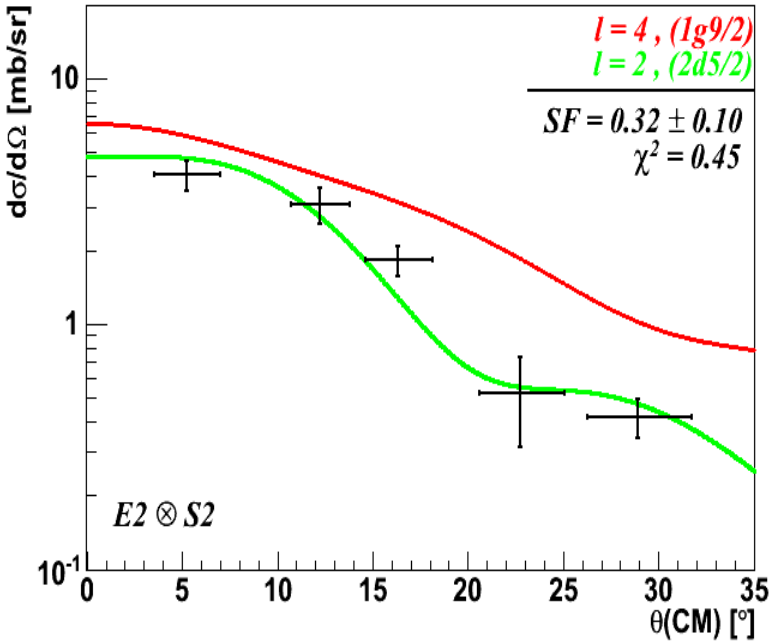

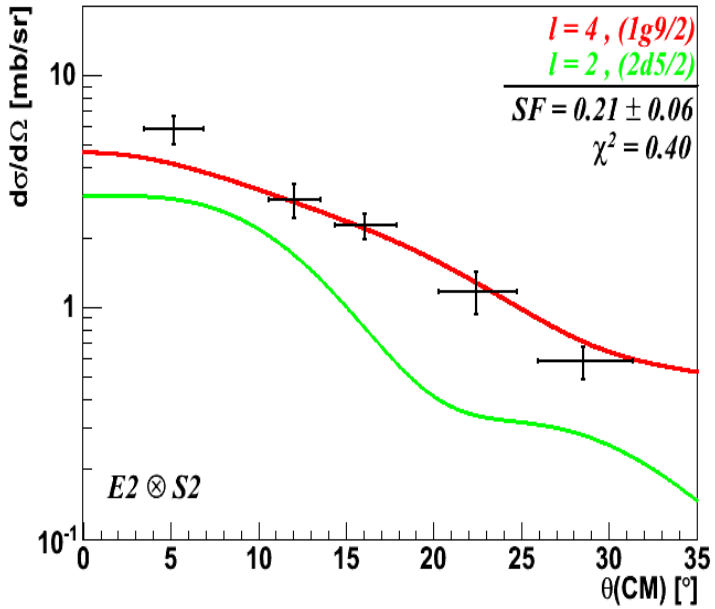

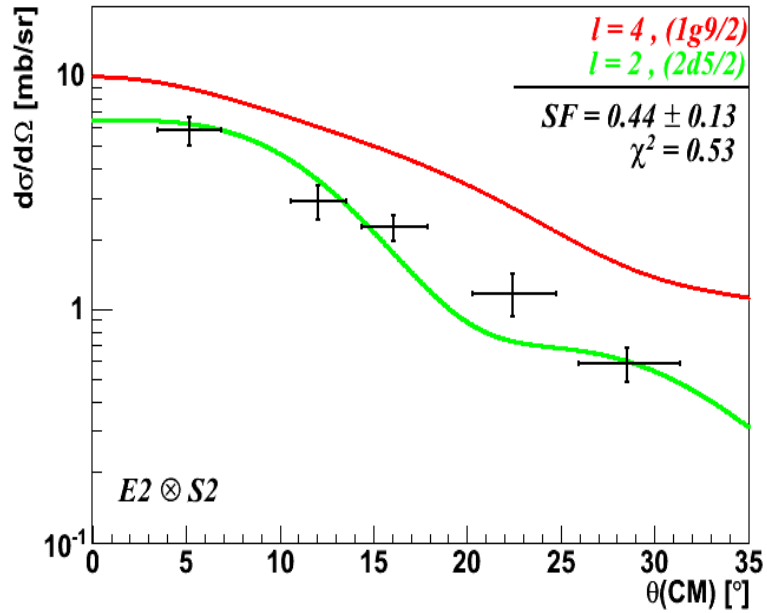

Experiment Vs Shell model calculations

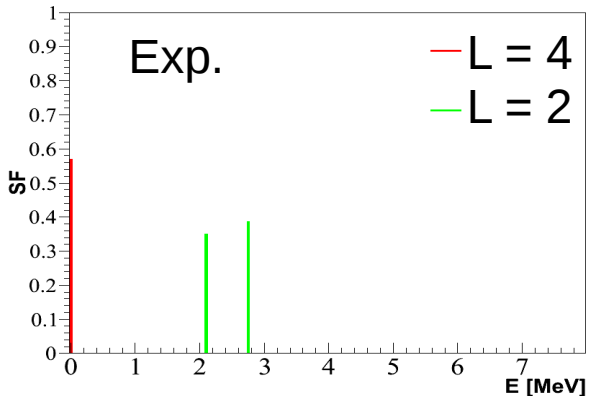

E_{exc}(Exp.) = 2.44 MeV

→ E_{exc} = 2.11 MeV

L = 2, SF = 0.36±0.13

→ E_{exc} = 2.76 MeV

L = 2, SF = 0.38±0.14

E_{exc}(Exp.) = 2.45 MeV

→ E_{exc} = 2.05 MeV

L = 2, SF = 0.32±0.10

→ E_{exc} = 2.74 MeV

L = 2, SF = 0.44±0.13

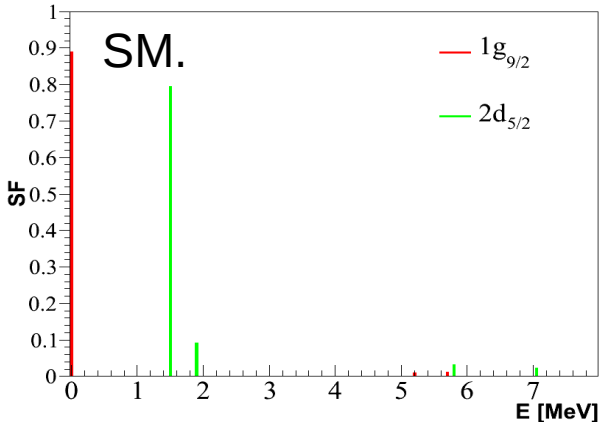

E_{exc}(SM) = 1.53 MeV

→ E_{exc} = 1.49 MeV

L = 2, SF = 0.79

→ E_{exc} = 1.92 MeV

L = 2, SF = 0.09

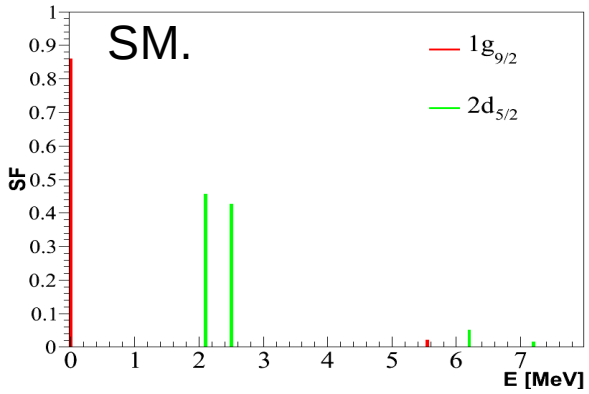

E_{exc}(SM) = 2.30 MeV

→ E_{exc} = 2.12 MeV

L = 2, SF = 0.46

→ E_{exc} = 2.50 MeV

L = 2, SF = 0.43

Diff. cross section analysis @ 4.19 MeV

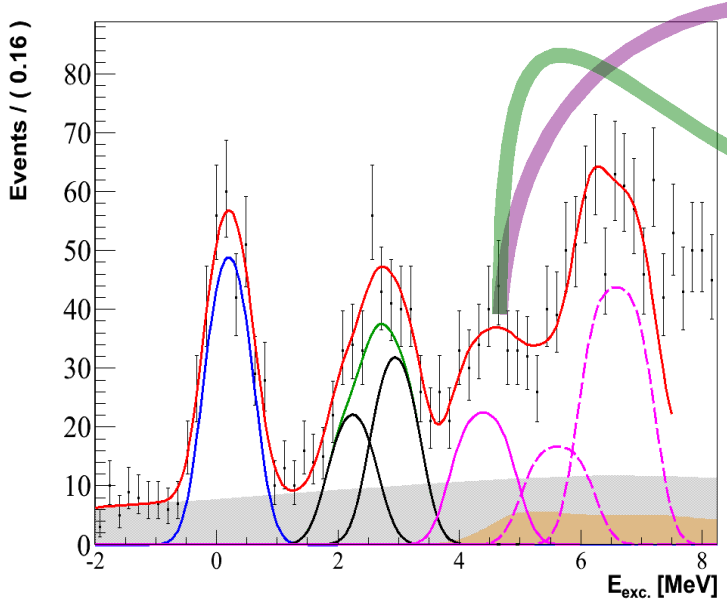

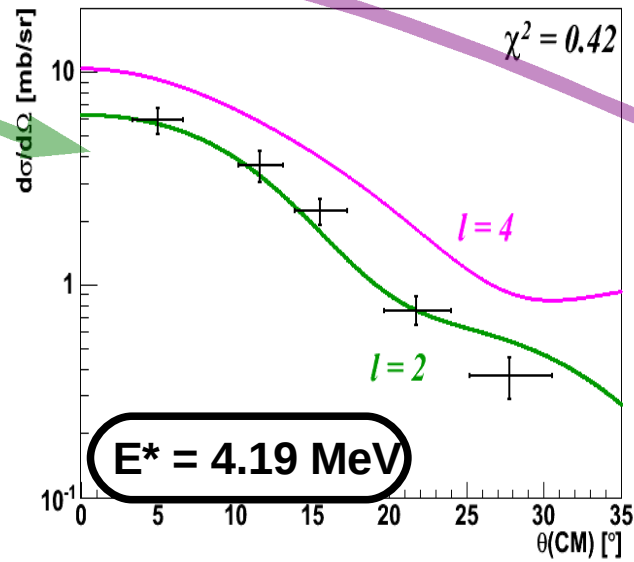

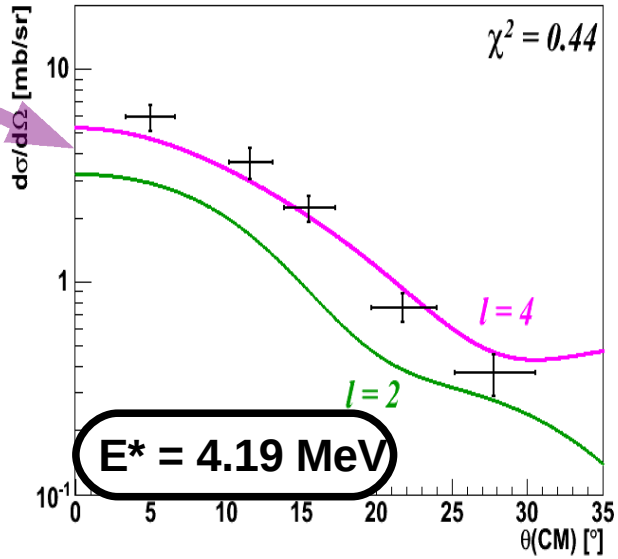

SF = 0.51 ± 0.15
SF = 0.26 ± 0.08

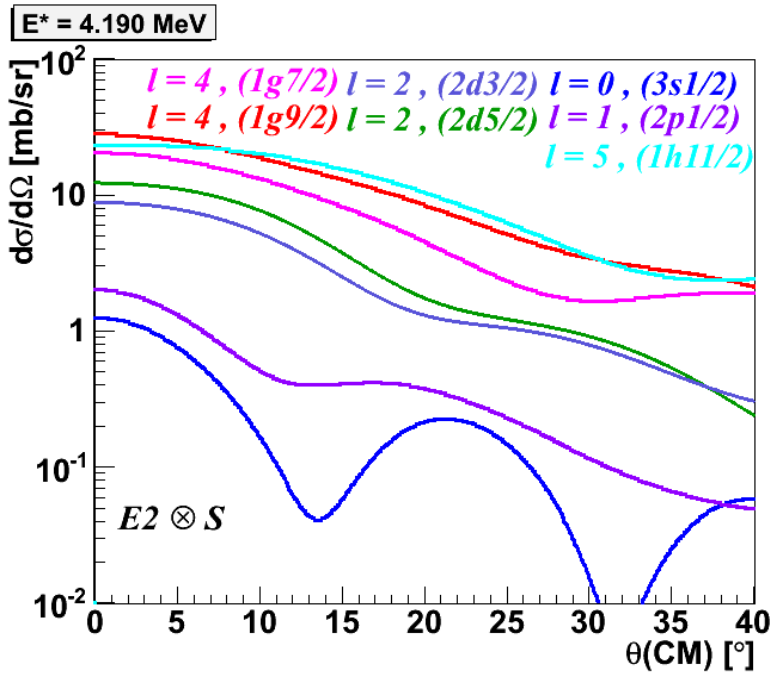

Diff. cross section analysis > Sn MeV